

Marianne Waagan

Eddy current losses in transformer windings

Master's thesis in Energy and Environmental Engineering

Supervisor: Arne Nysveen

May 2020

Marianne Waagan

Eddy current losses in transformer windings

Master's thesis in Energy and Environmental Engineering
Supervisor: Arne Nysveen
May 2020

Norwegian University of Science and Technology
Faculty of Information Technology and Electrical Engineering
Department of Electric Power Engineering

Preface

Here is the master thesis "Eddy current losses in transformer windings". This thesis is based on laboratory measurements and modelling in COMSOL multiphysics of a three phase transformer at 400/230 V.

This master thesis has been written to complete my master's degree in Energy and Environmental Engineering at NTNU. I was engaged in researching and writing this master thesis from January to May 2020.

This master thesis was written in collaboration with SINTEF. The master thesis was formulated together with my supervisor, Arne Nysveen, and co-supervisor, Svein Magne Hellesø. The work on this thesis gave me a greater understanding of transformers in general and was a learning opportunity in modelling.

Due to the COVID-19 pandemic hitting Norway in March, changes had to be done to the master thesis. I did my very best to complete the master thesis as planned, but because of restrictions set by NTNU, fewer measurements were performed than originally intended. Of the laboratory work, only 4 temperature measurement was performed in addition to resistance measurement, short circuit measurement and measurement of the circulating currents.

I want to thank my supervisor, Arne Nysveen. I have appreciated his guidance and support. His patience and willingness to explain concepts to me over and over again to ensure I truly understood them is something I have appreciated very much. I also want to thank my co-supervisor, Svein Magne Hellesø. He has always been willing to give helpful input, and he has through discussion and debate guided my through to finish all the needed models and measurements. The service lab also deserves thanks for helping me set up the experiments done in this master thesis.

I would like to thank all my wonderful classmates here at NTNU. They have brought laughter, friendship and academic insight to my five years here in Trondheim. I would also like to thank my parents, Monika Grønning and Olav Waagan. They have supported my through the highs and lows. From day one they have encouraged my curiosity, and without them, all my accomplishments would not have been possible. Lastly, I would like to thank Odd Arne Skjong, for proofreading, constructive criticism, and unfaltering support and patience throughout my five years here.

Marianne Waagan

Trondheim, May 29th, 2020

Abstract

The aim of this master thesis is to investigate a semi-analytical loss calculation method, especially when taking into account eddy current losses in transformer windings. This is done through comparisons between simulated and measured results, and through comparison between measurements and rated data from the producer. All of this is performed on a three phase 230/400 V test transformer. A large part of this thesis is to expand the work done in the specialization project[10] of the same name, by taking into consideration circulating currents and performing measurements.

The simulated results were found using COMSOL multiphysics. This was done by modelling a 3D model of the transformer to find the circulating currents and by modifying the 2D models created for the specialization project. The circulating currents were used to modify the three phase losses calculated in the specialization project. The data gathered from these simulations were processed using Microsoft Excel. The rated data used for comparison was acquired from the producer of the transformer, Noratel.

The types of measured result that were gathered varied. A short circuit heat run test was performed, being compared with the rated data. The resistance of the windings were measured both at room temperature, and after the heat run test. This was done to calculate the average temperature of the windings after a heat run test and the resistance of the windings at room temperature. Measurement of the circulating currents on the primary side of the transformer was performed using Rogowski coils. This was done to compare these currents with the simulated result. Thermocouples were used to measure the temperature increase in different turns, and was used to calculate the copper loss in the respective turns. This was done at 3 different current levels. To process this data, MATLAB and Microsoft Excel were used.

The short circuit test showed that the copper losses given in the rated data was performed at operating temperature of the windings. At the operating temperature, the difference between the measured and the rated loss was at 0.7 %. The three phase losses found at room temperature in the specialization project at 841.3 W increased to 931.7 W when taking into consideration circulating currents, causing the losses to increase with 10.7 %. It is still not at 1.11 kW, which is the copper losses registered at room temperature for the transformer. When comparing the simulated circulating currents in the primary winding and the measured circulating currents, it becomes clear that the difference is rather small, both in amplitude and phase angle.

From the resistance measurement, it became clear that the primary winding has the largest resistance. There were some differences between the measured and calculated value of the resistance at room temperature, 7.648 % in the secondary winding and 8.215 % in the primary winding. This difference is assumed to be due to inaccurate geometry assumptions of the transformer and inaccurate data about the area and resistivity of the conductor. For the resistance after the heat run test, it became clear that the calculated average temperature of the primary winding matched well with the measured temperature.

For the temperature measurements, the linearity in the first 10 minutes of measurements showed that the assumption of approximately adiabatic heating was valid. It was noted that the higher the current, the bigger the temperature increase would be. When using these temperature increases to calculate the power loss in the turns, there were some differences between the measured and simulated result depending on the winding parallel, regardless of current being applied. The cause of this was not found and further research would be beneficial.

The comparison between the magnetodynamic and the semi-analytical loss calculation method when considering circulating currents showed minute differences between the methods, and it is therefore assumed that they can be used interchangeably at 50 Hz. For the comparisons between the loss calculation methods with and without circulating currents, differences became clear depending on position of the winding parallel and can be explained using the leakage field and the geometry of the winding.

Sammendrag

Målet med denne masteroppgaven er å undersøke en semi-analytisk tapberegning metode, spesielt når man tar hensyn til virvelstrømstap i transformatorviklinger. Dette gjøres gjennom sammenligninger mellom simulerte og målte resultater, og gjennom sammenligninger av målte og nominell data fra produsenten. Alt dette utføres på en trefase 230/400 V testtransformator. En stor del av denne masteroppgaven er å utvide arbeidet som er gjort i fordypningsprosjektet [10] med samme navn, ved å ta i betraktning sirkulerende strømmer og utføre målinger på transformatoren.

De simulerte resultatene ble funnet ved bruk av COMSOL multiphysics. Dette ble gjort ved å modellere en 3D-modell av transformatoren for å finne de sirkulerende strømmene og ved å modifisere 2D-modellene som ble konstruert i fordypningsprosjektet. De simulerte sirkulerende strømmene ble brukt til å modifisere trefase-tapene som ble beregnet i fordypningsprosjektet. Dataene som ble samlet inn fra disse simuleringene ble behandlet ved hjelp av Microsoft Excel. De nominelle dataene som ble brukt til sammenligning ble anskaffet fra produsenten av transformatoren, Noratel.

De forskjellige type målinger som ble utført varierte. En kortslutningstest ble utført og sammenlignet med de nominelle dataene. Motstandsmålinger av transformatoren ble utført for å beregne gjennomsnittstemperaturen på viklingene etter en varmekjøringstest og motstanden til viklingene ved romtemperatur. Måling av sirkulerende strømmer på primærsiden av transformatoren ble utført ved bruk av Rogowski-spoler. Dette ble gjort for å sammenligne disse strømmene med det simulerte resultatet. Termoelementer ble brukt til å måle temperaturøkningen i forskjellige vindinger, og ble brukt til å beregne kobbertapet i de respektive vindingene. Dette ble gjort på 3 forskjellige strømmnivåer. For å behandle disse dataene ble MATLAB og Microsoft Excel brukt.

Kortslutningstesten viste at kobbertapene som ble oppgitt i de nominelle dataene ble utført ved nominell temperatur i viklingene. Ved nominell temperatur var forskjellen mellom det målte tapet og det nominelle tapet 0,7 %. Trefase-tapene som ble funnet ved romtemperatur i fordypningsprosjektet ved 841,3 W økte til 931,7 W når man tok i betraktning sirkulerende strømmer, en økning på 10,7 %. Det korrigerede tapet er fremdeles ikke på 1,11 kW, som er kobbertapene som er registrert ved romtemperatur for transformatoren. Når man sammenligner de simulerte sirkulerende strømmene i primærviklingen og de målte sirkulerende strømmene, er det tydelig at forskjellen er ganske liten, både i amplitude og fasevinkel.

Fra motstandsmålingen ble det klart at primærviklingen har størst motstand. Det var en viss forskjell mellom den målte og beregnede verdien av motstanden ved romtemperatur, 7.648 % i sekundærviklingen og 8.215 % i primærviklingen. Denne forskjellen antas å skyldes unøyaktige antagelser om geometri fra transformatoren og unøyaktig data om resistivitet og areal av lederen. For motstanden etter varmekjøringstest ble det klart at den beregnede gjennomsnittstemperaturen i primærviklingen stemte godt overens med den målte temperaturen.

For temperaturmålingene påviste lineariteten i de første 10 minuttene av målingene at antakelsen om tilnærmet adiabatisk oppvarming var gyldig. Det ble også tydelig at den aktive effekten var proporsjonal med temperaturøkningen. Når man brukte disse temperaturøkningene for å beregne effekttapet i svingene, var det noen forskjeller mellom det målte og simulerte resultatet avhengig av parallellen i viklingen, uavhengig av strøm. Årsaken til dette ble ikke funnet, og videre målinger vil være fordelaktig.

Sammenligningen mellom den magnetodynamiske og semi-analytiske tapberegning metoden når man vurderer sirkulerende strømmer, viste små forskjeller mellom metodene, og det antas derfor at de kan brukes om hverandre ved 50 Hz. For sammenligningene mellom tapsberegning metodene med og uten sirkulerende strømmer, ble forskjeller tydelige avhengig av parallellene i viklingene og kan forklares ved hjelp av lekkfeltet og viklingens geometri.

Contents

Preface	I
Abstract	II
Sammendrag	III
1 Introduction	1
2 Losses in transformer windings	3
2.1 The structure of a transformer	3
2.1.1 Windings	3
2.1.2 Core	4
2.1.3 Equivalent circuit of a transformer	4
2.2 Physics of a transformer	5
2.2.1 The leakage field of a transformer	5
2.2.2 Eddy currents in transformer windings	7
2.3 FEM calculations	8
2.4 Semi-analytical loss calculation method	9
2.5 Circulating currents	10
2.6 Temperature and transformer winding	10
2.6.1 Temperature and resistance	10
2.6.2 Adiabatic heating	11
3 Method	12
3.1 The test transformer	12
3.2 Short circuit measuring	14
3.3 Temperature measurement	19
3.3.1 Calculations	23

3.4	Resistance measurement	24
3.4.1	Constants and calculations	27
3.5	Circulating currents	27
3.5.1	The physics	29
3.5.2	Calculations	30
3.5.3	Measurements of circulating currents	31
3.6	Comparisons for different methods	31
3.6.1	Comparisons between magnetodynamic and semi-analytical loss calculation methods	32
3.6.2	The influence of circulating currents on calculated losses	32
4	Results	33
4.1	Short circuit measurement	33
4.2	Circulating currents	34
4.2.1	The currents modelled in COMSOL multiphysics	34
4.2.2	The measurement of the circulating current	36
4.2.3	Losses corrected for circulating currents	37
4.3	Resistance measurement	37
4.3.1	Before heat run test	37
4.3.2	After heat run test	38
4.4	Temperature measurement	39
4.4.1	The linear regression analyses	39
4.4.2	Comparisons between the temperature measurements	46
4.4.3	Losses and comparisons of losses	47
4.5	Comparisons for different simulation methods	50
5	Discussion	51
5.1	Short circuit measurement	51
5.2	Circulating currents	51
5.2.1	The measurement of the circulating current	52
5.3	Resistance measurement	52
5.3.1	Before the heat run test	52
5.3.2	After the heat run test	53
5.4	Temperature measurement	53
5.4.1	Linear regression analysis	53

5.4.2	Comparisons between measured and calculated power loss	54
5.5	Comparisons for different methods	55
6	Conclusion	57
7	Further works	58
	Appendices	60
A	Short circuit test	60
B	Resistance measurement	61
C	Temperature measurements	62
C.1	Current applied during temperature measurement	62
C.1.1	Half the nominal current	62
C.1.2	Nominal current	62
C.2	linear regression analyses	64
C.2.1	Half the nominal current	64
C.2.2	Nominal current	70
C.2.3	Twice the nominal current	78
D	Ratio between different methods	86

List of Figures

1.1	Transformers sorted by installation year in the distribution network, 1 kV to 22 kV [8, p.23].	2
2.1	Concentric windings.	3
2.2	Core-type transformers[7, p.12]. The upper two are 1-phase transformers, with the lower being a 3-phase transformer.	4
2.3	Equivalent circuit of a transformer [7, p.18].	4
2.4	Example of leakage fields in transformer cores [6, p.122].	5
2.5	Leakage window in a transformer with concentric windings[7, p.33].	6
2.6	Current density and field lines in windings.	7
2.7	Illustration for the semi-analytical loss calculation method.	9
2.8	Illustration for circulating currents in transformer windings.	10
3.1	The test transformer.	12
3.2	Short circuiting of the primary side of the test transformer.	13
3.3	Equivalent circuit for short circuit measuring of test transformer.	14
3.4	The transformers used as an energy source.	15
3.5	Equivalent circuit for short circuit measuring of test transformer.	16
3.6	The set up of the various measuring instruments.	17
3.7	Areas of placement of the thermocouples during short circuit heat run test.	17
3.8	Placement of thermocouples on the primary winding during short circuit measuring.	18
3.9	Placement of thermocouples on the primary winding during short circuit measuring.	18
3.10	Fastening of the thermocouples.	20
3.11	Areas of placement of thermocouples.	20
3.12	Placement of thermocouples on the primary winding.	21
3.13	Placement of thermocouples on the primary winding.	22
3.14	thermocouple placements on the secondary winding, upper turns.	22
3.15	thermocouple placements on the secondary winding, lower turns.	23

3.16	Circuit for measuring resistance on the secondary side.	25
3.17	Set up for resistance measurement on the primary side.	26
3.18	The cross section of the core leg with windings made in COMSOL.	28
3.19	The 3D model used to calculate the circulating currents, half section view of the transformer.	28
3.20	The area where Magnetic Insulation is used.	29
3.21	The definition of the windings using Coil.	29
3.22	The definition of current direction from Geometry Analysis in Coil.	30
3.23	The numbering system describing the winding parallels position in regards to the core.	30
3.24	The set up for measuring the circulating currents on the primary side.	31
4.1	The active power to the test transformer [kW].	33
4.2	The temperature [°C] registered at three different points during short circuit heat run test.	34
4.3	The phasor plot for the circulating currents in the primary winding.	35
4.4	The phasor plot for the circulating currents in the secondary winding.	36
4.5	The temperature [°C] measured by thermocouple 115 during heat run test.	39
4.6	The temperature [°C] and the linear regression analysis for thermocouple 110, from 0 to 10 minutes, when applying half nominal current.	40
4.7	The temperature [°C] and the linear regression analysis for thermocouple 110, from 0 to 10 minutes and from 1 to 2 minutes, half nominal current.	41
4.8	The temperature [°C] and the linear regression analysis for thermocouple 110, alpha and beta measurements.	42
4.9	The temperature [°C] and the linear regression analysis for thermocouple 110, comparing from 0 to 10 minutes and from 1 to 2 minutes, alpha measurement.	43
4.10	The temperature [°C] and the linear regression analysis for thermocouple 110, comparing from 0 to 10 minutes and from 1 to 2 minutes, beta measurement.	43
4.11	The temperature [°C] and the linear regression analysis for thermocouple 110, from 0 to 10 minutes, when applying twice nominal current.	44
4.12	The current [A] delivered to the test transformer in the time interval 1 to 2 minutes.	45
4.13	The temperature [°C] and the linear regression analysis for thermocouple 110, comparing from 0 to 10 minutes and from 1 to 2 minutes, twice nominal current.	45
4.14	The temperature [°C] measured at different currents applied.	46
4.15	The temperature [°C] measured at half and nominal current.	47
4.16	The major trend of the differences found in thermocouples, half the nominal current.	48
4.17	The major trend of the differences found in thermocouples, nominal current.	49
4.18	The major trend of the differences found in thermocouples, twice nominal current.	50
A.0.1	All measurements of the short circuit test.	60

B.0.1	Temperature [$^{\circ}\text{C}$] over time for resistance measurement.	61
C.1.1	The current [A] applied during temperature measurement for half nominal current.	62
C.1.2	The current [A] applied during the alpha temperature measurement for nominal current.	63
C.1.3	The current [A] applied during the beta temperature measurement for nominal current.	63
C.2.4	The temperature [$^{\circ}\text{C}$] and the linear regression analysis for thermocouple 107, from 1 to 2 minutes, at half the nominal current.	64
C.2.5	The temperature [$^{\circ}\text{C}$] and the linear regression analysis for thermocouple 108, from 1 to 2 minutes, at half the nominal current.	65
C.2.6	The temperature [$^{\circ}\text{C}$] and the linear regression analysis for thermocouple 109, from 1 to 2 minutes, at half the nominal current.	65
C.2.7	The temperature [$^{\circ}\text{C}$] and the linear regression analysis for thermocouple 111, from 1 to 2 minutes, at half the nominal current.	66
C.2.8	The temperature [$^{\circ}\text{C}$] and the linear regression analysis for thermocouple 112, from 1 to 2 minutes, at half the nominal current.	67
C.2.9	The temperature [$^{\circ}\text{C}$] and the linear regression analysis for thermocouple 113, from 1 to 2 minutes, at half the nominal current.	67
C.2.10	The temperature [$^{\circ}\text{C}$] and the linear regression analysis for thermocouple 114, from 1 to 2 minutes, at half the nominal current.	68
C.2.11	The temperature [$^{\circ}\text{C}$] and the linear regression analysis for thermocouple 115, from 1 to 2 minutes, at half the nominal current.	69
C.2.12	The temperature [$^{\circ}\text{C}$] and the linear regression analysis for thermocouple 116, from 1 to 2 minutes, at half the nominal current.	69
C.2.13	The temperature [$^{\circ}\text{C}$] and the linear regression analysis for thermocouple 107, from 1 to 2 minutes, alpha and beta measurement.	70
C.2.14	The temperature [$^{\circ}\text{C}$] and the linear regression analysis for thermocouple 108, from 1 to 2 minutes, alpha and beta measurement.	71
C.2.15	The temperature [$^{\circ}\text{C}$] and the linear regression analysis for thermocouple 109, from 1 to 2 minutes, alpha and beta measurement.	72
C.2.16	The temperature [$^{\circ}\text{C}$] and the linear regression analysis for thermocouple 111, from 1 to 2 minutes, alpha and beta measurement.	73
C.2.17	The temperature [$^{\circ}\text{C}$] and the linear regression analysis for thermocouple 112, from 1 to 2 minutes, alpha and beta measurement.	74
C.2.18	The temperature [$^{\circ}\text{C}$] and the linear regression analysis for thermocouple 113, from 1 to 2 minutes, alpha and beta measurement.	75
C.2.19	The temperature [$^{\circ}\text{C}$] and the linear regression analysis for thermocouple 114, from 1 to 2 minutes, alpha and beta measurement.	76
C.2.20	The temperature [$^{\circ}\text{C}$] and the linear regression analysis for thermocouple 115, from 1 to 2 minutes, alpha and beta measurement.	77
C.2.21	The temperature [$^{\circ}\text{C}$] and the linear regression analysis for thermocouple 116, from 1 to 2 minutes, alpha and beta measurement.	78

C.2.22 The temperature [°C] and the linear regression analysis for thermocouple 107, from 1 to 2 minutes, at twice nominal current.	79
C.2.23 The temperature [°C] and the linear regression analysis for thermocouple 108, from 1 to 2 minutes, at twice nominal current.	80
C.2.24 The temperature [°C] and the linear regression analysis for thermocouple 109, from 1 to 2 minutes, at twice nominal current.	80
C.2.25 The temperature [°C] and the linear regression analysis for thermocouple 111, from 1 to 2 minutes, at twice nominal current.	81
C.2.26 The temperature [°C] and the linear regression analysis for thermocouple 112, from 1 to 2 minutes, at twice nominal current.	82
C.2.27 The temperature [°C] and the linear regression analysis for thermocouple 113, from 1 to 2 minutes, at twice nominal current.	82
C.2.28 The temperature [°C] and the linear regression analysis for thermocouple 114, from 1 to 2 minutes, at twice nominal current.	83
C.2.29 The temperature [°C] and the linear regression analysis for thermocouple 115, from 1 to 2 minutes, at twice nominal current.	84
C.2.30 The temperature [°C] and the linear regression analysis for thermocouple 116, from 1 to 2 minutes, at twice nominal current.	84

List of Tables

3.1	Rated data of the test transformer.	13
3.2	Rated data of the one phase transformers.	14
3.3	The currents that is used during temperature measurement.	23
3.4	The constants used to calculate the temperature measurements.	23
3.5	Electrical data for copper [4].	27
3.6	The lengths of the parallels [m].	27
4.1	The absolute rms value of the currents in the different parallels.	34
4.2	The phase angles of the current in the different parallels.	35
4.3	The average rms absolute value for the currents in the secondary and primary windings [A].	36
4.4	The measured current and phase angle of phase u on the primary side.	37
4.5	The corrected losses in the test transformer[W].	37
4.6	The measured resistance in the windings before the heat run test.	37
4.7	The calculated and measured data from before the heat run test.	38
4.8	The measured resistance in the windings after the heat run test.	38
4.9	The resistivity and average temperature in the windings after the heat run test.	38
4.10	The losses [W/m] calculated from the temperature measured using half the nominal current.	47
4.11	The losses [W/m] calculated from the temperature measured using nominal current, alpha measurement.	48
4.12	The losses [W/m] calculated from the temperature measured using nominal current, beta measurement.	48
4.13	The losses [W/m] calculated from the temperature measured using twice nominal current.	49
5.1	The difference in % between the simulated and measured circulating current.	52
D.1	Difference in loss in % between the magnetodynamic and semi-analytical loss calculation method.	86
D.2	Difference in loss in % between the semi-analytical loss calculation method applying and not applying circulating currents, from turn 0 to 30 from the top.	87
D.3	Difference in loss in % between the semi-analytical loss calculation method applying and not applying circulating currents, from turn 30 to 61 from the top.	88

1 | Introduction

In this master thesis, the losses in transformer windings are investigated. Of particular interest are the losses associated with eddy currents. In transformer windings, the majority of the losses are ohmic losses. The eddy current losses are not equally distributed throughout the windings, but concentrates differently at different places in the windings. These areas with higher current density can generate hot spots and this again can reduce the expected life time of a transformer. There are several methods to model these losses. Some are numerical and require a lot of computation time and memory. Others are analytical and require less computational resources, but are less accurate. This master thesis is done in collaboration with SINTEF and builds on the work in the specialization project[10] with the same name. In this specialization project, the conclusion was that when low frequencies are used, from 75 Hz down to 25 Hz, a simplified semi-analytical loss calculation method showed sufficient accuracy during the testing. This semi-analytical loss calculation method calculates the static magnetic field of the transformer numerically with AC current applied, with the model not permitting eddy currents. The eddy current losses are added with analytical calculations based on the static magnetic field. In this master thesis, the loss calculations done in the specialization project are expanded on to include circulating currents due to the parallel circuits. This is done through constructing a 3D model of the transformer in COMSOL multiphysics, which is a "general-purpose simulation software for modeling designs, devices, and processes in all fields of engineering, manufacturing, and scientific research"[5].

An important aim of this master thesis, is to compare the simulated result, both modified from the spezialication project and found in newer models, with experimental data found through measurement in various places in the windings. This data is gathered through experiments performed in Elektrovarmelab at NTNU. The comparisons are made to see if the models constructed in COMSOL match the actual physical effect in the transformer and to evaluate the accuracy of the semi-analytical loss calculations method in the windings. This is done by applying several different currents on the transformer and accessing the result compared with the COMSOL models. Another aim is to compare the different loss calculation methods.

The goal for this master thesis, is to do the loss calculations within acceptable times of computation. For a purely numerical calculation of losses in a transformer, it would require a lot of computational resources. In a 3D FEM calculation, the vector field would have to be calculated numerically, in X, Y and Z direction. This would require many nodes and many unknowns that need to be calculated. To be able to simplify this loss calculation is an important goal for this project in collaboration with SINTEF. This data will be used by SINTEF in calculation of temperature development in transformers.

This master thesis is a part of a larger project. The larger motivations for SINTEF for this project are to increase the expected life time of transformers, conduct condition estimations and predict safe operation of older transformers that are found throughout the Norwegian energy infrastructure. Power transformers are an essential part of the electrical power infrastructure. Many of the transformers are installed several decades ago, as can be observed in Figure 1.1. This figure presents the amount of transformers in use in the distribution network in Norway sorted by year of installation[8]. The x-axis represents the installation year while the y-axis represents the amount of transformers. The transformers in Figure 1.1 are part of the distribution network in Norway, with voltage levels from 1 kV to 22 kV.

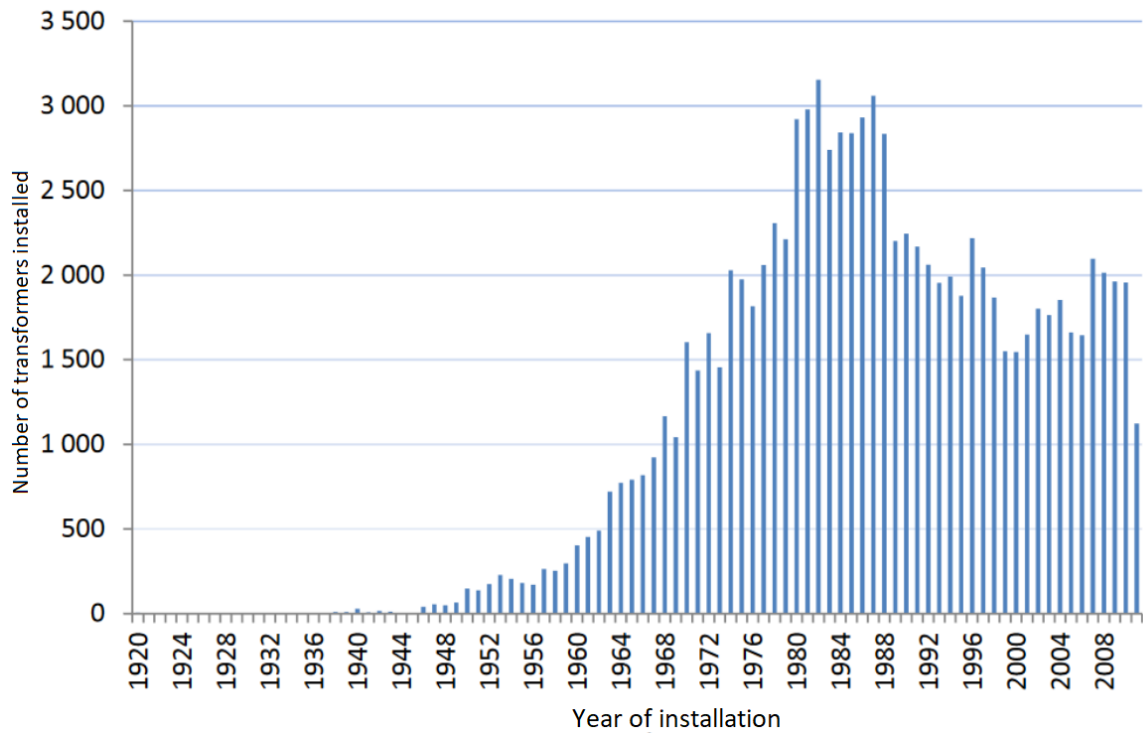


Figure 1.1: Transformers sorted by installation year in the distribution network, 1 kV to 22 kV [8, p.23].

As one can see from the above figure, many of the older transformer are still in operation. The replacing of transformers have been moderate throughout the years, which in turn means that the average age of a transformer is increasing continuously. It should be noted that even though the average age of the transformers is high, the condition of the transformers is generally good. In fact, many of the transformer are surpassing their expected life time. This may be due to the fact that the transformers have often been used with moderate loads instead of full loads, and due to design margins being quite large because of inaccurate design premises.

SINTEF have been tasked with determining the magnitude and distribution of losses in transformer, as part of a project that aims to determine the temperature of the windings, with funding from The Research Council of Norway and several major players in the electrical power industry. This is done to better estimate the life time of a transformer from it's hottest point. The sources of thermal activity in a transformer are the losses due to current in the copper windings, the electromagnetic losses in the iron core of the transformer and in the structural parts such as the transformer tank. In this master thesis, only the thermal activity from the copper windings are considered. Especially the losses associated with eddy current losses in the copper turns are of interest.

The goal of this project with SINTEF, is to be able to better use the existing infrastructure. This would mean to increase loading on these older transformers or extend their lifetime. Another important goal is to be able to calculate the thermal effects occurring in a transformer with limited knowledge of the geometry and still make these thermal calculations accurately. By increasing the accuracy of the calculations, the losses can be found more precisely and the hot spots these losses generate in a transformer can be more accurately mapped out. Regarding limited knowledge of geometry, old transformers often lack documentation and to get the exact geometry of the transformer, it needs to be taken out of use, transported, opened and studied. This takes time and resources, and a new transformer could easily be the cheaper option in such a case. So by not needing the exact geometry of the transformer, the owners of the energy infrastructure could save money.

This master thesis is structured so that the first section following the introduction is about losses in transformer windings. This section explains the theory which is the basis for the rest of the work in the thesis. Then follows the method section, which details information about the transformer used in the measurement is presented, the set up for the short circuit heat run test, the resistance measurement, the comparisons between the different methods used, the temperature measurement and the calculations performed, and COMSOL models will be presented. The next section is the result section. Here, the result, be it from experiments or the models constructed in COMSOL, are presented. To comment and discuss these result, the section discussion will follow the result. Lastly, the conclusion to summarize the most important points of this thesis will be presented, followed by further work to wrap up this master thesis. The appendix, with additional data, measurements and calculations, is found at the very end of the master thesis.

2 | Losses in transformer windings

2.1 The structure of a transformer

A functional definition of a power transformer is that it is an electrical device transferring electrical energy from one winding to one or several other windings that are magnetically coupled. This is done by having a time varying current in one of the transformer windings producing a time varying magnetic flux. This magnetic flux induces an EMF in the other transformer windings. Both of these windings are wound around a common transformer core. The main usage of a power transformer is to lower or elevate the voltage, reducing power losses during transportation of power.

To understand a transformer more practically, the main parts of a transformer are presented. Those are the windings and the core. In addition to those parts that are presented, a transformer consists of the structural parts that keep the windings and core in place. Oil insulated transformers have transformer tanks while air insulated transformers often have enclosures. Some transformers do not have a protective outer surface like the two described above.

2.1.1 Windings

A large variety of winding types are available in order to meet the different demands of current and voltage levels in the windings. These are concentric winding, layer winding, foil winding, interleaved helical winding, helical winding disc winding and regulation winding[7]. Since the test transformer has concentric windings, this winding arrangement is further discussed.

The concentric winding arrangement is the most common type. Normally the low voltage winding is the winding set closest to the core-leg, with the high voltage winding placed outside the low voltage winding. This is done since the low voltage winding require less isolation, making it occupy less space. Since less insulation is used, the total length of the secondary and primary winding is reduced and the total amount of copper needed is reduced. How this winding arrangement looks like is illustrated in Figure 2.1.

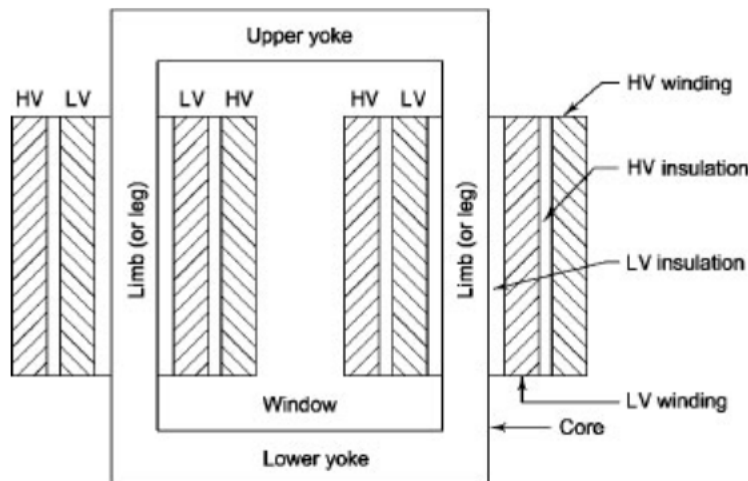


Figure 2.1: Concentric windings.

2.1.2 Core

The transformer core is the path of the magnetic field such that currents and voltages can be transformed from the primary to the secondary side. There are two main types of transformer cores mostly used today. Those are the core-type transformers and shell-type transformer. Since the test transformer is a core-type transformer, this type is further assessed.

The core-type transformer is the most common type in the power grid. The windings are usually placed around the legs [7]. In Figure 2.2, both 1-phase and 3-phase core-type transformer are illustrated.

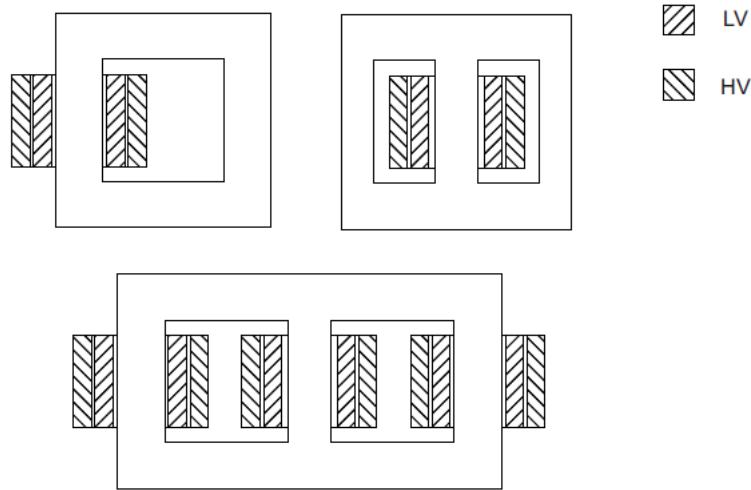


Figure 2.2: Core-type transformers[7, p.12]. The upper two are 1-phase transformers, with the lower being a 3-phase transformer.

2.1.3 Equivalent circuit of a transformer

To describe a transformer electrically, a circuit diagram is used. This diagram is shown in Figure 2.3. This is a per phase representation.

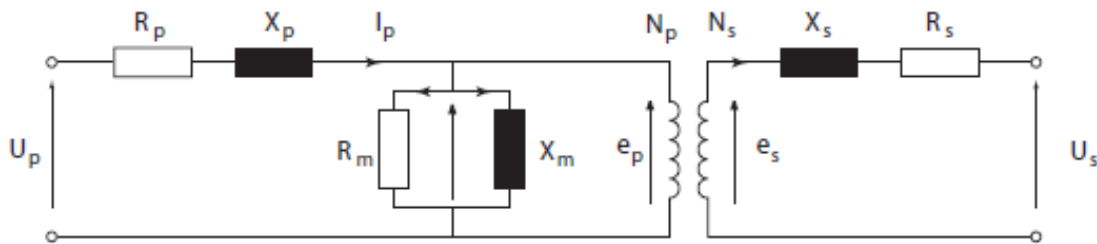


Figure 2.3: Equivalent circuit of a transformer [7, p.18].

The above equivalent circuit is valid for frequencies approximately below 400 Hz [7, p.18]. The different constants in Figure 2.3 represent various voltages, current and impedances. The explanation of these are found below itemized.

- U_p : The voltage applied on primary side.
- I_p : The current flowing from the primary side.
- R_p : The ohmic resistance in the primary winding. Lies between 0.01 to 0.0025 pu, depending on the size of transformer.
- X_p : The primary leakage reactance. Arrives from the flux leakage that goes through air. Lies between 0.05 to 0.025 pu, depending on the transformer.

- R_m : The resistance that represents no load losses of the transformer.
- X_m : The magnetizing reactance.
- E_p : The induced voltage on the primary side.
- N_p, N_s : The number of turns on the primary and secondary side, respectively.
- E_s : The induced voltage on the secondary side.
- X_s : The secondary leakage reactance. Lies between 0.05 to 0.025 pu, depending on the transformer.
- R_s : The ohmic resistance of the secondary windings. Lies between 0.01 to 0.0025 pu, depending on the size of transformer.
- U_s : The voltage the secondary side receives.

It should be noted that the magnetizing current, the current that feeds R_m and X_m , normally lies between 0.02 and 0.05 pu[3, p.81]. This current is so small because the normal per unit values for R_m and X_m are very high by design.

2.2 Physics of a transformer

2.2.1 The leakage field of a transformer

In a transformer core, there are several fields present. There is the mutual field of the core, the field that is flowing from the primary to the secondary coil. This is done by setting up a magnetic field in primary coil by applying current. This magnetic field then flows through the iron core and will induce a voltage in the secondary coil[6, p.122]. This can be observed in Figure 2.4 by the arrow underneath the mutual flux in the core.

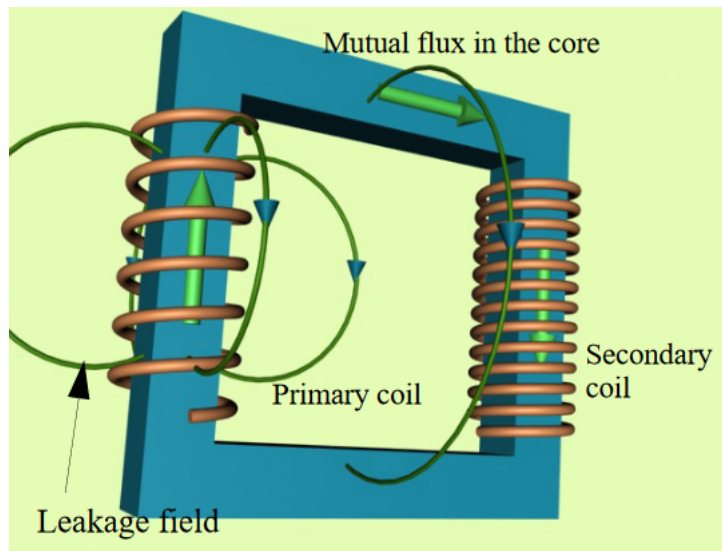


Figure 2.4: Example of leakage fields in transformer cores [6, p.122].

There is also a leakage flux in the transformer, as demonstrated in Figure 2.4. The leakage field in the primary coil will not reach the secondary coil and result in a voltage drop over the transformer and additional eddy current losses induced in various parts of the transformer[6, p.122]. Though not shown, the leakage field during loaded operation will occur in both primary and secondary coils.

The leakage field can be explained by using Ampere's law. It states the following as seen in Equation 2.1.

$$\oint_C H dl = I \quad (2.1)$$

This equation says that the magnetic field strength, H , around a closed curve, C , is proportional to the total current inside the curve. For a transformer, Equation 2.1 can be further simplified to Equation 2.2.

$$H \cdot L = N \cdot I \quad (2.2)$$

For this simplification, assumptions about the curve and the H field are made. The assumptions are that the H field is sufficiently close to zero to be negligible in the core and is constant in air, assuming that the yoke is placed directly on top of the winding, and that L is the height of the windings in the transformer. I is the applied current [A], N is the turn number.

In the iron core, the H field is close to zero due to the fact that the permeability of the core is so high. This causes most of the H field to be situated in the air. During normal operation of the transformer, the applied current and the turns create the right side of Equation 2.2. To fulfil ampere's law, a magnetic field must exist. Most of the magnetic field in the transformer travel through the iron core due to the low permeability in the iron core. Yet there is always a leakage field, since there is an alternative path for the magnetic field to travel, which is through air.

Leakage field and concentric windings

To describe how the leakage field travels through a concentric winding, which is the type of winding arrangement the test transformer has, Figure 2.5 is used. This figure describes the value of the axial leakage flux. The magnetic field and its direction is described by the red arrows. The above plot shows the axial flux density in the leakage window.

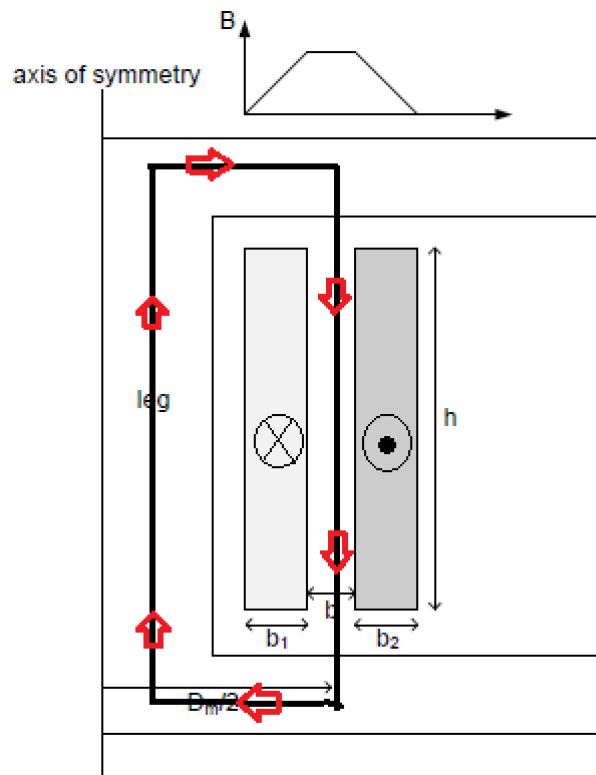


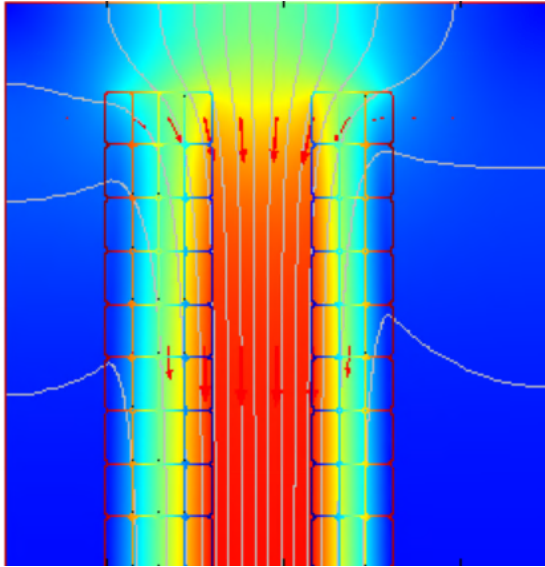
Figure 2.5: Leakage window in a transformer with concentric windings[7, p.33].

This figure is valid during short circuit testing, as perfect amp-turn balance is achieved. This is due to the fact that the magnetizing current discussed in section 2.1.3 is so small compared with the current in the windings, so when there is a short circuit, none of the current will pass through R_m and X_m from Figure 2.3. This causes equal amounts of current to flow in opposite directions in the windings of the transformer, as represented in Figure 2.5.

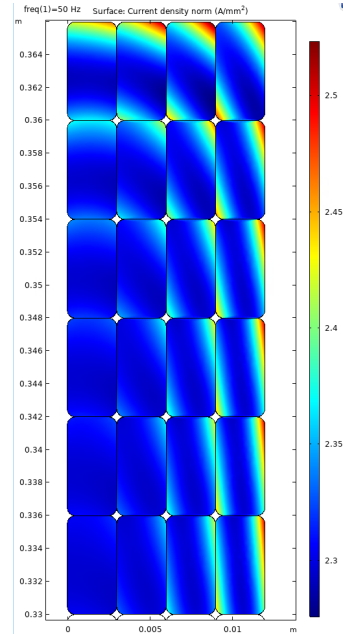
As discussed earlier, since the permeability is so high within the iron core, the H -field within the core is assumed to be close to zero. This causes the flux density to increase linearly through the first inner winding. In the air gap between the windings, the flux density is assumed to be constant. This due to the fact that the normal component of a B field when going from one material to the other is constant[9, p.73]. Through the outer winding, the flux density will

reduce linearly to zero [7, p.33], making the leakage flux outside of the windings, zero. This is why there is no axial leakage flux outside of the concentric windings.

In real life, there is never just an axial leakage field. Since the yoke can not be right next to the windings, both because of cooling of the windings and to isolate the windings from earth, there is also a radial leakage field. The effect of this field is that it creates currents within turns that are pushed upwards and downwards in the turns. This can be observed in Figure 2.6. Figure 2.6b shows the current density when applying an AC current, while Figure 2.6a shows the field lines of the leakage field. In Figure 2.6, red represent higher values and blue represent lower values, both for current and flux density.



(a) The field lines in a transformer[10].



(b) The current density with AC current applied[10].

Figure 2.6: Current density and field lines in windings.

The effect of the radial leakage field is mostly on the top and the bottoms in the windings, as can be observed in Figure 2.6b. When observing the angle of the field lines in Figure 2.6a, one can observe that the above statement is correct. Further from the top of the windings, the radial leakage field is so small that it is negligible and the axial leakage field dominates.

2.2.2 Eddy currents in transformer windings

In this section, an explanation of eddy currents in transformer windings is presented. This is based on the explanation first found in the specialization project[10], and is reused with small modifications to the text.

Eddy current loss in transformer windings can be defined as "power loss in conductors resulting from magnetic leakage field in windings and from the flow of eddy currents in parallel windings or in parallel winding strands[1, p.6]." It should be noted that for measurements of loss, it's not possible to separate the transformer stray losses from the eddy current loss[1, p.6].

Eddy currents in the each strand shift the current density. This due to the amount of flux each part of the winding is subjected to is different. This causes a difference in induced voltage, according to Faraday's law of induction, as seen in Equation 2.3.

$$\epsilon = -\frac{d\phi}{dt} \quad (2.3)$$

where ϵ is the induced EMF and ϕ is the flux. As seen in the above equation, this causes a difference in the induced voltage within the strand dependent on position. One would think that this would cause a radial voltage drop with in

the strand. This does not occur though. What happens is that currents get induced, but unevenly within the strand. The Equation that describes how this happens is Ohm's law shown in Equation 2.4.

$$J = \sigma \cdot E \quad (2.4)$$

Where J is the current density, E is the electric field and σ is the conductivity. How the electric field varies is explained in the following paragraphs.

In a conservative field, which is curlfree, we can set the electric field to be equal a gradient of a potential. This is presented in Equation 2.5. These equations describe what happens during magnetostatic conditions.

$$\nabla \times \vec{E} = 0 \quad (2.5a)$$

$$\vec{E} = -\nabla V \quad (2.5b)$$

The jump from Equation 2.5a to 2.5b is possible due to the fact that the field is conservative.

When adding the time perspective into it, others equations emerge. From the Faraday-Maxwell equation, shown in Equation 2.6, the relationship between electric field and flux density is shown.

$$\nabla \times \vec{E} = -\frac{\partial \vec{B}}{\partial t} \quad (2.6)$$

Next, the vector field gets introduced in Equation 2.7.

$$\nabla \times \vec{A} = \vec{B} \quad (2.7)$$

Using Equation 2.7 and 2.6, a relationship between vector field and electric field is presented in Equation 2.8.

$$\nabla \times \vec{E} = -\frac{\partial(\nabla \times \vec{A})}{\partial t} \quad (2.8a)$$

$$\nabla \times \vec{E} = -\nabla \times \frac{\partial \vec{A}}{\partial t} \quad (2.8b)$$

$$\nabla \times (\vec{E} + \frac{\partial \vec{A}}{\partial t}) = 0 \quad (2.8c)$$

$$\vec{E} + \frac{\partial \vec{A}}{\partial t} = -\nabla V \quad (2.8d)$$

The last leap from Equation 2.8c to 2.8d is possible due to the relationship shown in Equation 2.5. The gradient is a constant in each cross section of the winding that is normal to the current direction. The derivative vector field varies within the strand, due to the flux density varying within the winding. This causes the electric field to vary within the strand of the winding. From Equation 2.4, one can observe that this causes the current density to vary within in the winding strand. This again causes the potential radial voltage drop to become zero, since the varying vector field is considered EMF. This is in effect the cause of eddy current in windings.

2.3 FEM calculations

To do all the calculations done in COMSOL, the Finite Element Method, or FEM, is used. "The FEM is a particular numerical method for solving partial differential equations in two or three space variables. To solve a problem, the FEM subdivides a large system into smaller, simpler parts that are called finite elements. This is achieved by a particular space discretisation in the space dimensions, which is implemented by the construction of a mesh of the object: the numerical domain for the solution, which has a finite number of points.[12]"

2.4 Semi-analytical loss calculation method

For the semi-analytical loss calculation method to be used in simulations of the transformer, an AC current is set on the terminals of the transformer, while no eddy currents are allowed by the model. From there, the losses associated with the copper are found and mapped out. This is the first step in finding the total losses using the semi-analytical loss method. These losses are associated with the resistance of the copper, calculated using Equation 2.9.

$$R = \frac{\rho \cdot l}{A} \quad (2.9)$$

Where R is the ohmic resistance, the ρ is the resistivity of the material, l is the length of the conductor and A is the cross section area of the conductor. When calculating the resistance in the transformer, the resistances R_1 and R_2 , the winding resistances presented in Figure 2.3 are the resistances of interest. From here, the resistance is multiplied with the current squared, and the DC losses for the conductor are presented.

The second part of these calculations are to use an analytical equation to calculate the additional eddy current losses in the winding. This is done while applying the same AC current on the conductor. An article[1] on thermal modelling in transformers was used.

The losses in the windings from the eddy currents can be calculated using Equation 2.10[1, p.14].

$$P = \frac{\omega^2}{24 \cdot \rho} \cdot (B_x^2 \cdot T_y^2 + B_y^2 \cdot T_x^2) \quad (2.10)$$

Where P is the additional eddy current loss, ω is the angular frequency and ρ is the resistivity of the material in $[\Omega]$. It should be mentioned that this equation is valid assuming a small conductor size compared with the depth of penetration. To explain B and T, Figure 2.7 is used.

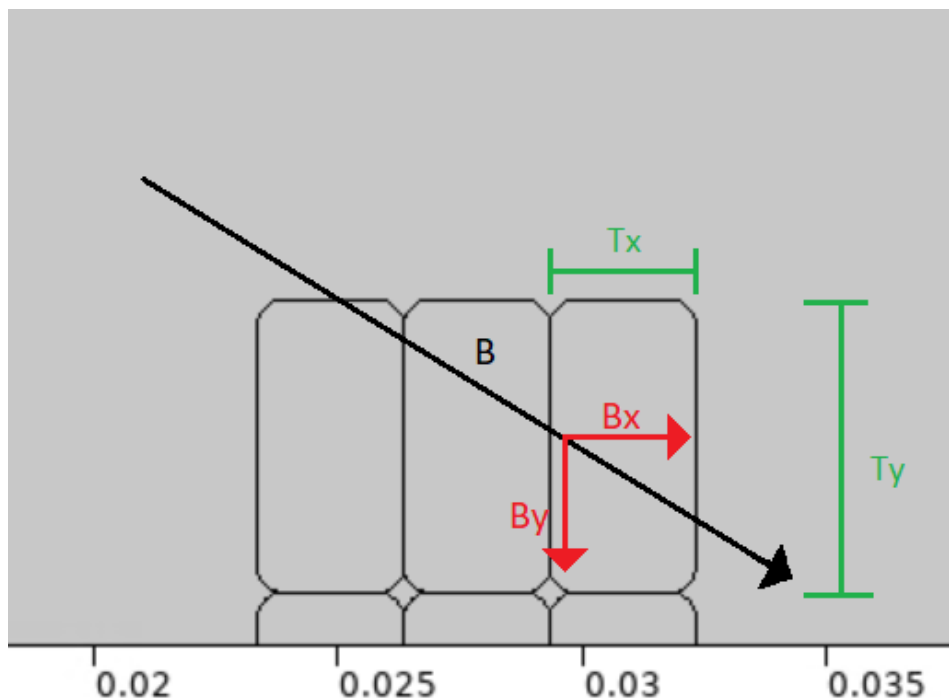


Figure 2.7: Illustration for the semi-analytical loss calculation method.

In this case, B is the peak leakage field that enters the turn, with B_x and B_y being the vector components of the leakage field. T is the dimensions of the winding, with T_x and T_y being the lengths in their respective directions for a 2D system.

From the specialization project, it was shown that at the lower frequencies, this semi-analytical loss method worked very well compared to a purely magnetodynamic AC model[10]. When the semi-analytical loss method is applied to the 3D model, this makes the calculations much easier due to the fact that the current is uniform in the windings. With this knowledge, COMSOL does not need to calculate the current density, which demands a lot of computational resources. Therefore, the loss calculations can be done quicker, with less partitions and still keep the accuracy. The leakage field is found from the applied current and put into Equation 2.10 to calculate the losses in each turn of the winding. The greater the DC current, the larger the flux elements will be.

2.5 Circulating currents

Circulating currents may occur when multiple turn conductors are connected in parallel, such as in the test transformer. This is due to different impedances in each parallel due to different lengths, and differences in leakage field that induces different currents. This causes each different radial turn to be linked with a different leakage field, which causes circulating currents to flow in each turn to balance out the voltage difference between them. The current will flow back and forth between the parallel turns. These circulating currents generate additional losses in the windings and can add to the generation of hot spots[2]. Since circulating currents are dependent on the leakage field different radial turns are subjected to, the geometry is important for the amount of circulating currents that may occur. The current is equal through out each parallel, the circulating currents are flowing between the parallels. This phenomena is presented visually in Figure 2.8.

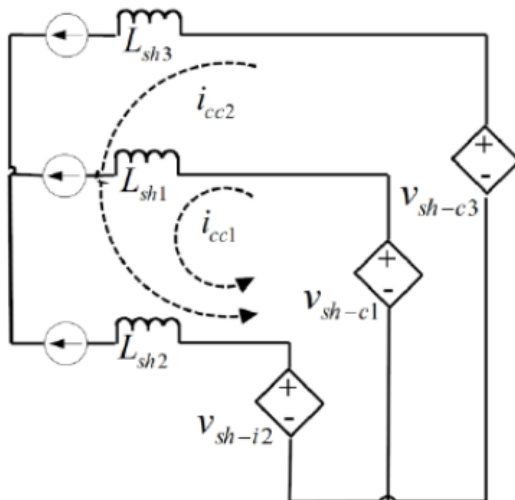


Figure 2.8: Illustration for circulating currents in transformer windings.

Many designs of transformer windings have continuously transposed conductors, or CTC cables, or use transposition of the conductor to reduce the occurrence of circulating currents in transformer windings[7, p.26]. This is done so that each conductor from parallel to parallel are subjugated to equal amount of leakage field. The losses associated with circulating currents are unwanted and increases the total losses in the transformer.

2.6 Temperature and transformer winding

In this section, temperature and how it affects the windings in a transformer is presented.

2.6.1 Temperature and resistance

For most materials, the resistance rises with the temperature. This is the case for the common electrical conductors aluminium and copper. For the relationship between resistivity and temperature, a linear approximation can be used. This relationship is presented in Equation 2.11.

$$\rho(T) = \rho_0 \cdot [1 + \alpha(T - T_0)] \quad (2.11)$$

where ρ_0 is the resistivity at temperature T_0 , α is the temperature co-efficient of resistivity and T is the temperature measured.

The assumption of linearity is only valid within an interval of the temperature. This is because α is different at different temperatures. It is therefore common to name the temperature of which α is referenced. If the temperature is too far away from the reference temperature, the assumption of linearity is not valid[11].

2.6.2 Adiabatic heating

Adiabatic heating occurs when all the losses generated heat up an object and not the surroundings. An example of this occurring is when the heating process happens more quickly than the time needed to cool, using conduction or convection.

For transformer windings, this can occur at the beginning of applying load to the windings. This is due to the fact that the difference in temperature between the windings and the surrounding air is close to zero. Thus virtually no convection takes place. Since the generation of heat due to the applied power occurs so quickly, the cooling effects do not occur until the difference in temperature increases. Therefore the generation of heat in transformer windings happening at the beginning of applying load can be considered close to adiabatic. This means that the temperature increase is associated solely with the energy applied to the transformer from an energy source.

To calculate the energy supplied to the test transformer during adiabatic heating, one can use the heat capacity of the copper in the winding. This is done using Equation 2.12.

$$Q = C_p \cdot V(T_2 - T_1) \cdot \rho \quad (2.12)$$

From the above equation, Q represent the energy, C_p is the heat capacitance of the material, V is the volume of what is being heated, T_2 and T_1 is the end and start temperature, respectively and ρ is the density of the material in question.

Due to the assumption of adiabatic heating, the power applied to the copper conductor can be determined form the change in temperature. This is shown in Equation 2.13.

$$P = \frac{\partial Q}{\partial t} = C_{p,cu} \cdot \rho_{cu} \cdot A_{cu} \cdot l_v \cdot \frac{\partial T}{\partial t} \quad (2.13)$$

Many of the same constants appear in Equation 2.12 and in Equation 2.13. The new constants in the equation are A_{cu} and l_v , representing the area of the cross section and the length of the conductor respectively.

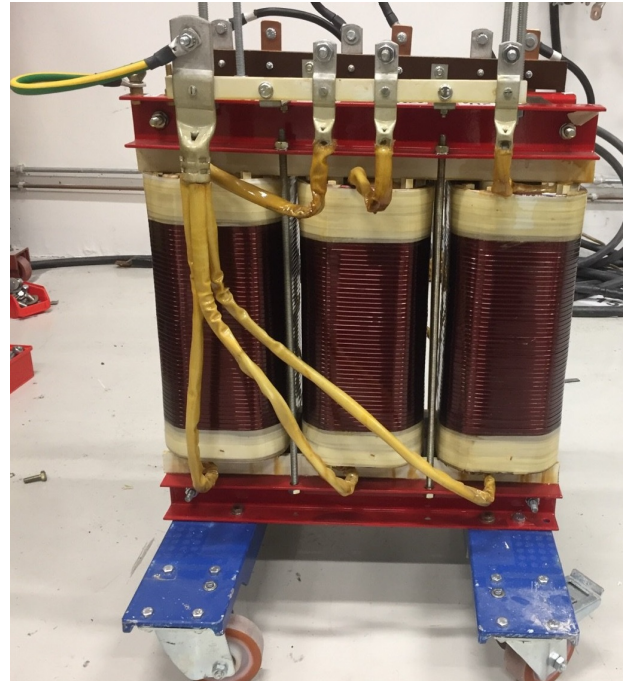
3 | Method

3.1 The test transformer

The test transformer used in this master thesis is a 400/230 V three phase transformer delivered by the producer Noratel AS. It was delivered to NTNU on 24.04.2008. This test transformer has concentric windings made out of copper. The windings are around an iron core of the core-type construction. The test transformer can be observed in Figure 3.1. The vector group of the transformer is dYN11, as provided by Noratel.



(a) The primary side of the test transformer.



(b) The secondary side of the test transformer.

Figure 3.1: The test transformer.

From Figure 3.1a, one can see that it is connected using delta configuration, while Figure 3.1b shows that the secondary side is connected in the star configuration.

Relevant data found in the production schematics provided by Noratel, are presented below in table 3.1.

Table 3.1: Rated data of the test transformer.

Constant	Value	Explanation
S	80 KVA	Apparent power
V_{prim}	230 V	Voltage on primary side
I_{prim}	205.4 A	Current on primary side
V_{sec}	400 V	Voltage on secondary side
I_{sec}	115.5 A	Current on secondary side
P_{core}	600.22 W	Core losses
P_{cu}	1329.37 W	Copper losses
P_{ec}	104.13 W	Eddy current losses

All of the above values are given with their RMS values.

To do the short circuit measurements and the temperature measurement on the test transformer, the measurements must be performed while short circuiting the primary side. This is mainly done to achieve ampere-turn balance, which gives more accurate calculations of the currents. This is also done to limit the apparent power used during measurement. If these tests were to be done using 80 kVA, it would be necessary with a rather large ohmic resistance to handle so much apparent power and this would produce heat. It would also increase the level of danger for the people conducting these tests, as the voltage level would have to increase during measurement. The down side to this is that one has to be particularly careful with the applied voltage, as applying voltage quickly and carelessly could cause the current to increase quickly to many times the nominal current. This in turn could cause harm to equipment and people.

The short circuit of the primary side is presented in Figure 3.2.



Figure 3.2: Short circuiting of the primary side of the test transformer.

3.2 Short circuit measuring

A short circuit measurement is performed to measure the copper losses and to compare the measured result to the calculated result during design and measured on the actual transformer by Noratel.

To do this, these instruments were used:

- Keysight InfiniVision DSOX2014A Oscilloscope
- Fluke 438 Series II POWER QUALITY AND MOTION ANALYSER
- Fluke 117 True RMS multimeter
- Fluke i1000s AC current probe
- Fluke i430-FLEXI-TF-II
- Agilent 34972A, Data logger

These various instruments are connected as shown in Figure 3.3. This is the equivalent circuit that shows the setup of the short circuit measuring.

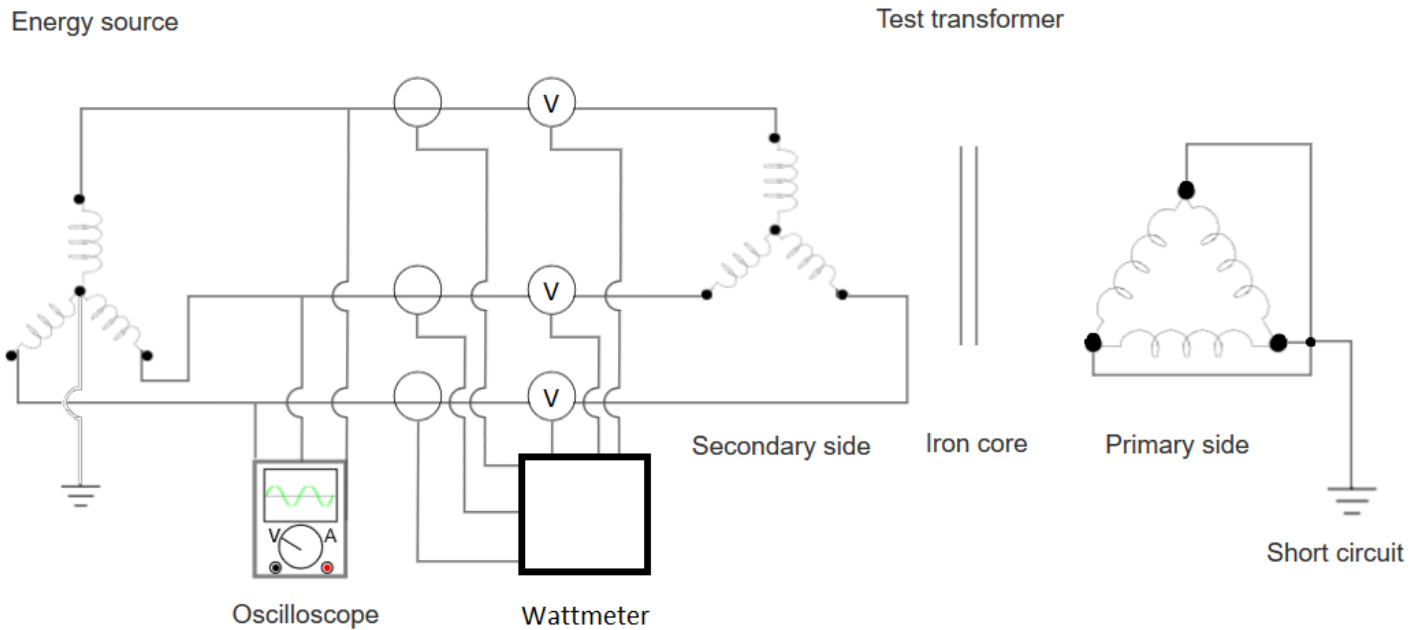


Figure 3.3: Equivalent circuit for short circuit measuring of test transformer.

Three transformers located at NTNU is used as the energy source. Each of the transformer are one phase transformers produced by National Transformer and were received by NTNU in 1987. The rated data is presented in table 3.2.

Table 3.2: Rated data of the one phase transformers.

Constant	Value	Explanation
S	250 kVA	Apparent power
V_{prim}	2 · 400 V	Voltage on primary side
I_{prim}	312 A	Current on primary side
V_{sec}	25-75 V	Voltage on secondary side
$I_{sec,max}$	3333-10 000 A	Current on secondary side

These transformers are shown in Figure 3.4.



Figure 3.4: The transformers used as an energy source.

Each of the transformers are fed by an individual variac. Since these transformers are one-phase transformers, the terminals of the phases are connected in a star configuration to make them operate as a three-phase transformer. This is shown in Figure 3.5, where the black circuit box is used to create the star point.



Figure 3.5: Equivalent circuit for short circuit measuring of test transformer.

Following this, the terminals of the energy source transformer are set on the terminals of the test transformer on the secondary side of the test transformer. The primary side of the transformer is short circuited. The node where the three phases get connected gets connected to ground. The current and the voltage from the energy source transformer is applied by manual control for each phase.

The oscilloscope, as shown in Figure 3.3, is used to monitor the wave form of the current being applied. This allows a better overview of the currents and makes it easy to monitor for harmonics and noise on the current. The current probes are connected to the oscilloscope and are what register the current wave form. This is shown in Figure 3.6.

The Fluke 438 Series II POWER QUALITY AND MOTION ANALYSER, which is referred to as the wattmeter in Figure 3.3, is used to measure the current, voltage and power being provided from the energy source transformer to the test transformer. This is done using voltage alligator clips and the i430-FLEXI-TF-II Rogowski coils. The voltage alligator clips measure the applied voltage while the Rogowski coils measure the current transferred. How these various measuring instruments are placed is presented in Figure 3.6.

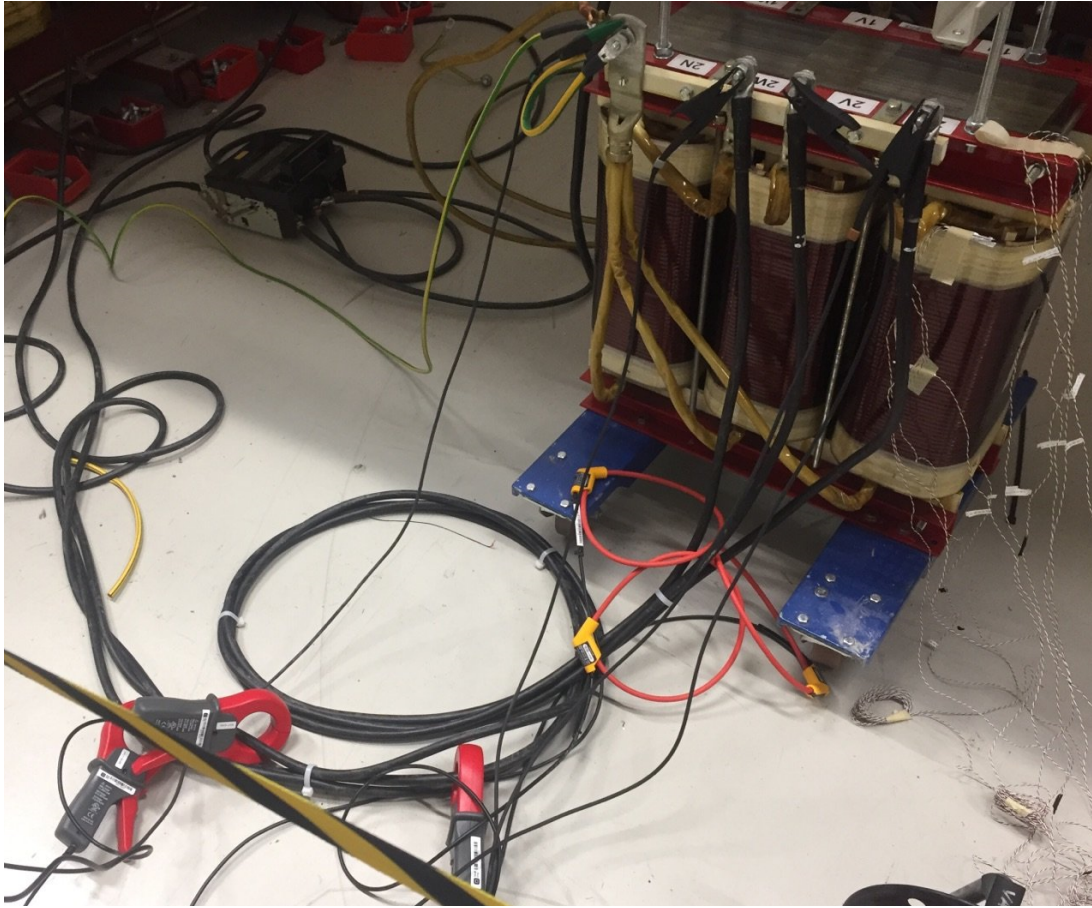


Figure 3.6: The set up of the various measuring instruments.

The black alligator clips measure the voltage, the red rings are the Rogowski coils and the grey and red current clamps are connected to the oscilloscope.

The current is set to the nominal primary current of 115 A RMS. Thermocouples that register the temperature are placed onto the windings. They are placed within the blue and yellow rectangles seen in Figure 3.7, a bird's-eye view of the test transformer. It should be noted that the blue rectangle covers the primary windings underneath the yoke.

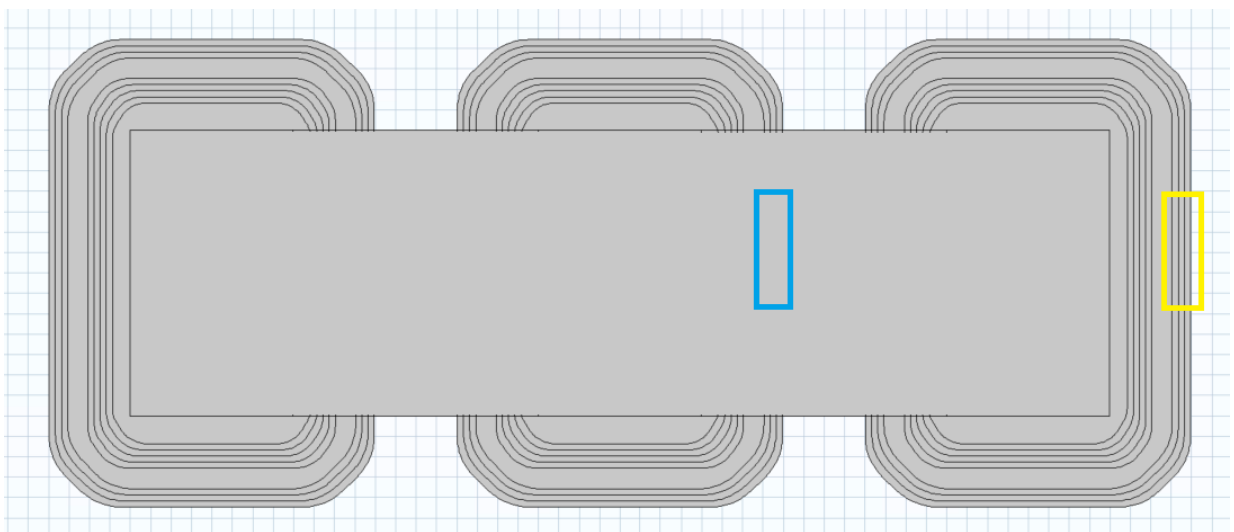
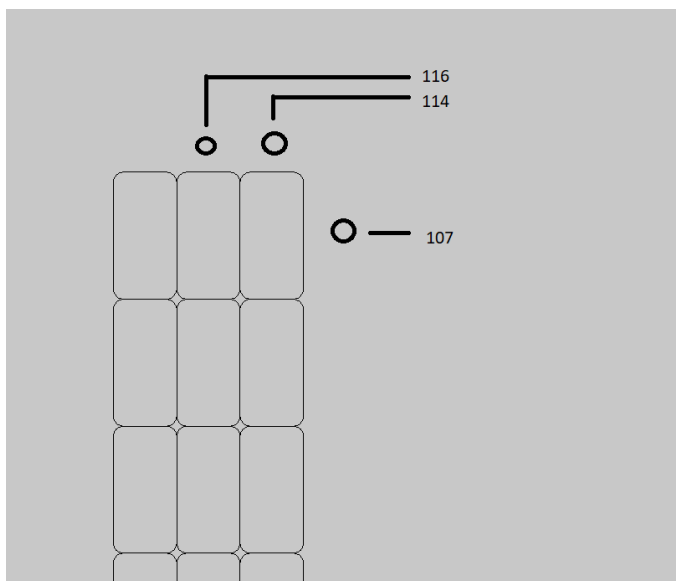
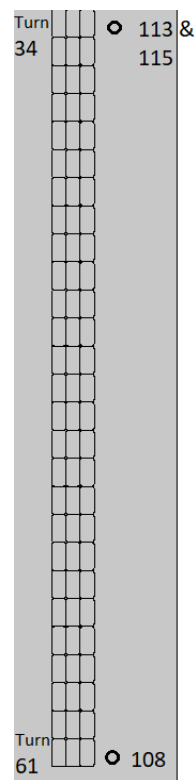


Figure 3.7: Areas of placement of the thermocouples during short circuit heat run test.

The thermocouples found within the yellow rectangle are placed as seen in Figure 3.8.



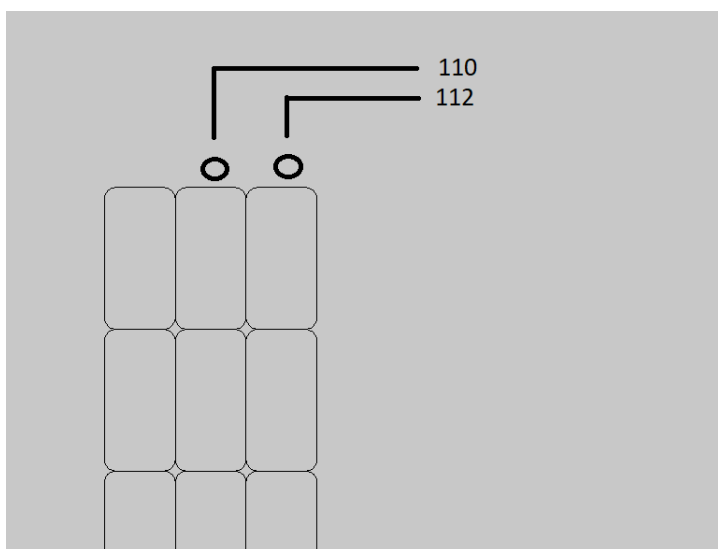
(a) The placement of the thermal nodes in the upper part of the winding.



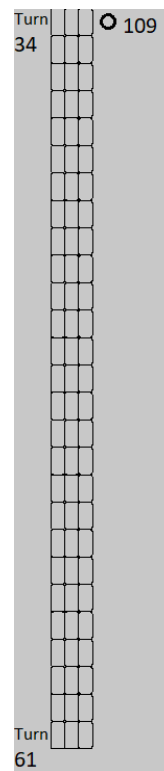
(b) The placement in the lower and middle part of the thermocouples in the winding.

Figure 3.8: Placement of thermocouples on the primary winding during short circuit measuring.

To present the placement of the thermocouples within the blue rectangle, Figure 3.9 is used.



(a) The placement of the thermal nodes in the upper part of the winding.



(b) The placement in the middle part of the thermocouples in the winding.

Figure 3.9: Placement of thermocouples on the primary winding during short circuit measuring.

In addition to the thermocouples shown in Figure 3.9 and 3.8, there are the thermocouples 105 and 111, which measure the room temperature and the iron core temperature, respectively.

These thermocouples are connected to the data logger and is used to measure the temperature of the windings. This is done until the temperature increase becomes so small that one can assume equilibrium. At this temperature, the apparent power transferred to the test transformer is registered.

3.3 Temperature measurement

In this section, how the measurement of the temperature rise at various currents is described in detail.

To conduct the temperature measurement, various instruments were used. The most important instruments are the following:

- Keysight InfiniiVision DSOX2014A Oscilloscope
- Agilent 34972A, Data logger
- Fluke 438 SERIES II, ANALYSATOR POWER QUALITY
- Fluke I430-Flexi-TF-II
- Fluke i1000s AC current probe

These various instruments are connected as shown in Figure 3.3. As one can observe from Figure 3.3, this set up for temperature measurement is identical to the set up for short circuit measurement.

The wattmeter from Figure 3.3 is used to measure the current and the voltage applied to the test transformer from the energy source transformer. This is especially to make sure the current is balanced in the three phases and has the correct amplitude. The wattmeter is also used to measure the applied power from the energy source transformer. Fluke I430-Flexi-TF-II Rogowski-coils are the instruments used to measure the current.

As with the short circuit measurement explained in Section 3.2, the oscilloscope is used to monitor the wave form, which is made possible using the current clamps connected to the oscilloscope.

The data logger is not shown in Figure 3.3, as it is presented further down. The temperature is measured by thermocouples connected to the data logger. The sampling rate for the thermocouples is set at 1 Hz. In total there are 10 thermocouples that are connected to various turns in the windings. They are connected using a mix of aluminium tape and kapton tape, a heat resistant tape. This was done to secure that the thermocouples were thoroughly fastened to the winding, while still being thermally isolated from the surrounding air. The electrical junction of the thermocouple was fastened with aluminum tape, then kapton tape was placed on top of it. This method of fastening the thermocouple is illustrated in Figure 3.10. This figure shows the placement of thermocouples 112, 116 and 107.

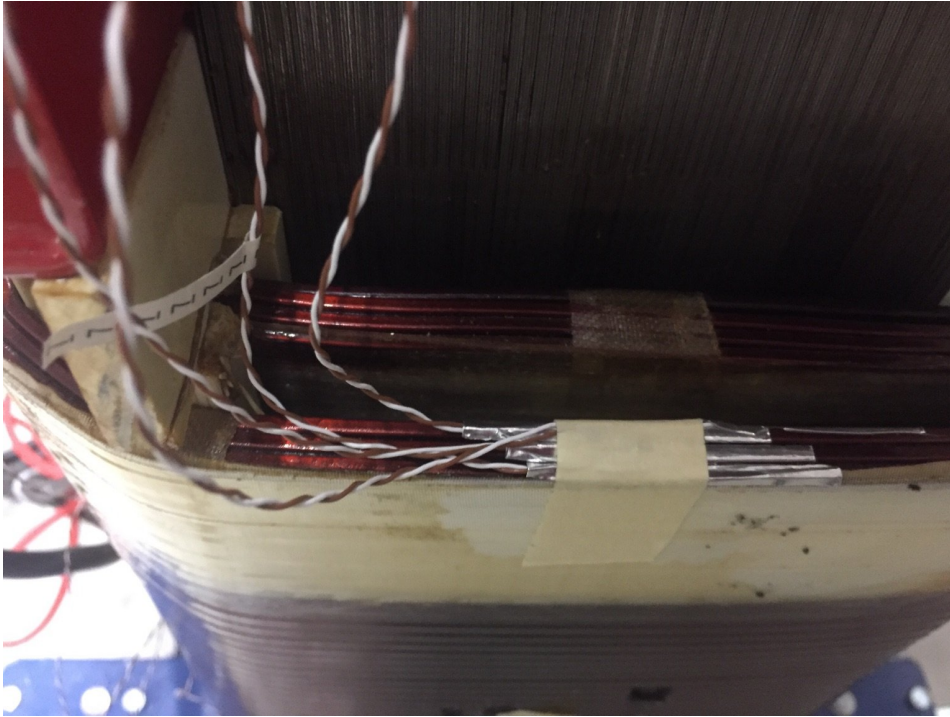


Figure 3.10: Fastening of the thermocouples.

The thermocouples are placed at different places of the primary winding. These areas, represented by coloured rectangles, are presented in Figure 3.11.

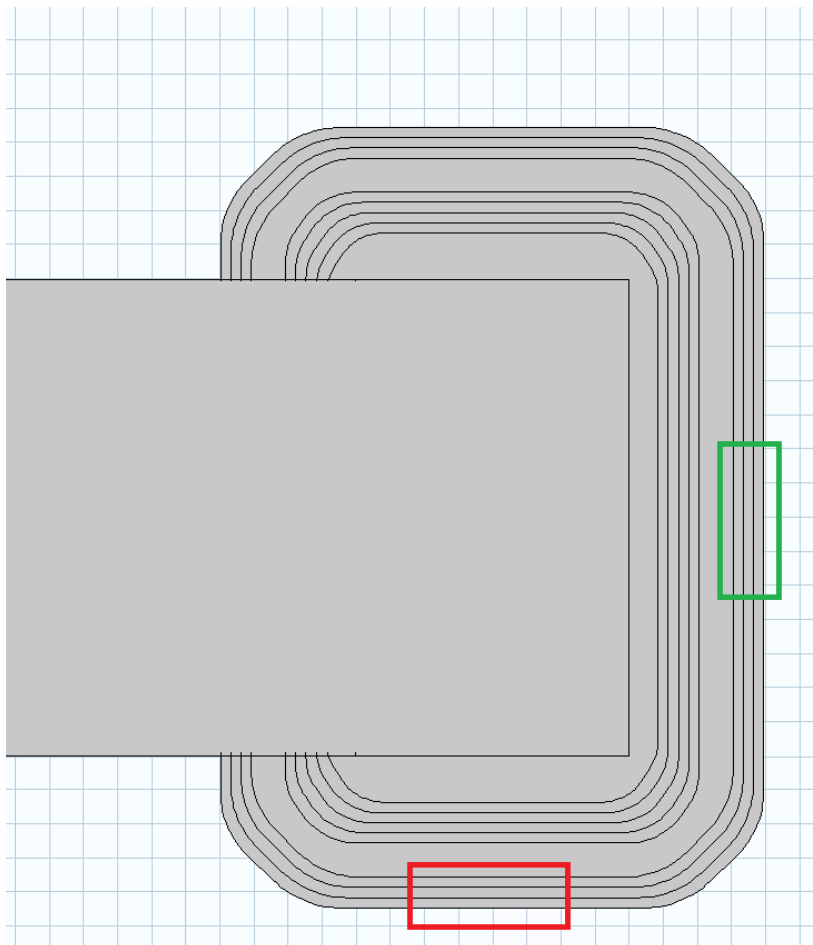
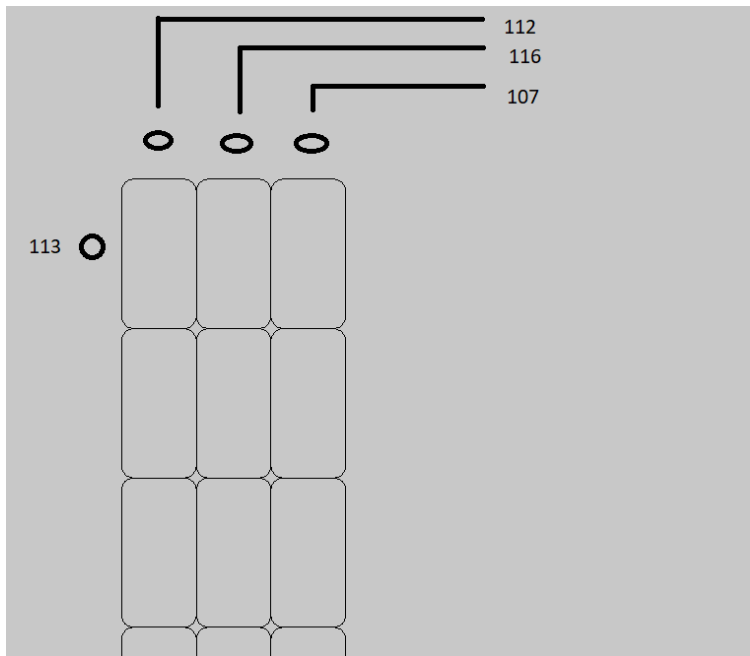


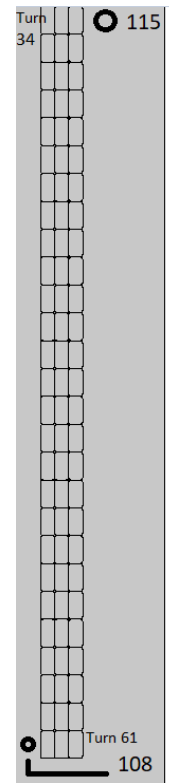
Figure 3.11: Areas of placement of thermocouples.

The large, grey rectangle in Figure 3.11 represent the yoke and the thin bands represent the parallels in the winding. It should be noted that none of the thermocouples are placed underneath the yoke and that the placements are distinct from what is presented in Section 3.2. All of these thermocouples are placed on phase u.

For the thermocouple situated in the green rectangle, the placement observed in Figure 3.12 was used. Each circle illustrate where one thermocouple is placed.



(a) The placement of the thermal nodes in the upper part of the winding.

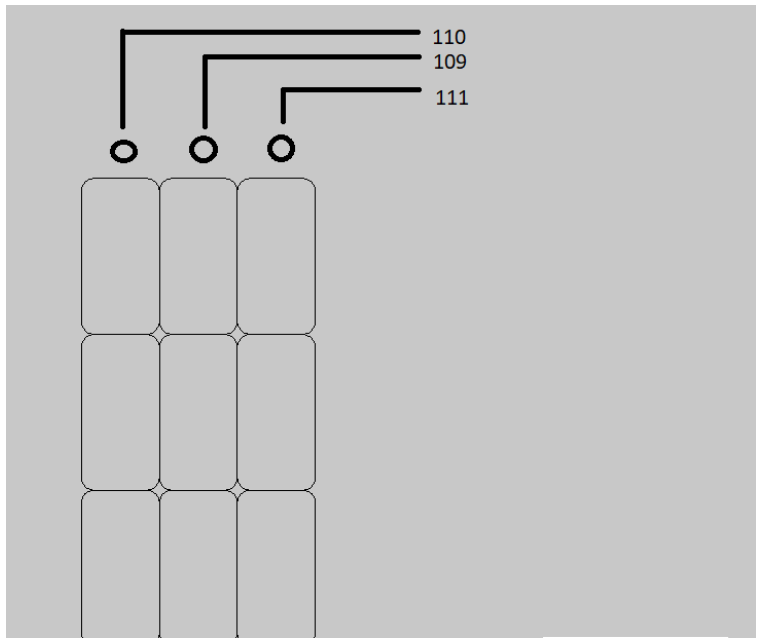


(b) The placement in the lower and middle part of the thermocouples in the winding.

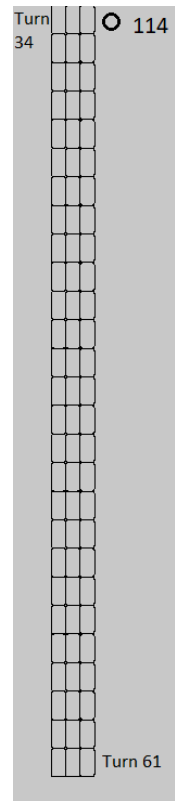
Figure 3.12: Placement of thermocouples on the primary winding.

It should be understood from Figure 3.12b that thermocouple 108 is placed in the leakage channel while thermocouple number 115 is placed on the outer side of primary winding. From Figure 3.12a, it should be understood that thermocouple 113 is placed in the leakage channel.

For the thermocouple situated in the red rectangle, the placement seen in Figure 3.13 was used.



(a) The placement of the thermal nodes in the upper part of the winding.



(b) The placement in the middle part of the thermocouples in the winding.

Figure 3.13: Placement of thermocouples on the primary winding.

The thermocouple 114 in Figure 3.13b should be understood such that it is placed on the outer side of the primary winding.

For the secondary winding, the thermocouples are placed as seen in figures 3.14 and 3.15. These thermocouples are placed within the green rectangle.

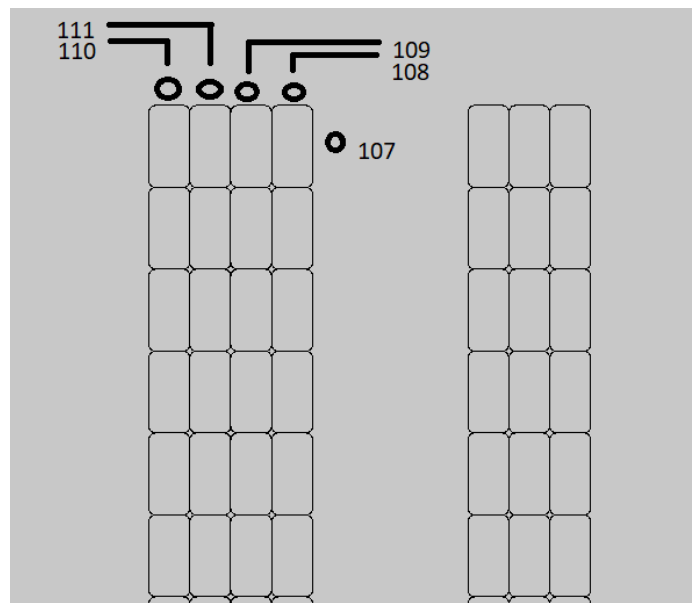


Figure 3.14: thermocouple placements on the secondary winding, upper turns.

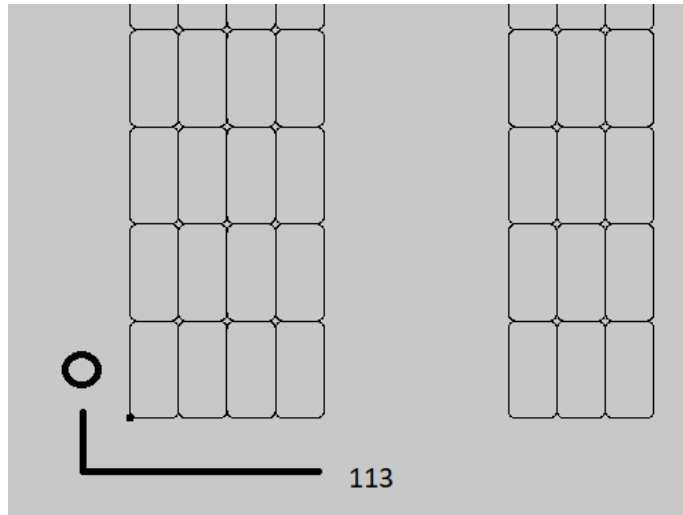


Figure 3.15: thermocouple placements on the secondary winding, lower turns.

The two above figures are placed within the red square for the secondary windings. thermocouple 107 can be understood to be placed in the leakage channel, while thermocouple 113 is located on the inside of the secondary winding, facing the iron core.

The power quality analyzer is used to figure out how much energy is consumed in the transformer windings. It is also used to observe the amount of current that is applied to the transformer windings. The data logger on the power quality analyzer is set to 1 Hz.

The current that is applied on the transformer windings varies with the different measurements. The currents that are applied on the windings are presented in Table 3.3.

Table 3.3: The currents that is used during temperature measurement.

Current applied	
I_1	0.5 · nominal current
I_2	nominal current
I_3	2 · nominal current

In this case, the current is the nominal current of the secondary winding with a rms value of 115 A.

3.3.1 Calculations

In this section, the calculations using the data from the experiment is presented.

When calculating the active power from heat added to the windings using Equation 2.13, the constants heat capacity and mass density must be decided. These are presented in table 3.4.

Table 3.4: The constants used to calculate the temperature measurements.

Constants	
Heat capacity [J/(kg K)]	385
Mass density [kg/m ³]	8940

Using the assumption that the heating during the first 10 minutes is adiabatic, a linear regression analysis is used on the data collected. This is done using the function LINEST in excel. This gives a line of best fit gradient and a line of best fit intercept. With this, a function of time is found to describe the temperature.

As seen from Equation 2.13, the derivative of the temperature as a function of time is needed. For the case of adiabatic

heating, this is the line of best fit gradient from the LINEST function. Using this together with the decided constants, the active power delivered can be calculated.

When the active power from the measurements is calculated, this result gets compared with the result from the COMSOL model. This is done as presented in equation

$$\eta_{temp} = \frac{P_{measured} - P_{simulated}}{P_{simulated}} \cdot 100 \quad (3.1)$$

Where $P_{measured}$ represent the active power measured with the laboratory set up, $P_{simulated}$ is the active power that is found using the models in COMSOL and η_{temp} is the difference between these two in %.

For the representation of the major trends, a histogram plot is used. The average difference measured in thermocouples placed at similar places in the winding is found and presented as the plot.

3.4 Resistance measurement

One of the measurements performed on this transformer is resistance measurements. This is done first at room temperature and then after a heat run test. This is done while short circuiting the primary side.

The main goal of the resistance measuring is to investigate the characteristics of the test transformer. It is also done to calculate and compare data from measurements with the technical data provided by the manufacturer of the transformer. The resistance after the heat run test is used to calculate the average temperature of the windings with nominal current applied to them.

The test are done using Megger MTO 210 OHMMETER TRANSFORMATOR. Only two set of voltage alligator clips are available using this ohmmeter. The last resistance must be tested after the last two, making this measurement occur at slightly lower temperatures. This ohmmeter supplies DC current for the measurements.

To measure the primary side, the changes to the original set up presented in Figure 3.16 must be done. The labels represent measuring points.

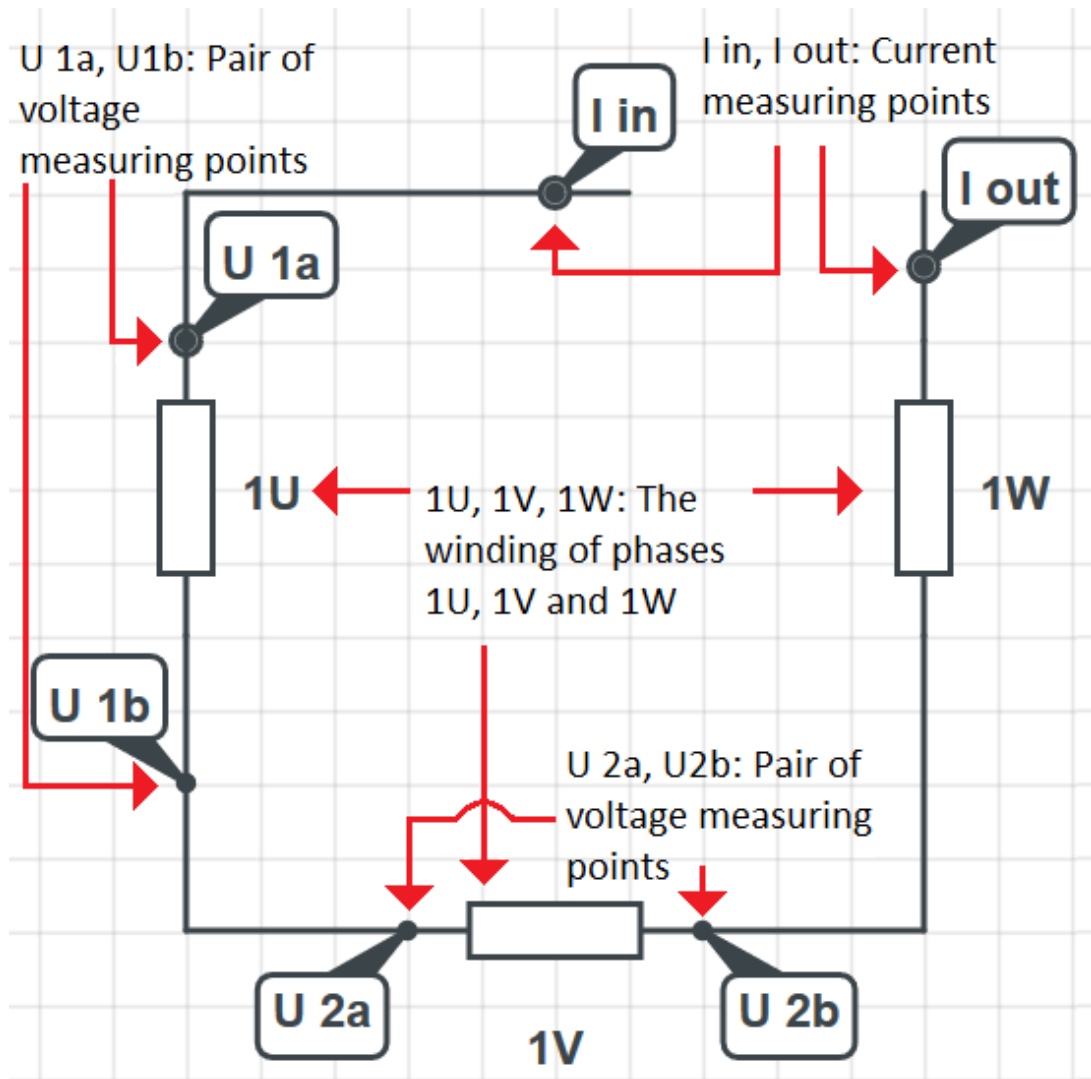


Figure 3.16: Circuit for measuring resistance on the secondary side.

The delta connection must be opened up, so no current can flow within the connection. The current is injected to the ends of the undone delta connection, represented by the measuring points I out and I in in Figure 3.16. Furthermore, the voltage alligator clips must be placed as shown in Figure 3.16. It should be noted that one of the voltage alligator clip pairs must be relocated to before and after phase 1W when the first round of measurement is performed.

For measurement the resistance on the secondary side, the changes presented in Figure 3.17 must be done. The labels represent the measuring points.

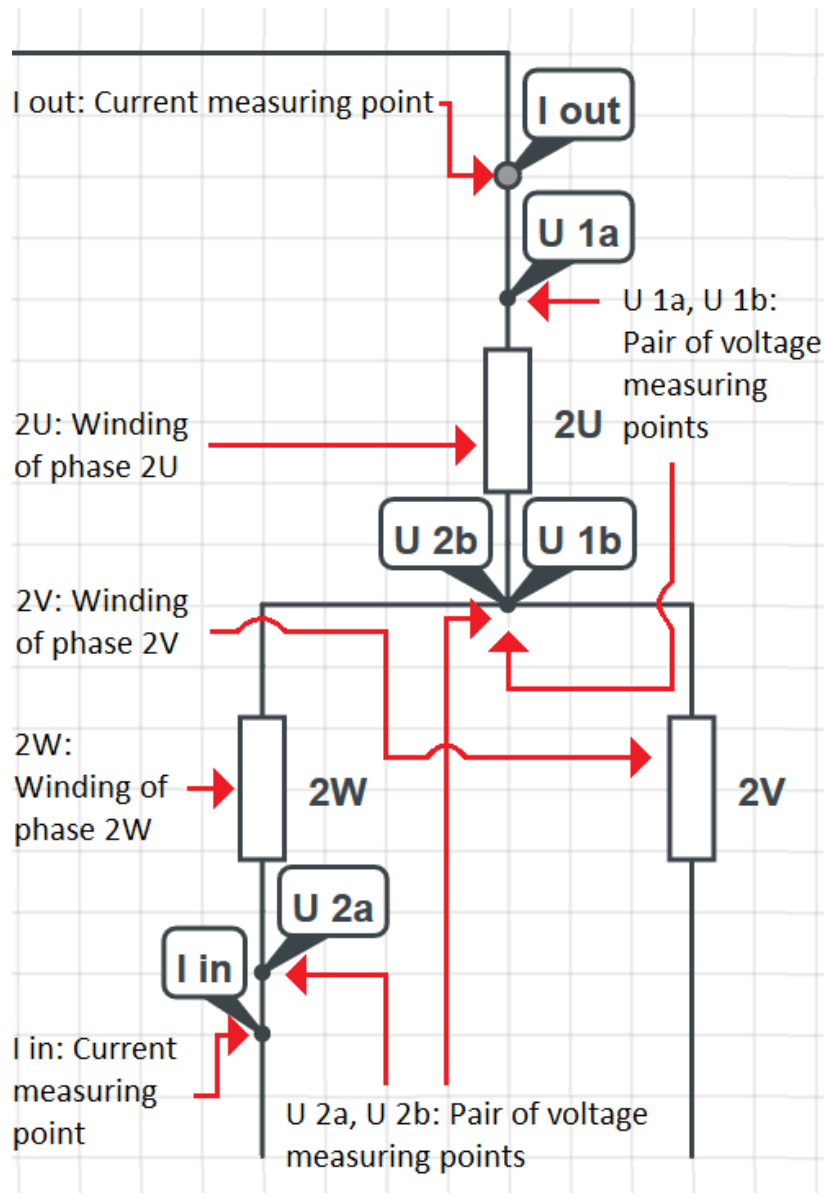


Figure 3.17: Set up for resistance measurement on the primary side.

The secondary side of the transformer is connected to the energy source transformer. When measuring the resistance, two of the connections to the power source must be opened up, as seen in Figure 3.17. This causes no current to circulate, not to the energy source transformer nor within the circuit.

The current measuring points are connected as seen in Figure 3.17. This connection causes the current to flow through two windings simultaneously. To measure the third winding, the I in measuring point is moved underneath the 2V winding. The voltage alligator clips are placed over each of the phases, as shown in Figure 3.17. Each of the pairs of voltage alligator clips have one of the terminals in the star point of the star configuration on the primary side. This way the voltage drop over the winding is registered. When measuring the last winding, the voltage alligator clip U 2a must be moved underneath 2V.

For the resistance measurements performed at room temperature, haste is not something to take into consideration, due to the temperature being constant throughout the measurement. When measuring the resistances after a heat run test however, time is of the essence. Therefore everything must be ready for attaching the alligator clips and a partner is recommended to get the measurements as quickly as possible after applied current is disconnected.

Thermocouples are used to register the temperature in various places of the transformer. The temperature will be measured until an increase in temperature is small and the temperature of the winding reaches steady state. The placement of the thermocouples is the same as in the measurements of the temperature, presented in figures 3.12, and 3.13.

3.4.1 Constants and calculations

When calculating the resistivity, a few constants must be decided to use Equation 2.11. They are found in Table 3.5.

Table 3.5: Electrical data for copper [4].

Constants	Value	Unit
ρ_0	$1.72 \cdot 10^{-8}$	$\Omega \cdot m$
T_0	20	$^{\circ}C$
α_{20}	0.00393	$1/^{\circ}C$

For calculating the resistance at room temperature, Equation 2.9 are used, together with the knowledge of the length and the cross sections of the windings and the turns. Then this result is compared with the measured resistance.

Since the resistances in the windings are connected in parallel, the resistance must be calculated taking this into consideration to be able to compare it with the resistance measured. For the primary winding, the resistance that can be calculated as presented in Equation 3.2.

$$R_{primary} = \frac{1}{A \cdot \left(\frac{1}{l_{prim,1}} + \frac{1}{l_{prim,2}} + \frac{1}{l_{prim,3}} \right) \rho_{cu}} \quad (3.2)$$

For calculating the resistance in the secondary winding, Equation 3.3 is used.

$$R_{secondary} = \frac{1}{A \cdot \left(\frac{1}{l_{sec,1}} + \frac{1}{l_{sec,2}} + \frac{1}{l_{sec,3}} + \frac{1}{l_{sec,4}} \right) \rho_{cu}} \quad (3.3)$$

The lengths of the parallels are found from measurements of the core leg and the gaps between the windings, and multiplied by the amount of turns. This is done in COMSOL after measurements of the test transformer. They are presented below in Table 3.6.

Table 3.6: The lengths of the parallels [m].

Lengths of parallels [m].							
	Secondary				Primary		
Parallel	1	2	3	4	1	2	3
Length [m]	31.0	32.4	33.8	35.2	40.1	41.5	42.8

To find the resistivity after the heat run test, the relationship presented in Equation 3.4 is used. This is used since the cross section area and length of the conductor is equal for before and after the heat run test.

$$\frac{R_{room,temp}}{R_{heat,run}} = \frac{\rho_{room,temp}}{\rho_{heat,run}} \quad (3.4)$$

The resistivity found using Equation 3.4 can be used to discover the average temperature of the winding using Equation 2.11. This temperature gets compared with the temperature measured with thermocouple 115, as seen in Figure 3.8b.

3.5 Circulating currents

To investigate the effect of the circulating currents on the losses, a 3D model of the transformer is built in COMSOL.

This was done by first creating a 2D model of the cross section of the core leg with windings. This model can be seen in Figure 3.18.

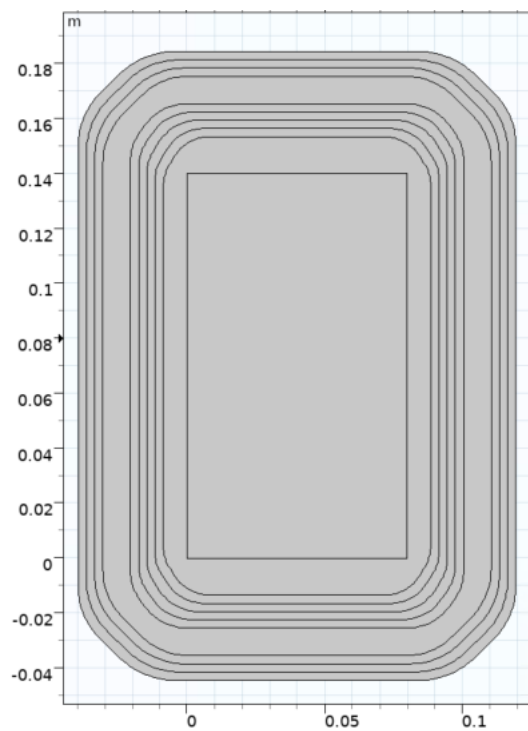


Figure 3.18: The cross section of the core leg with windings made in COMSOL.

The square in the middle represent the core leg, and the thin bands around the core legs represent the windings of the transformer. The model in Figure 3.18 is then extruded into a 3D model and the core is built around the windings. The result of this can be seen in Figure 3.19.

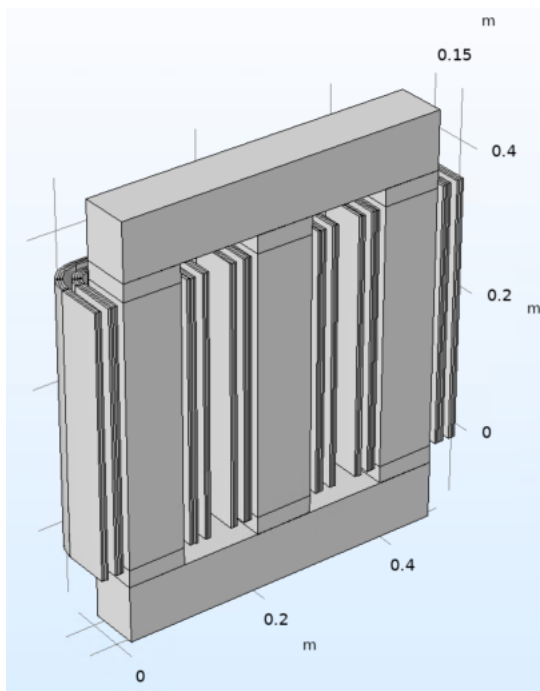


Figure 3.19: The 3D model used to calculate the circulating currents, half section view of the transformer.

It should be noted that Figure 3.19 is a half section view of the transformer. This is done to reduce the computation time and the size of the problem reducing the demands of the computational resources.

3.5.1 The physics

For the physics in COMSOL, Magnetic Fields are chosen. For the surface of the half section view, the boundary condition Magnetic Insulation is chosen. This can be observed in Figure 3.20.

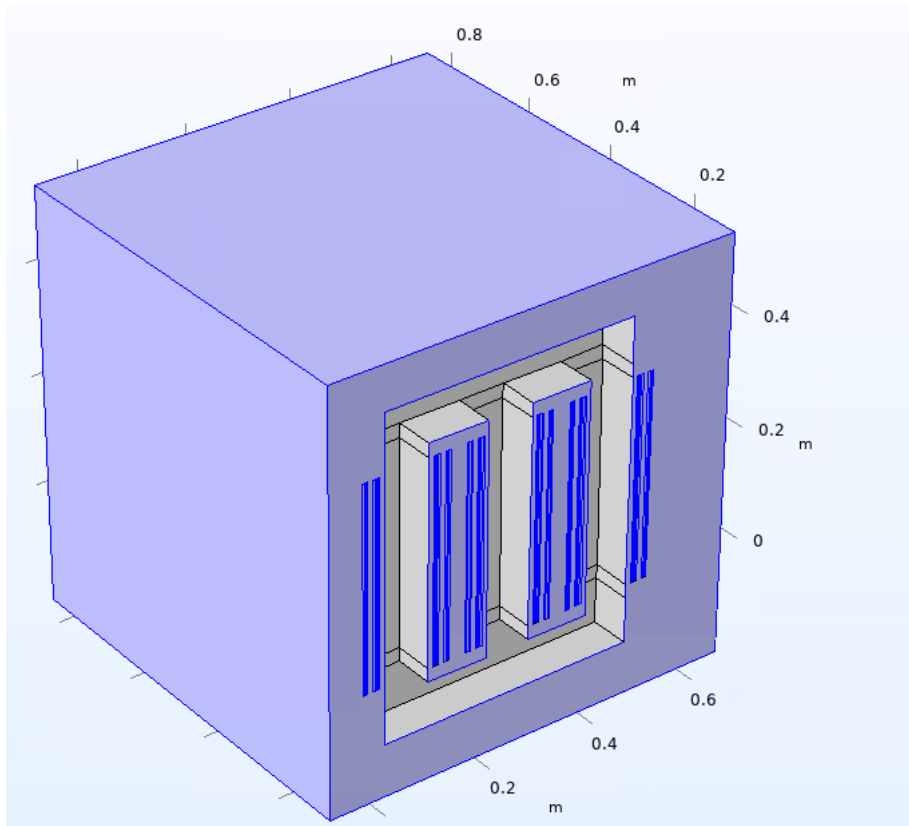


Figure 3.20: The area where Magnetic Insulation is used.

This configuration is done since this boundary represents the plane in which current will flow in the normal direction, which is the case for the windings in this model.

Further, the boundary condition Perfect Magnetic Conductor is chosen. This is set to the boundaries close to the core. This causes the magnetic field to have no tangential component, and to only point in the normal direction. This is done as a simplification, because this is the same as claiming that the iron core in the transformer is ideal, meaning it has infinitely high permeability. In reality this is not so, but since the permeability of iron is so high, it is close enough to use in calculations.

For the windings, the Coil function is elected. The different windings are chosen depending on their phase and whether they are primary or secondary windings. An example of this can be seen in Figure 3.21.



(a) The definition of the inner primary winding using Coil. (b) The definition of the inner secondary winding using Coil.

Figure 3.21: The definition of the windings using Coil.

For the primary windings, as seen in Figure 3.21a, the voltage is set to 0 V since the primary side is short circuited.

For the secondary windings, as seen in Figure 3.21b, the voltage is set to a value such that the nominal current is achieved in the primary winding. Each of the phases have the coil voltage displaced by 120° in respect to one another. For both windings, the coil type Numeric is elected due to the a-typical shape of the windings. Further, Geometry Analysis is added to the coils and the input and the output of the current is elected to help define the direction of the current in the winding. This is illustrated in Figure 3.22 where Geometry Analysis is used on a secondary winding parallel for phase w.

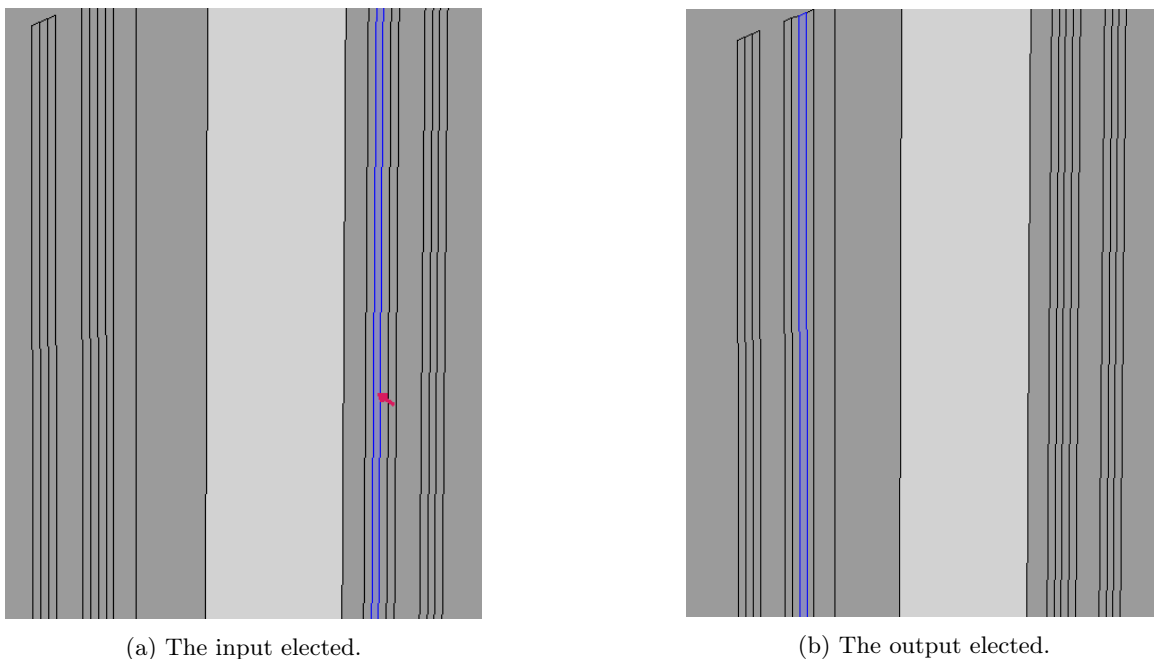


Figure 3.22: The definition of current direction from Geometry Analysis in Coil.

3.5.2 Calculations

To be able to understand the calculations, the numbering system used to label the parallels of the test transformer must be explained. This is presented in Figure 3.23, and describe how the parallels are located compared to the core.

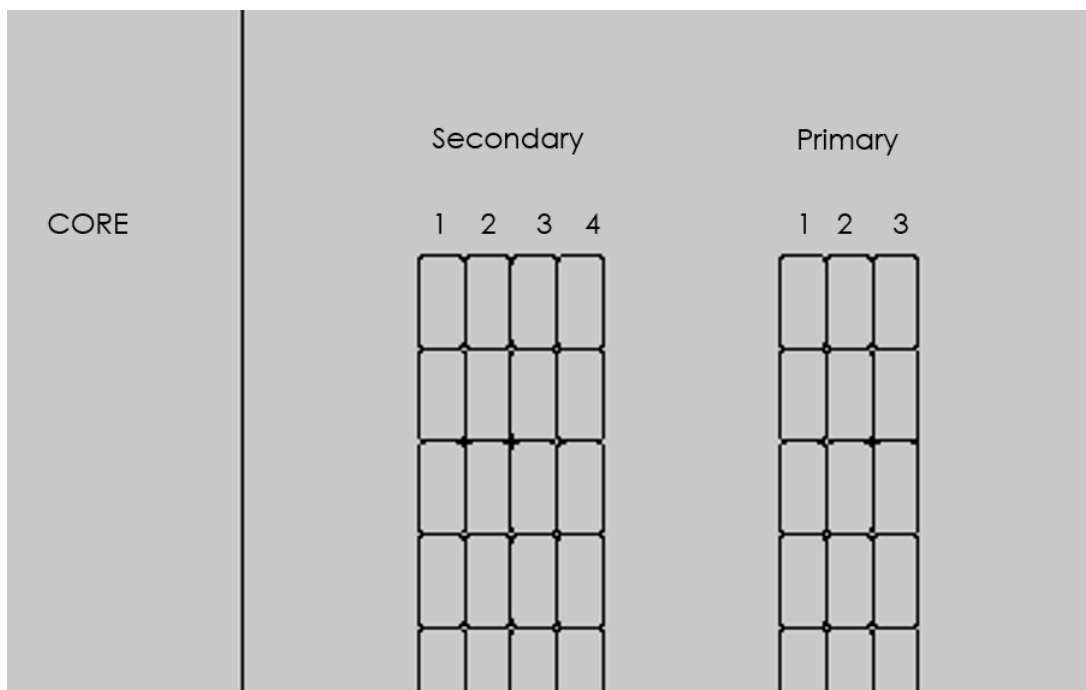


Figure 3.23: The numbering system describing the winding parallels position in regards to the core.

After the study is run, the currents and their phase angles in each coil parallel are found. Then these currents are added in their respective parallel in the 2D models made in the specialization project [10]. These are used to calculate the total losses considering circulating currents.

3.5.3 Measurements of circulating currents

To check the calculations performed using the simulation explained above, measurements of the currents in the parallels conductors are performed. This is done by using the wattmeter and the Fluke I430-Flexi-TF-II Rogowski coils. The parallel conductors close the terminal has one Rogowski coil placed around each of the parallels. This set up can be observed in Figure 3.24.

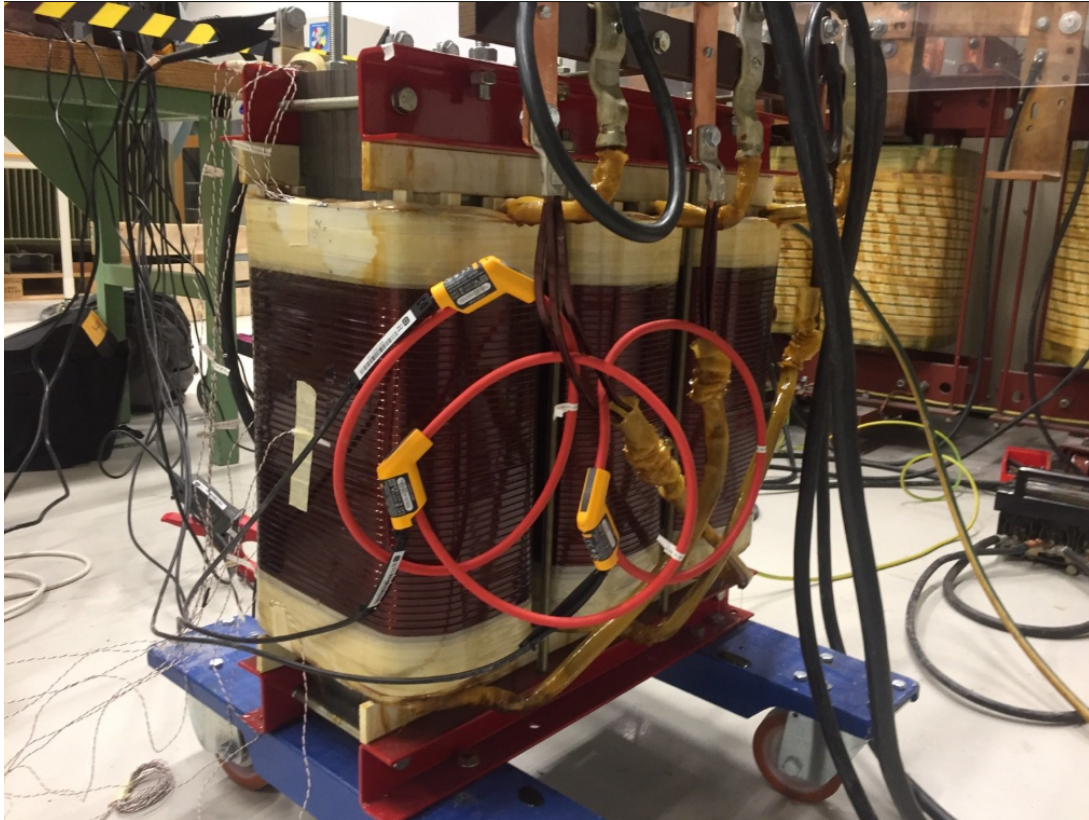


Figure 3.24: The set up for measuring the circulating currents on the primary side.

Rated current is applied during measurement. The currents and the phase angles measured are compared with the values from the simulation. Measurements are only performed in one phase, as it is assumed that this gives sufficient data for comparison with the modelled circulating currents.

3.6 Comparisons for different methods

In this section, the method behind finding the ratio between the magnetodynamic loss calculation method and the semi-analytical loss method is presented. Both methods are performed in the frequency domain. These calculations are based on COMSOL models done in the specialization project[10] and work done in this master thesis. All comparisons are done for a 2D model of the transformer.

3.6.1 Comparisons between magnetodynamic and semi-analytical loss calculation methods

The first comparison investigated is the ratio between the magnetodynamic loss calculation method and the semi-analytical loss calculation method. The ratio is calculated using Equation 3.5. In both cases, circulating currents are taken into consideration.

$$n_{methods} = \frac{P_{AC} - P_{semianalytical}}{P_{semianalytical}} \cdot 100 \quad (3.5)$$

where $n_{methods}$ is the difference between the methods in percent, P_{AC} is the losses found using the magnetodynamic loss calculation method and $P_{semianalytical}$ are the losses found using the semi-analytical loss calculation method.

3.6.2 The influence of circulating currents on calculated losses

Here, the difference between the losses simulated in COMSOL multiphysics when taking into consideration the circulating current and when it is not considered is investigated. The result that does not include circulating currents is found in the specialization project[10]. For the case with the circulating current, this is found by using the current from the 3D COMSOL model, as described in Section 3.5, and applying these in the windings in the 2D COMSOL model created in the specialization project. For this comparison, the currents in the parallels in phase u is used. This is also the case for the comparison of the magnetodynamic and semi-analytical loss calculations method.

To calculate this difference, Equation 3.6 is used.

$$n_{cc} = \frac{P_{wo,cc} - P_{w,cc}}{P_{w,cc}} \cdot 100 \quad (3.6)$$

where n_{cc} is the difference between losses when and when not taking into consideration circulating currents, $P_{wo,cc}$ represents the losses without taking into consideration circulating currents and $P_{w,cc}$ represents the losses taking into consideration the circulating currents. This comparison is done using the semi-analytical loss calculation method.

4 | Results

4.1 Short circuit measurement

In this section, the result from the short circuit heat run test is presented.

The total active power delivered to the test transformer during the short circuit test is presented in Figure 4.1. The x axis shows the time of the day of the measurement while the y axis shows the active power.

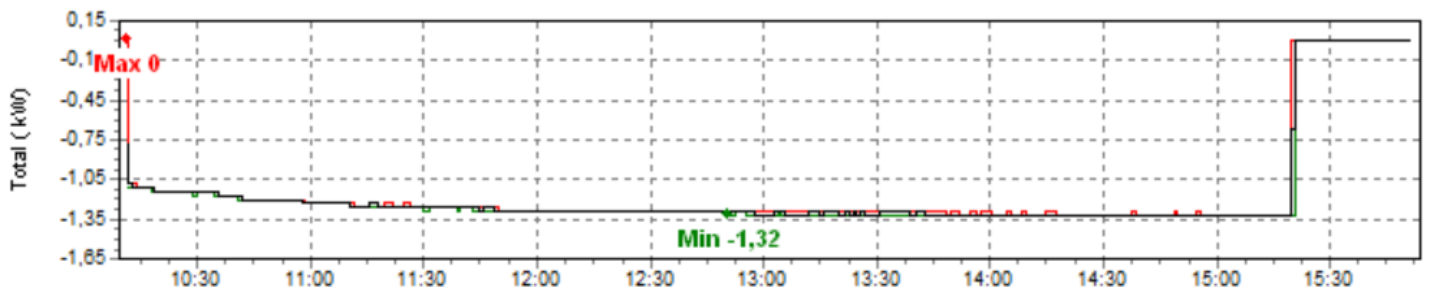


Figure 4.1: The active power to the test transformer [kW].

From the above figure, one can see that the active power delivered over time goes from -1.11 kW to -1.32 kW as the windings are heated up. After reaching -1.32 kW, the active power stabilizes and only changes when the power is turned off at the end of the measurement. Take notice that the negative power means the power is delivered from the energy source transformer to the test transformer.

When to end the test is chosen based on the temperature. The temperature at the thermocouples 109, 110 and 112, as presented in Figure 3.9, are shown in Figure 4.2. These thermocouples are chosen to show the trend of the temperature increase. The x axis is the passage of time in minutes while the y axis is the temperature in °C.

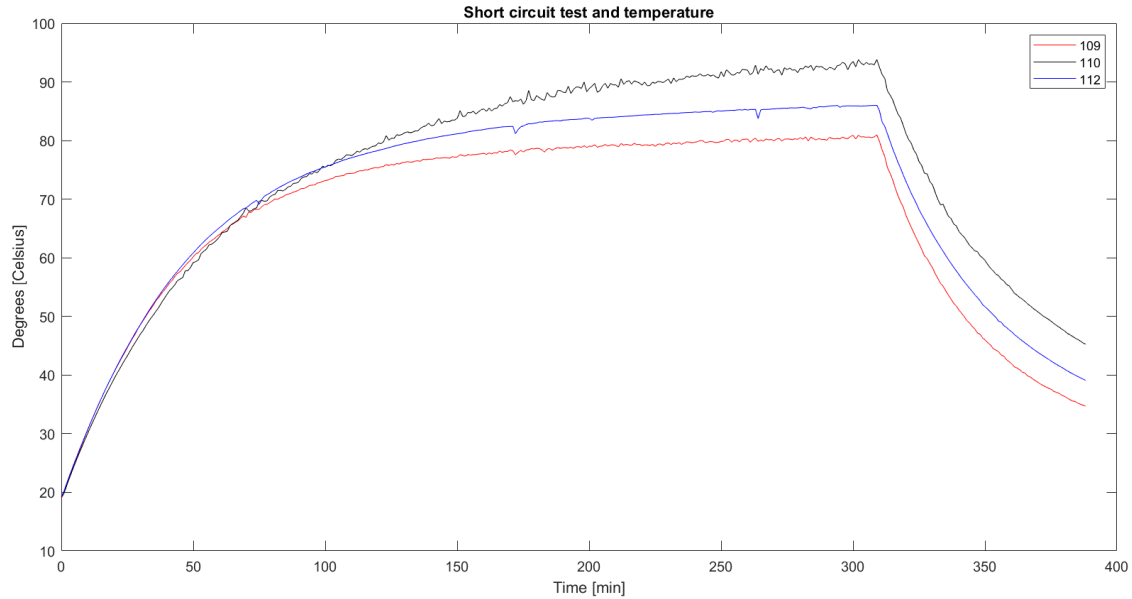


Figure 4.2: The temperature [$^{\circ}\text{C}$] registered at three different points during short circuit heat run test.

In Figure 4.2, one can observe that after about 120 minutes, the temperature increase is reduced, though not eliminated. There is still a slight increase in temperature up the end of the experiment. From 122 minutes to 309 minutes, there is a increase of 7 % in the temperature. When the active power is turned off at 309 minutes, the temperature decreases quickly. The rest of the temperature measurements are found in Section A of the appendix.

4.2 Circulating currents

In this section, the result having to do with the correction of the losses due to the circulating currents are presented.

4.2.1 The currents modelled in COMSOL multiphysics

Here, the currents in each parallel are presented, for both secondary and primary windings, both amplitude and phase angle with corresponding phasor plots. Lastly, the calculated average absolute currents for each phase is calculated.

Absolute value of the current

In Table 4.1, the absolute rms values of the current in the windings are presented. The currents in each parallel is presented together with their phases. Results for both secondary and primary windings are shown.

Table 4.1: The absolute rms value of the currents in the different parallels.

Absolute rms value of current [A]							
	Secondary				Primary		
Parallel	1	2	3	4	1	2	3
Phase u	28.8	28.3	30.3	37.1	43.1	38.3	36.8
Phase v	28.7	28.2	30.2	37.0	43.2	38.3	36.7
Phase w	28.8	28.3	30.3	37.1	43.2	38.3	36.6

The absolute value for the currents in the primary windings are similar to each other, likewise for the currents in the secondary windings. The largest currents are situated in the parallels close to the leakage channel. This occurs for all

the phases. The currents get smaller the further from the leakage channel the parallels are, with the exception being parallel 1 and 2 in the secondary winding, with parallel 2 being slightly smaller than parallel 1.

The phase angle of the current

The phase angles, both for the secondary and the primary winding is presented in Table 4.2. This done for each phase and all of the parallels.

Table 4.2: The phase angles of the current in the different parallels.

Phase angle of the current [°]							
	Secondary				Primary		
Parallel	1	2	3	4	1	2	3
Phase u	32.4	43.6	65.2	89.3	-103	-125	-135
Phase v	-87.7	-76.4	-54.7	-30.7	136	116	105
Phase w	152	163	-175	-150	16.5	-4.1	-15.0

From the above table, one can observe large variation between the angles, for both primary and secondary winding. There is also variation between each phase and between each parallel. These variations in phase angle and the absolute rms value of the currents are demonstrated as vectors in the Figures 4.3 and 4.4. The longest vectors in each phase represent the total current in that phase.

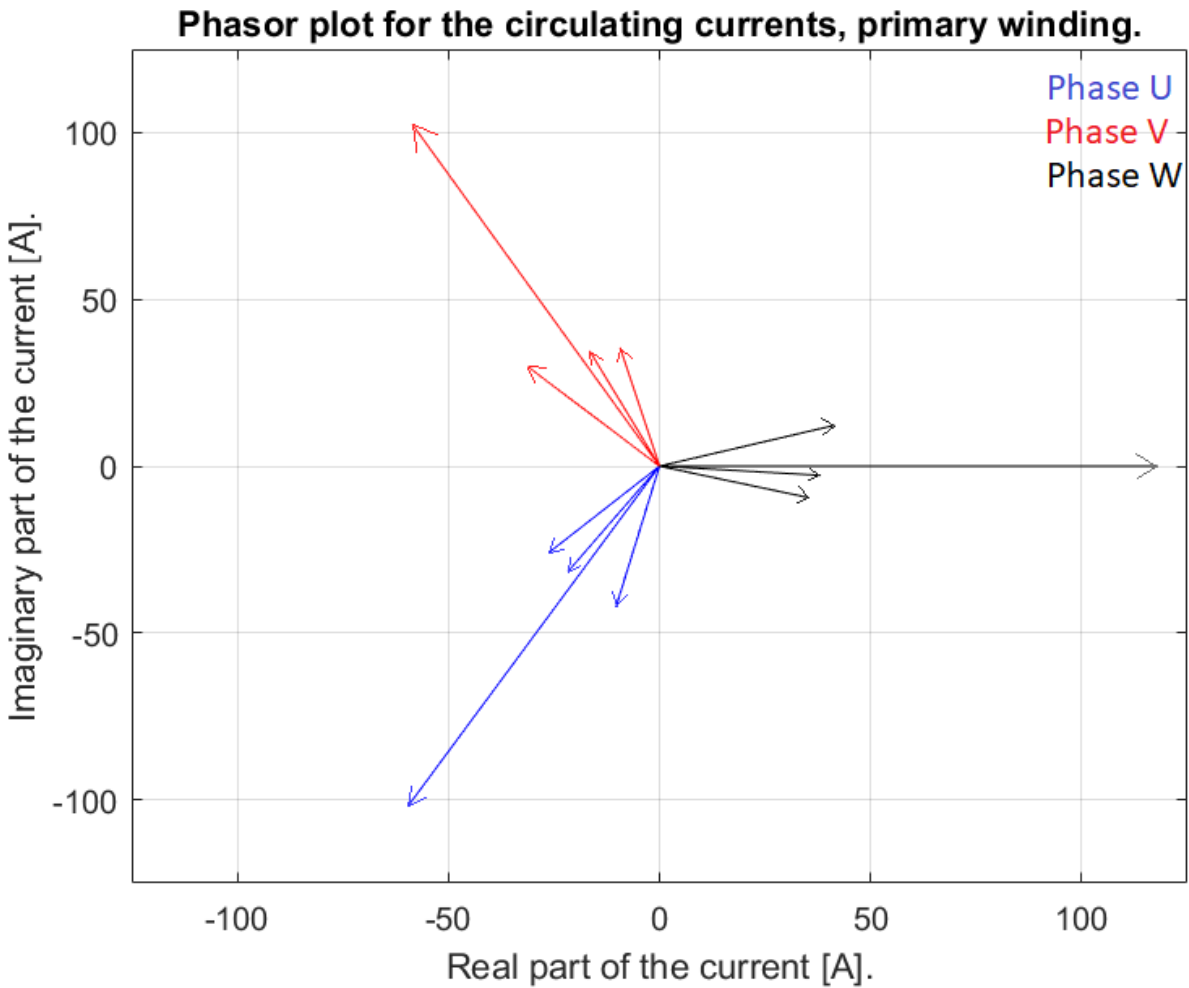


Figure 4.3: The phasor plot for the circulating currents in the primary winding.

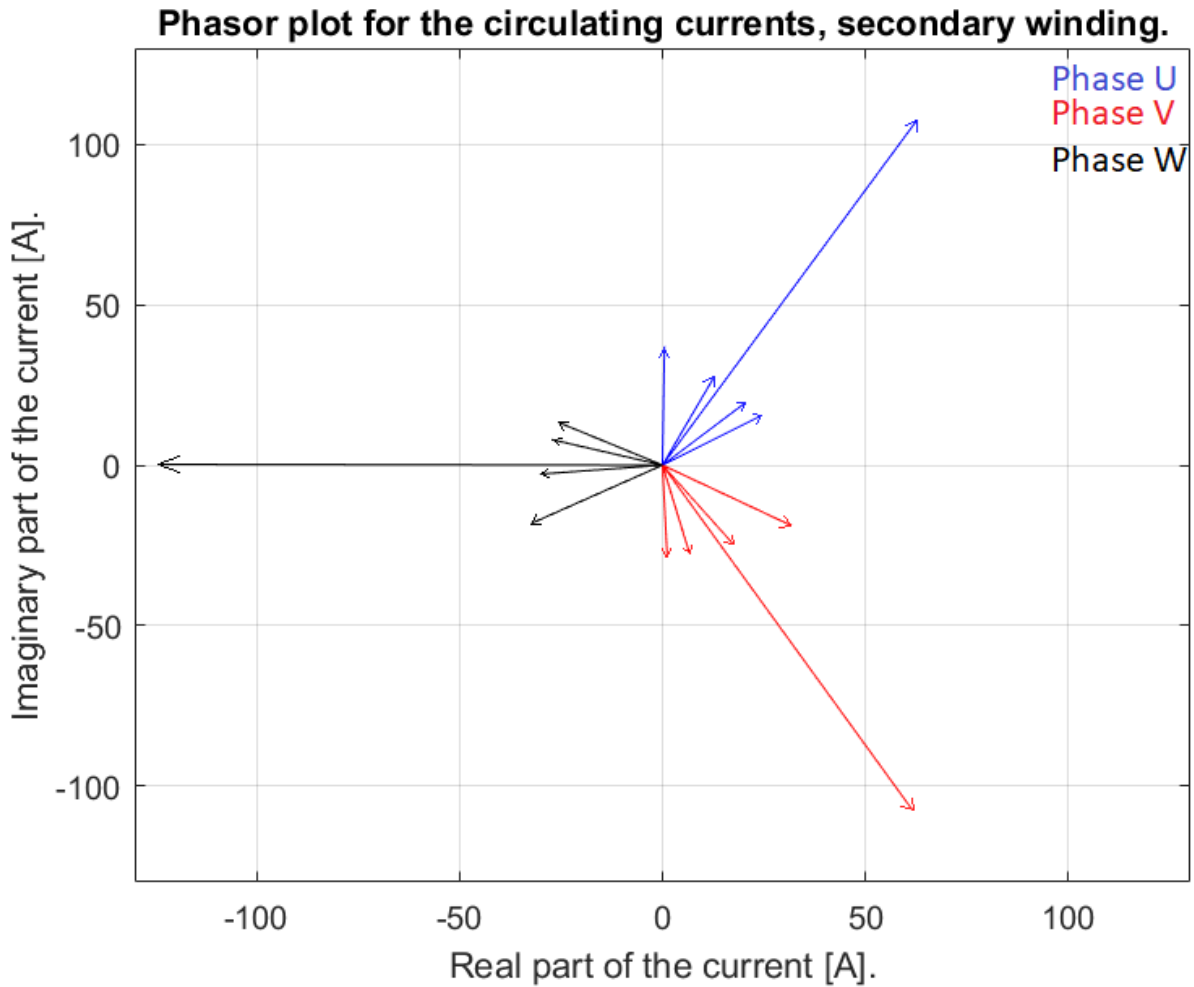


Figure 4.4: The phasor plot for the circulating currents in the secondary winding.

The average value of the current

In the table below, the calculated average absolute values for the different phases are presented in Table 4.3. It presents the average absolute values for the current in both the secondary and the primary windings.

Table 4.3: The average rms absolute value for the currents in the secondary and primary windings [A].

The average rms absolute current [A]		
	secondary	Primary
Phase u	28.8	38.4
Phase v	28.7	38.4
Phase w	28.8	38.4

For both the windings, the average rms current for the different phases are quite similar.

4.2.2 The measurement of the circulating current

In this section, the losses measured in phase u of the transformer on the primary side is presented. The absolute value and the phase angle of the current is presented in Table 4.4.

Table 4.4: The measured current and phase angle of phase u on the primary side.

Data from measurement of the circulating current			
Parallels	1	2	3
Absolute value of current [A]	42.7	37.3	36.9
Phase angle of the current[°]	75	56	47

Comparing the result in Tables 4.1 and 4.4, one can observe that the absolute values are quite similar.

4.2.3 Losses corrected for circulating currents

In this section, the losses calculated using the result from Section 4.2.1 are presented. The losses in each of the phases are presented together with the total losses in Table 4.5.

Table 4.5: The corrected losses in the test transformer[W].

The losses after correction for circulating currents [W]	
Loss, phase u	310.9
Loss, phase v	310.1
Loss, phase w	310.7
Total loss	931.7

The losses presented in Table 4.5 are quite similar in each phase, with the losses in phase v being marginally smaller.

4.3 Resistance measurement

In this section, the result from the resistance measuring is presented.

4.3.1 Before heat run test

Here, the resistances measured before the heat run test are presented. This is done for both the primary and secondary winding.

The measurements are performed with 10 A applied. The resistance in both the secondary and primary winding is presented in Table 4.6. The results for the different phases is included in this table.

Table 4.6: The measured resistance in the windings before the heat run test.

	Secondary	Primary
u [$m\Omega$]	8.47	14.3
v [$m\Omega$]	8.44	14.2
w [$m\Omega$]	8.47	14.2
Average [$m\Omega$]	8.46	14.2

From the above table, one can see that the resistance in the different phases are quite similar. The resistance is larger in the primary winding compared to the secondary.

In Table 4.7, various data used in calculations and comparisons are presented. The % difference is the difference between the measured and the calculated resistance of the windings. The resistivity and resistance calculated are found using the method presented in Section 3.4.1.

Table 4.7: The calculated and measured data from before the heat run test.

	Secondary	Primary
Temperature measured [$^{\circ}\text{C}$]	19.03	19.03
Resistivity calculated [$\Omega \cdot m$]	$1.71 \cdot 10^{-8}$	$1.71 \cdot 10^{-8}$
Resistance calculated [Ω]	0.00786	0.0131
Average resistance measured [Ω]	0.00846	0.00142
% difference	7.65	8.22

The measured resistance is larger than the calculated resistance. The difference is larger in percent for the primary winding than for the secondary winding, but not by a large margin.

4.3.2 After heat run test

In this section, the result from the resistance measurement after the heat run test is presented, both for secondary and primary windings. It should be noted that the measurements on the different phases happens at different times after disconnecting the current, making them occur at different temperatures in the windings.

In Table 4.8, the result of the resistance measurement after reaching a steady temperature is measured. The table presents the resistances in both windings and in all the phases. The various times the measurement was done after disconnecting the applied current from the primary side is also shown.

Table 4.8: The measured resistance in the windings after the heat run test.

	Secondary		Primary	
	Resistance after 4 min	Resistance after 6 min	Resistance after 2 min	Resistance after 6 min
u [$m\Omega$]	10.41	10.33	17.52	17.4
v [$m\Omega$]	10.56			17.5
w [$m\Omega$]		10.36	17.47	
Average [$m\Omega$]	10.5	10.4	17.5	17.5

From Table 4.8, as with Table 4.6, one can observe that the resistance in the windings are still larger in the primary windings. In both windings, it is clear that the resistance is reduced in the second measurement. It should be noted that the measurement in phase v is the largest of the phases in both secondary and primary winding.

When performing calculations, the average value of the resistances for the secondary and primary winding is used. The method of these calculations are found in Section 3.4.1. The result is presented in Table 4.9.

Table 4.9: The resistivity and average temperature in the windings after the heat run test.

	Secondary	Primary
Resistivity [$\Omega \cdot m$]	$2.11 \cdot 10^{-8}$	$2.105 \cdot 10^{-8}$
Average temperature [$^{\circ}\text{C}$]	77.7	76.9

As can be observed in the above table, the resistivity is slightly higher in the secondary winding compared with the primary winding. The average temperature of the windings is also higher in the secondary winding.

In Figure 4.5, the temperature of the thermocouple 115, which is placed at the middle of the primary winding as seen in figure 3.8b, is presented. The x-axis represent time in minutes while the y-axis represent temperature in $^{\circ}\text{C}$.

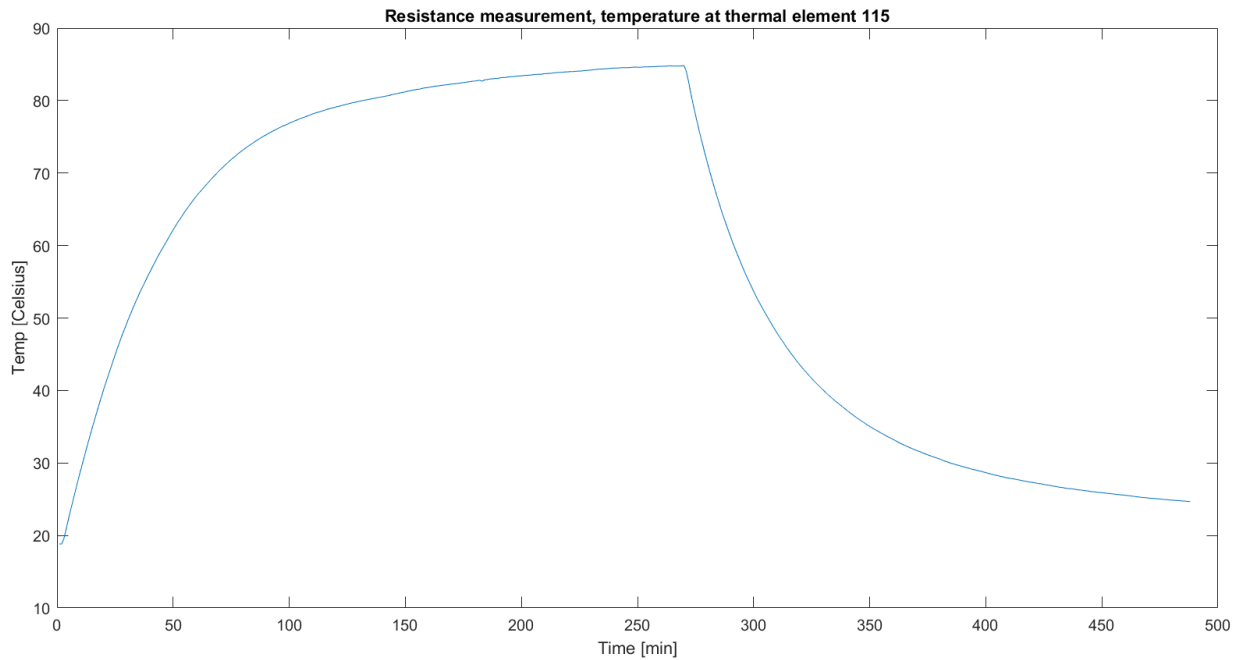


Figure 4.5: The temperature [$^{\circ}\text{C}$] measured by thermocouple 115 during heat run test.

From studying the temperature plot in Figure 4.5, it becomes clear that the temperature registered in thermocouple 115 is 78.5°C 4 minutes after the current is shut off. The rest of the temperature plots for the resistance measurement is presented in Section B in the appendix.

4.4 Temperature measurement

In this section, the results from the temperature measurements are presented. All of the results are presented for the thermocouple 110, which is placed as seen in Figure 3.13a. The rest of the measurements are presented in Section C.2 in the appendix. First the result from the linear regression analyses is presented for the currents shown in Table 3.3, then comparisons between the measurements at the different currents are displayed. Lastly, comparisons between the losses measured and simulated are made.

4.4.1 The linear regression analyses

In this section, the comparisons between the temperature measurements and the linear regression analyses performed are presented. The method behind these analyses are presented in Section 3.3.1.

Half nominal current

In Figure 4.6, the comparison between the temperature measured by thermocouple 110 and the linear regression analysis based on measured data is made. This measurement presented in Figure 4.6 was performed with half the nominal current. The red plot shows the actual temperature while the blue plot shows the line formed using the linear regression analysis.

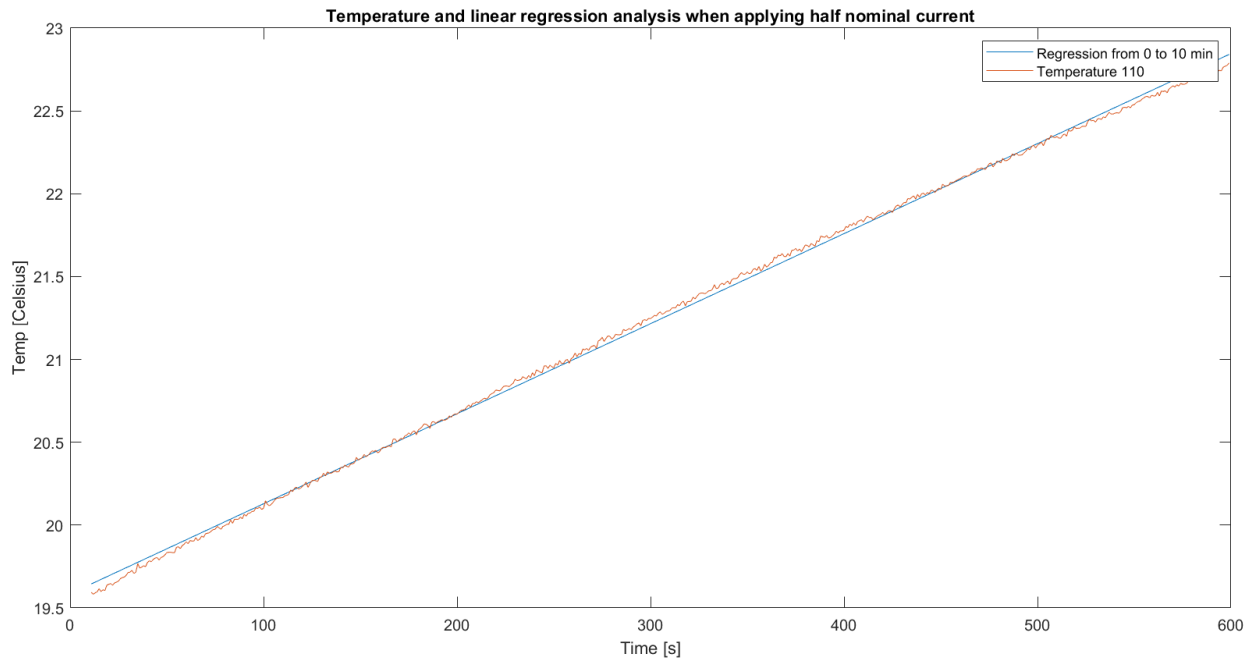


Figure 4.6: The temperature [°C] and the linear regression analysis for thermocouple 110, from 0 to 10 minutes, when applying half nominal current.

One can observe from the above figure that the two lines matches well. There is a rather small temperature increase when applying half the nominal current. The line from the regression analysis can be described as done in Equation 4.1.

$$y = 0.00544 \cdot x + 19.6 \quad (4.1)$$

where y represent the temperature and x is time in seconds. From the above equation, it becomes clear that the gradient is quite small, only $0.00544 \text{ }^\circ\text{C}$ per second.

A comparison between the linear regression analysis done from 0 to 10 minutes and from 1 to 2 minutes is presented in Figure 4.7. The yellow plot is the gradient suggested for from 0 to 10 minutes, the red plot is the gradient suggested from 1 to 2 minutes and the blue, dashed plot is the actual temperature measured in this time interval. The average current supplied in this time interval is 58.5 A.

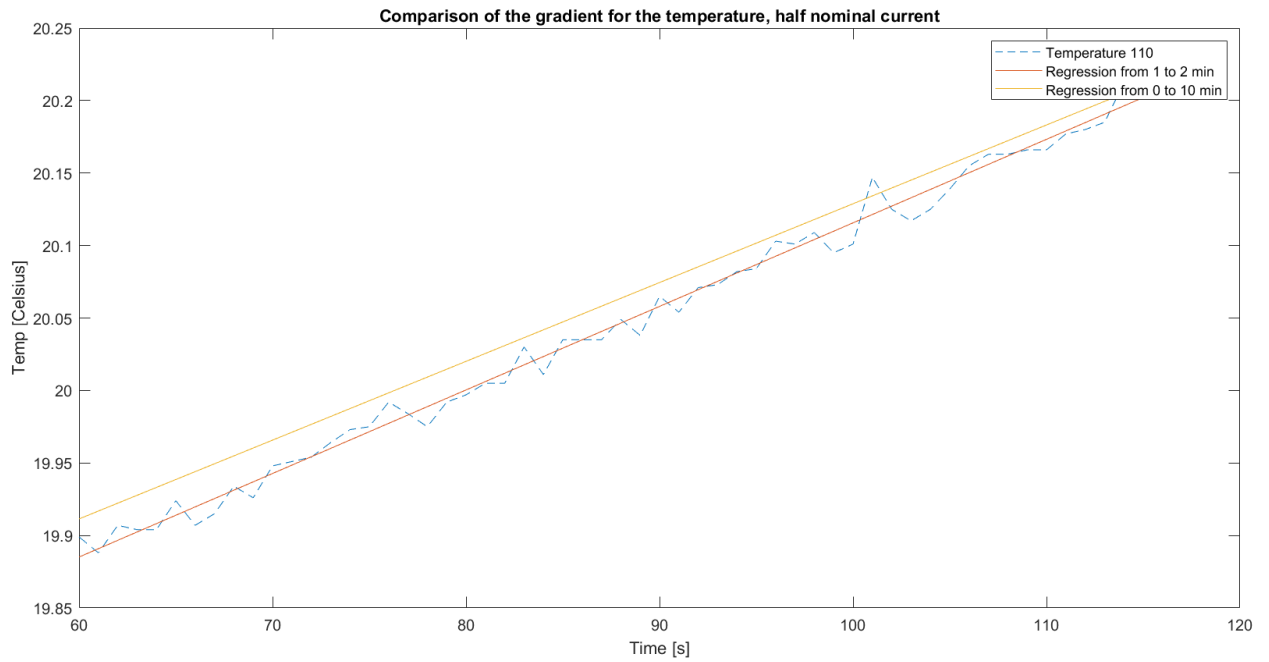


Figure 4.7: The temperature [°C] and the linear regression analysis for thermocouple 110, from 0 to 10 minutes and from 1 to 2 minutes, half nominal current.

From Figure 4.7, it can be perceived that the plot for the linear regression analysis from 1 to 2 minutes matches the temperature measurement better than the plot for 0 to 10 minutes. It should be noted there is some noise on the measurement of the temperature. The line from the regression analysis done from 1 to 2 minutes can be described as done in Equation 4.2.

$$y = 0.00576 \cdot x + 19.5 \quad (4.2)$$

The rest of the gradients and the temperature measurements for half of the nominal current can be found in Section C.2.1 in the appendix.

Nominal current

For nominal current, two measurements were performed, named alpha and beta measurement. They are found in this section. The average room temperature when performing the alpha and beta measurement were 19.0 C and 20.3 C respectively.

In Figure 4.8, the comparison between the temperature measured by thermocouple 110 and the linear regression analysis based on the measured data is made. The blue and yellow dashed lines show the actual temperatures in the beta and alpha measurements respectively, while the red and purple lines show the plots formed using the linear regression analysis for the beta and alpha measurements, respectively.

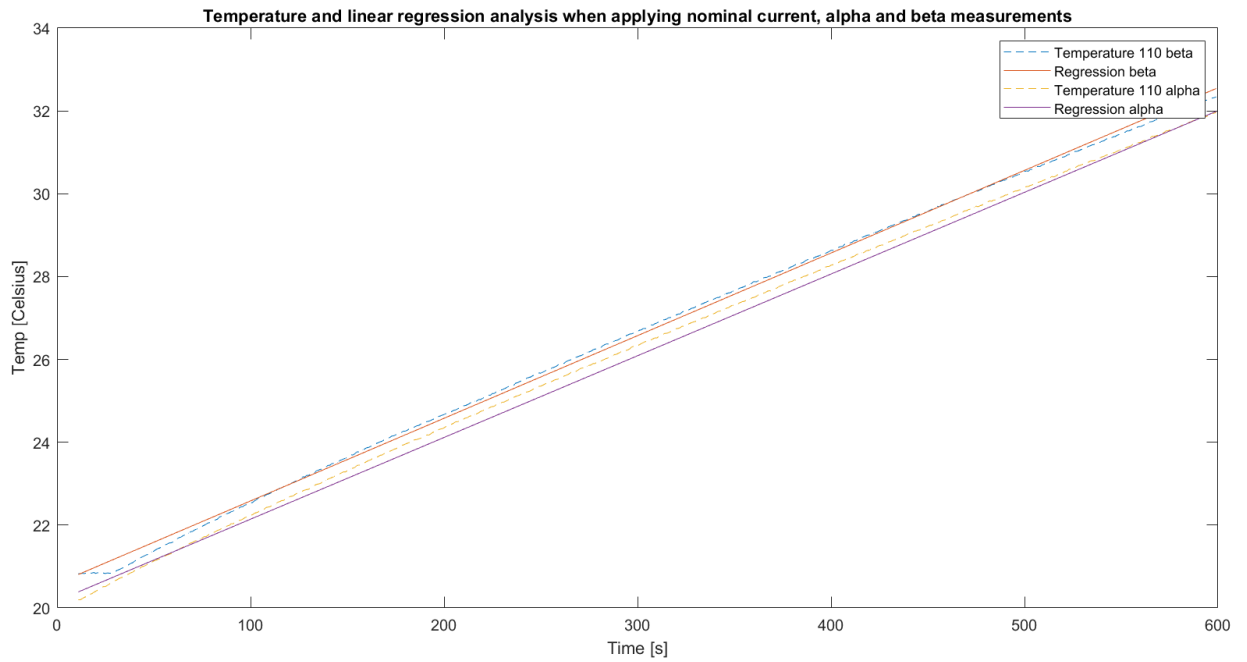


Figure 4.8: The temperature [°C] and the linear regression analysis for thermocouple 110, alpha and beta measurements.

One can observe from the above figure that the two lines match fairly well. The line from the regression analysis for the alpha and beta measurement can be described as done in equations 4.3 and 4.4 respectively.

$$y_{alpha} = 0.0197 \cdot x + 20.2 \quad (4.3)$$

$$y_{beta} = 0.0200 \cdot x + 20.6 \quad (4.4)$$

where y represent the temperature and x is time in seconds.

In Figures 4.9 and 4.10, comparisons between the linear regression analysis done from 0 to 10 minutes and from 1 to 2 minutes are presented.

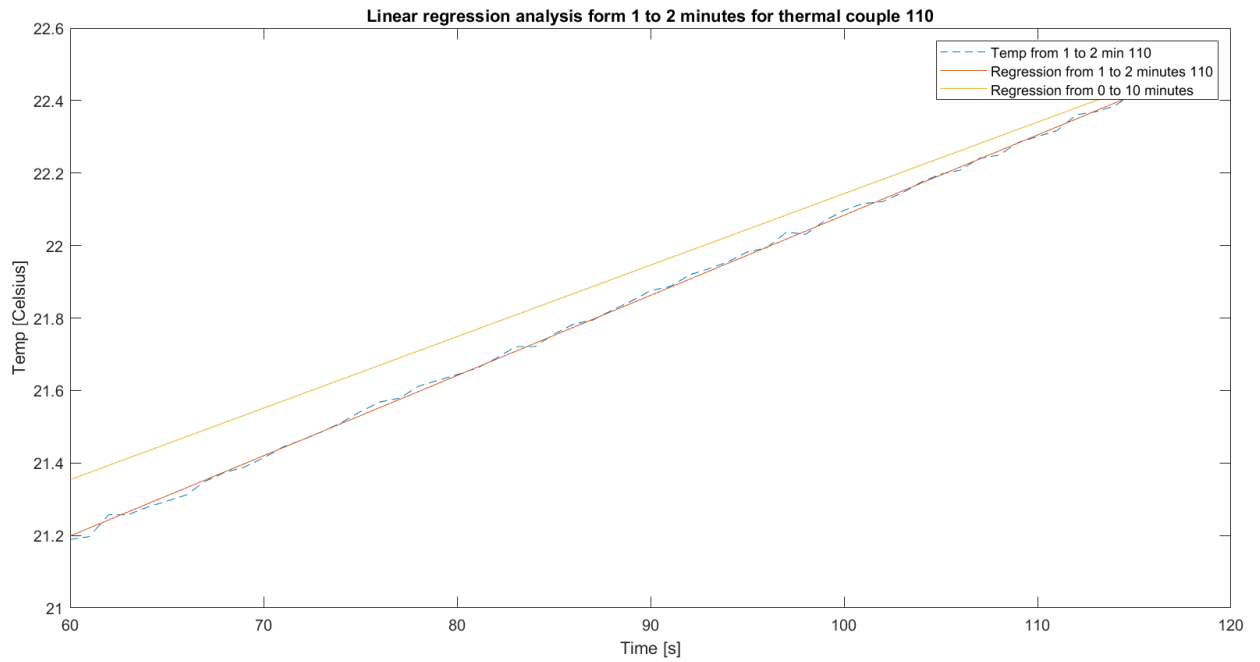


Figure 4.9: The temperature [°C] and the linear regression analysis for thermocouple 110, comparing from 0 to 10 minutes and from 1 to 2 minutes, alpha measurement.

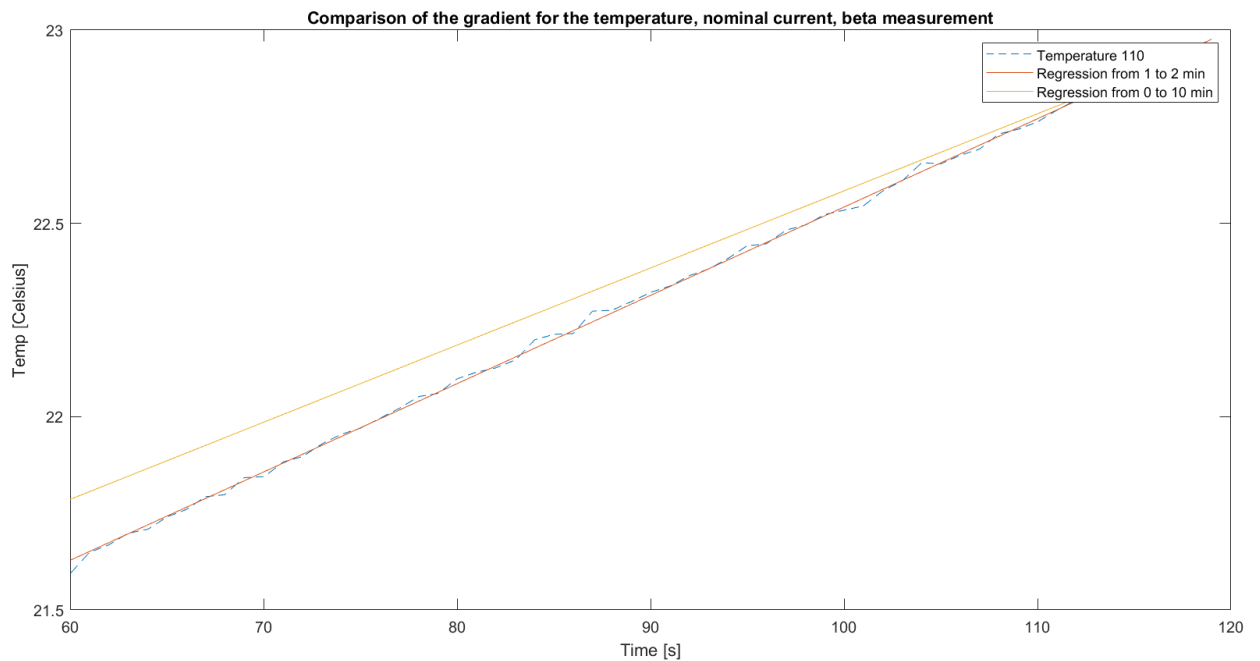


Figure 4.10: The temperature [°C] and the linear regression analysis for thermocouple 110, comparing from 0 to 10 minutes and from 1 to 2 minutes, beta measurement.

From figures 4.9 and 4.10, one can observe that the linear regression analysis done using data points from 1 to 2 minutes matches better with the measured temperature compared with the linear regression analysis from 0 to 10 minutes. The gradient is very similar for both measurements, but the beta measurements starts at a higher temperature at the 1 minute mark. The plots from the regression analysis done from 1 to 2 minutes can be described as done in equations 4.5 and 4.6.

$$y_{alpha} = 0.0221 \cdot x + 19.9 \quad (4.5)$$

$$y_{beta} = 0.0228 \cdot x + 20.3 \quad (4.6)$$

The rest of the temperature measurements done with their respective linear regression analyses at nominal current is presented in Section C.2.2.

Twice nominal current

In Figure 4.11, the comparison between the temperature measured by thermocouple 110 and the linear regression analysis based on the measured data is made. This figure presents the result for twice nominal current. The red plot shows the actual temperature while the blue plot shows the line formed using the linear regression analysis.

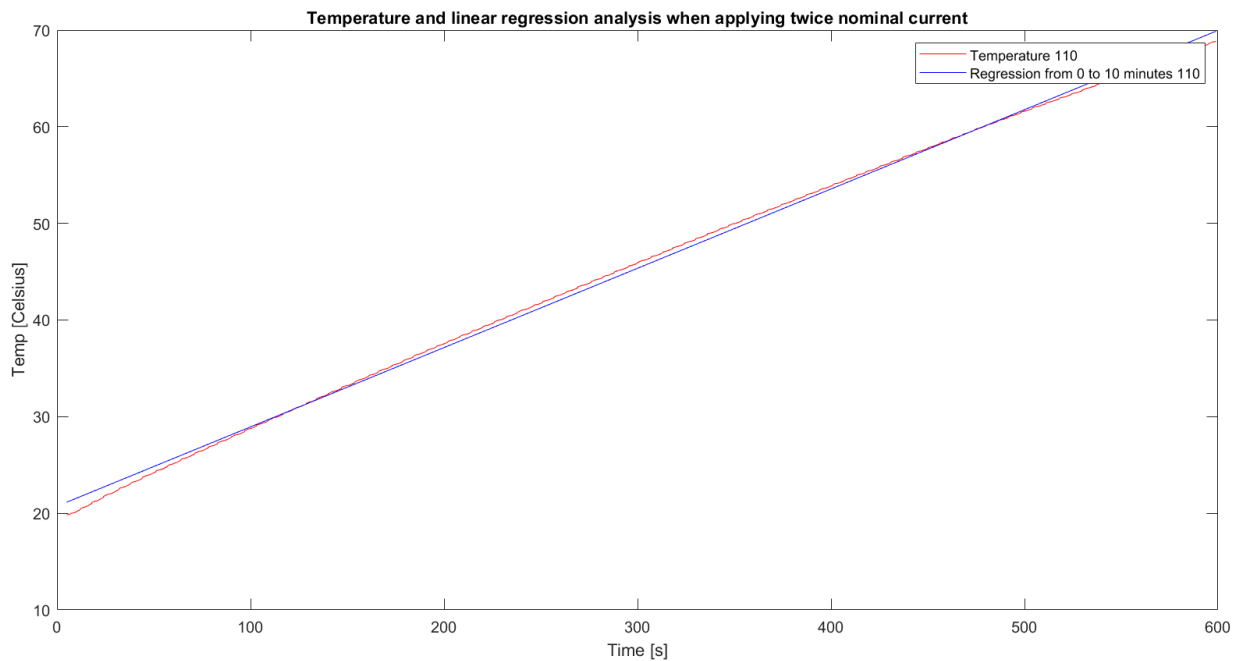


Figure 4.11: The temperature [°C] and the linear regression analysis for thermocouple 110, from 0 to 10 minutes, when applying twice nominal current.

One can observe from the above figure that the two lines match fairly well. It should be noted that the temperature increase is quite large, as it reaches almost 68 °C within 10 minutes. The line from the regression analysis can be described as done in Equation 4.7.

$$y = 0.0821 \cdot x + 20.7 \quad (4.7)$$

As done with half and full nominal current, a comparison between the linear regression analysis done from 0 to 10 minutes and from 1 to 2 minutes is performed. The current applied in this time interval is presented in Figure 4.12. It shows the current dropping from 232 A to 231 A within a minute.

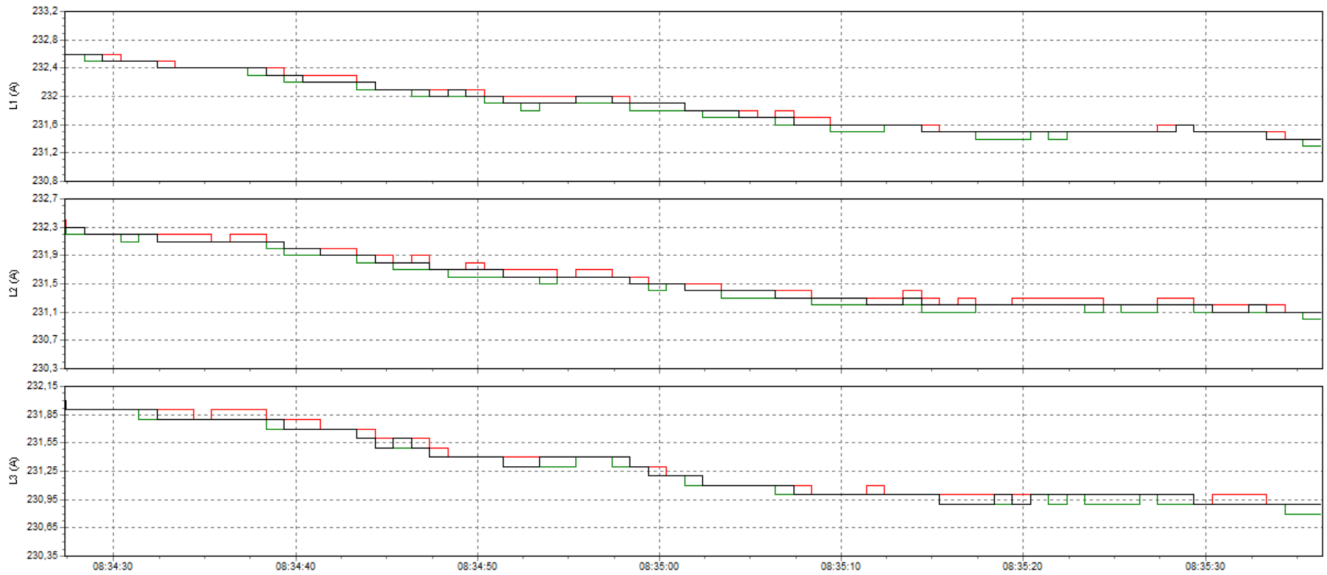


Figure 4.12: The current [A] delivered to the test transformer in the time interval 1 to 2 minutes.

The comparison between the linear regression analysis done from 0 to 10 minutes and from 1 to 2 minutes is shown in Figure 4.13.

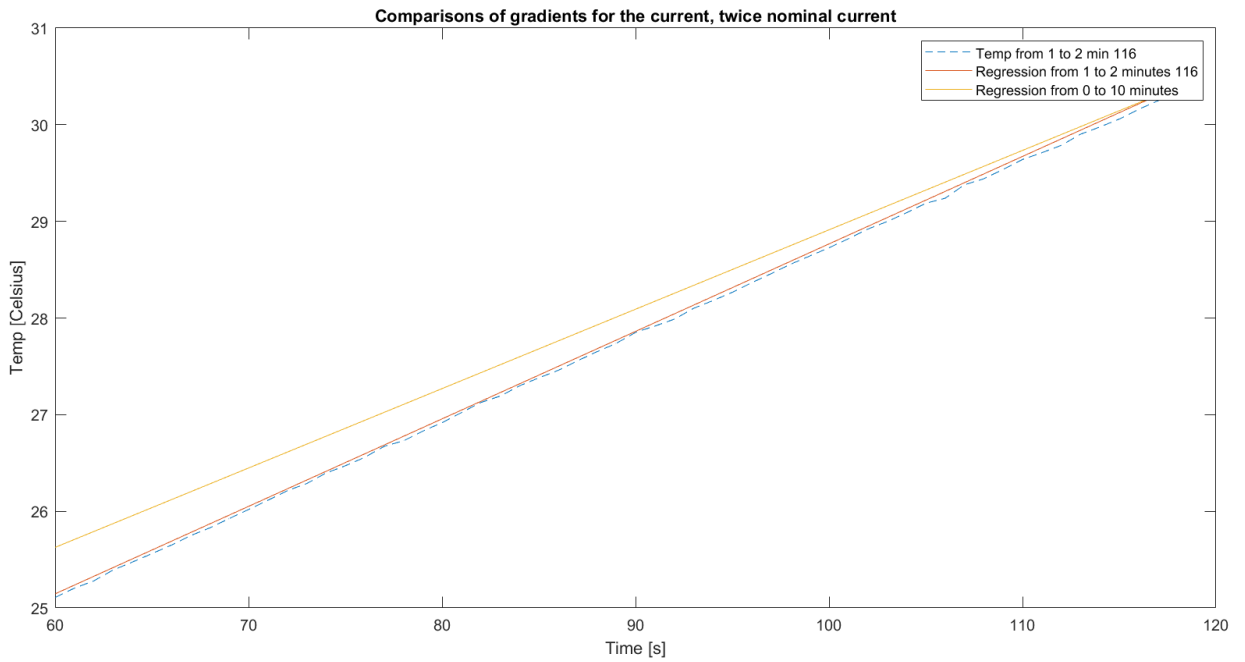


Figure 4.13: The temperature [°C] and the linear regression analysis for thermocouple 110, comparing from 0 to 10 minutes and from 1 to 2 minutes, twice nominal current.

As observed previously with currents at nominal and half nominal current, the plot from the linear regression analysis from 1 to 2 minutes is closer to the temperature measured in this time interval than the plot from 0 to 10 minutes. The temperature measurement is much closer to the plot suggested compared with what was observed in Figure 4.7 for half the nominal current. The line from the regression analysis done from 1 to 2 minutes can be described as done in Equation 4.8.

$$y = 0.0910 \cdot x + 19.7 \quad (4.8)$$

The rest of the gradients and the temperatures for the measurements done at twice nominal current can be observed in Section C.2.3 in the appendix.

4.4.2 Comparisons between the temperature measurements

To further illustrate the differences in the temperature measurements performed at different currents, there will be comparisons in this section. All comparisons are within the time interval 1 to 2 minutes. For the measurement at nominal current, the alpha measurement is presented.

First, a comparison between all three temperature measurements at the three currents is presented. It can be seen in Figure 4.14. The yellow plot is for twice the nominal current, the red plot is for the nominal current and the blue plot is for half the nominal plot.

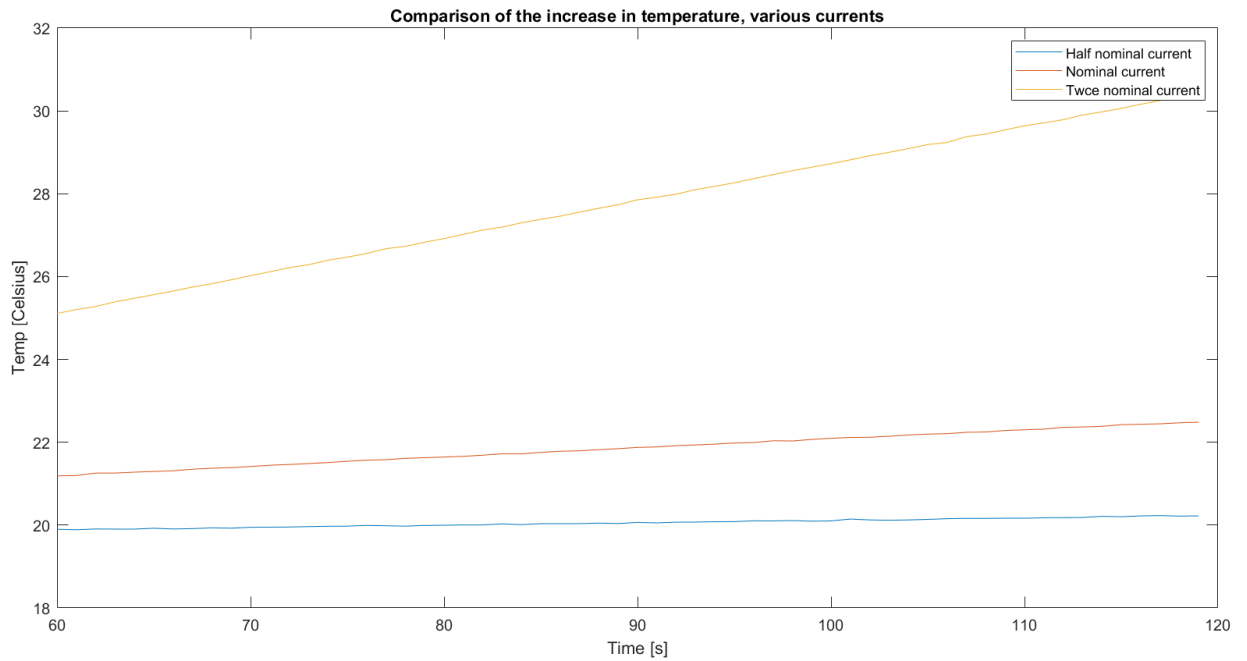


Figure 4.14: The temperature [°C] measured at different currents applied.

From the above figure, it becomes clear that the increase in temperature is largest for the measurements done at twice the nominal current. It is so much larger that the temperature increases of the other plot is hard to observe.

To better illustrate the difference in temperature increase between nominal current and half nominal current, Figure 4.15 is presented. It presents the temperature increase at when these currents are applied. The colours of the plots correspond with the colours of the plots in Figure 4.14.

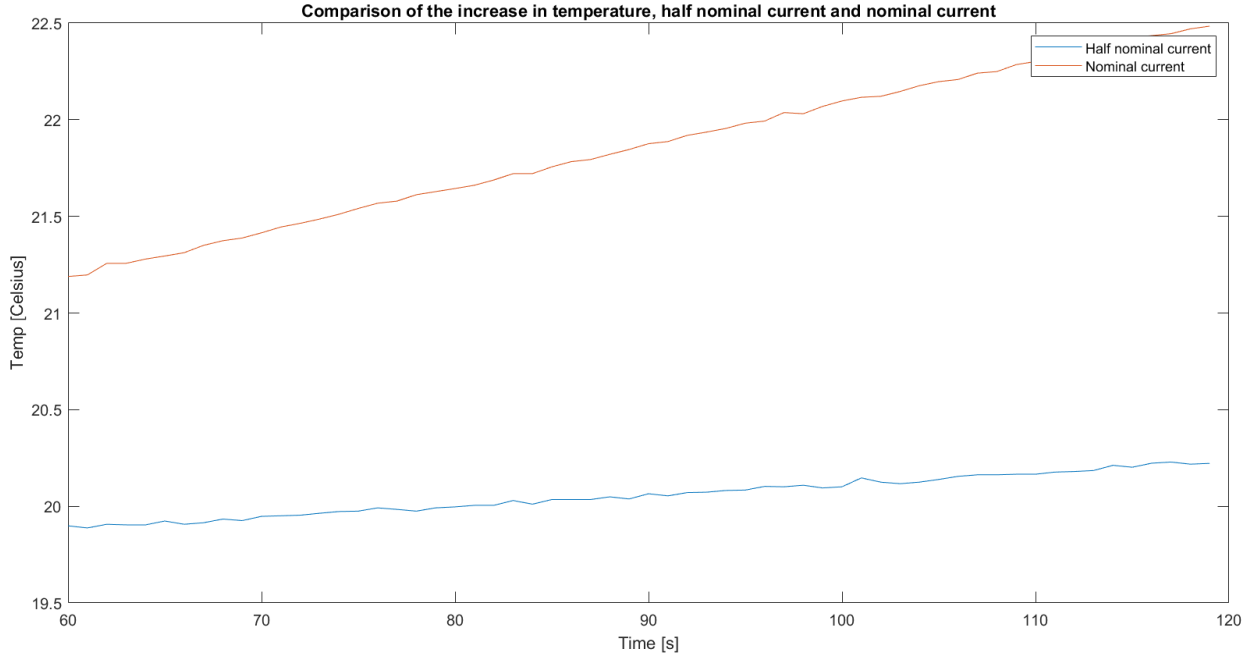


Figure 4.15: The temperature [$^{\circ}\text{C}$] measured at half and nominal current.

By observing the above figure, it becomes clear that the temperature increase when applying the nominal current is substantially larger than when half the nominal current is applied. The increase in temperature at half of the nominal current is quite small within this time interval.

4.4.3 Losses and comparisons of losses

In this section, the losses calculated from the temperature measurement is presented together and compared with the simulated losses using COMSOL. The major trends of the thermocouples are also presented in histograms in this section. The placements of the thermocouples are presented in Figures 3.12 and 3.13. The measured losses are found using the method described in Section 3.3.1.

Half the nominal current

The losses, both from measurements and from COMSOL simulations are presented in Table 4.10. In the same table, the difference between these 2 values are presented in percent. They are for the losses at half the nominal current.

Table 4.10: The losses [W/m] calculated from the temperature measured using half the nominal current.

Thermocouple	107	108	109	110	111	112	113	114	115	116
From measurements [W/m]	0.354	0.322	0.357	0.357	0.348	0.368	0.364	0.390	0.369	0.357
From simulations [W/m]	0.330	0.458	0.361	0.458	0.330	0.458	0.458	0.328	0.328	0.361
Difference in %	7.18	-29.7	-1.09	-22.0	5.38	-19.6	-20.5	18.9	12.4	-1.08

From the above table, one can observe that the difference between the measured and simulated loss varies on which parallel the thermocouple is placed. For the thermocouples 116 and 109 placed at parallel 2 in the primary winding, the difference is quite small, being at around 1 %. The thermocouples 112, 110 and 113 placed at parallel 1 have one of the largest differences, at around 20 %. In parallel 3, for the uppermost turns, the difference is between 7 and 5 % for the thermocouples 107 and 111. For thermocouples 114 and 115, which are placed around turn number 30, the difference varies between 12.4% and 18.9 %. The largest difference is measured by thermocouple 108. These trends are summed up in Figure 4.16.

Trends in thermocouples at half of nominal current

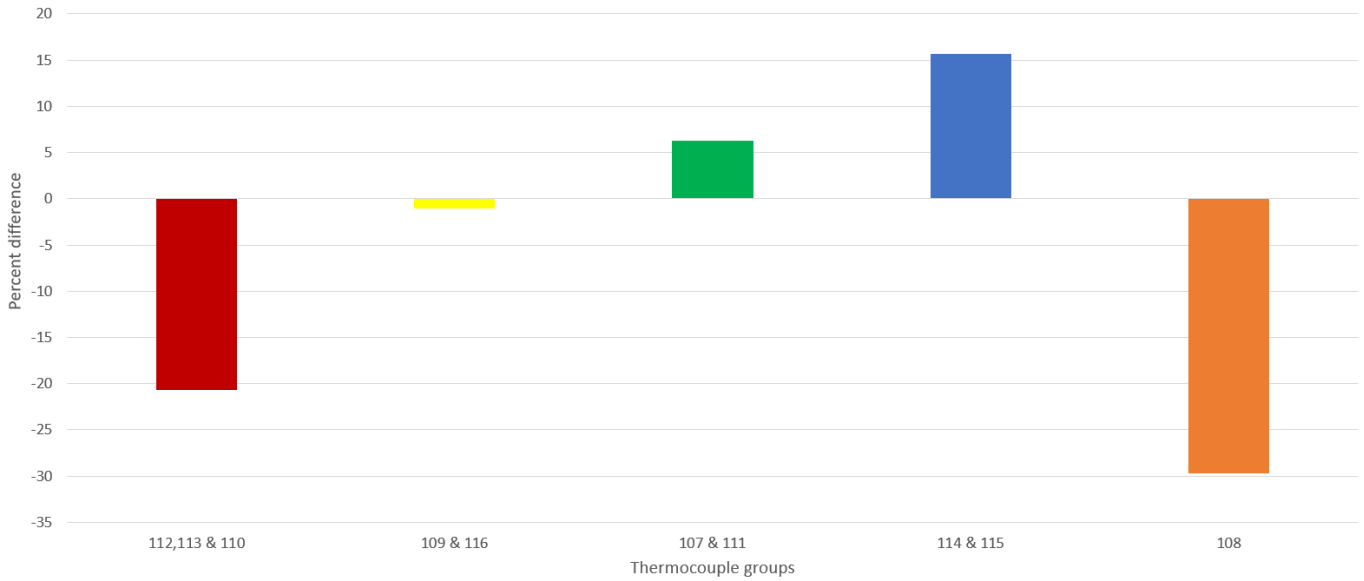


Figure 4.16: The major trend of the differences found in thermocouples, half the nominal current.

The gradients used to calculate the measured power loss are found in Equation 4.2 and Section C.2.1 in the appendix.

Nominal current

In Tables 4.11 and 4.12, the losses calculated from the temperature measured is presented with the thermocouple where the temperature measurement was registered. The difference between these two values are also presented. This is done using nominal current.

Table 4.11: The losses [W/m] calculated from the temperature measured using nominal current, alpha measurement.

Thermocouple	107	108	109	110	111	112	113	114	115	116
Measurements [W/m]	1.34	1.17	1.36	1.37	1.35	1.41	1.42	1.43	1.43	1.36
Simulations [W/m]	1.27	1.77	1.39	1.77	1.27	1.77	1.77	1.27	1.27	1.39
Difference in %	5.37	-33.81	-2.29	-22.42	5.55	-20.1	-19.8	12.5	12.8	-2.17

Table 4.12: The losses [W/m] calculated from the temperature measured using nominal current, beta measurement.

	107	108	109	110	111	112	113	114	115	116
From measurements[W/m]	1.37	1.16	1.40	1.42	1.38	1.45	1.46	1.44	1.44	1.41
Simulations [W/m]	1.27	1.77	1.39	1.77	1.27	1.77	1.77	1.27	1.27	1.39
Difference in %	7.51	-34.1	0.299	-19.9	7.91	-18.0	-17.2	13.2	13.8	1.48

From the above tables, one can observe that the general trends found in Table 4.10 are present for the cases with nominal current. There are variations between the alpha and beta measurement, which gives varying differences. These differences are seldom more than 2.5 % off one another. These trends are summed up in Figure 4.17.

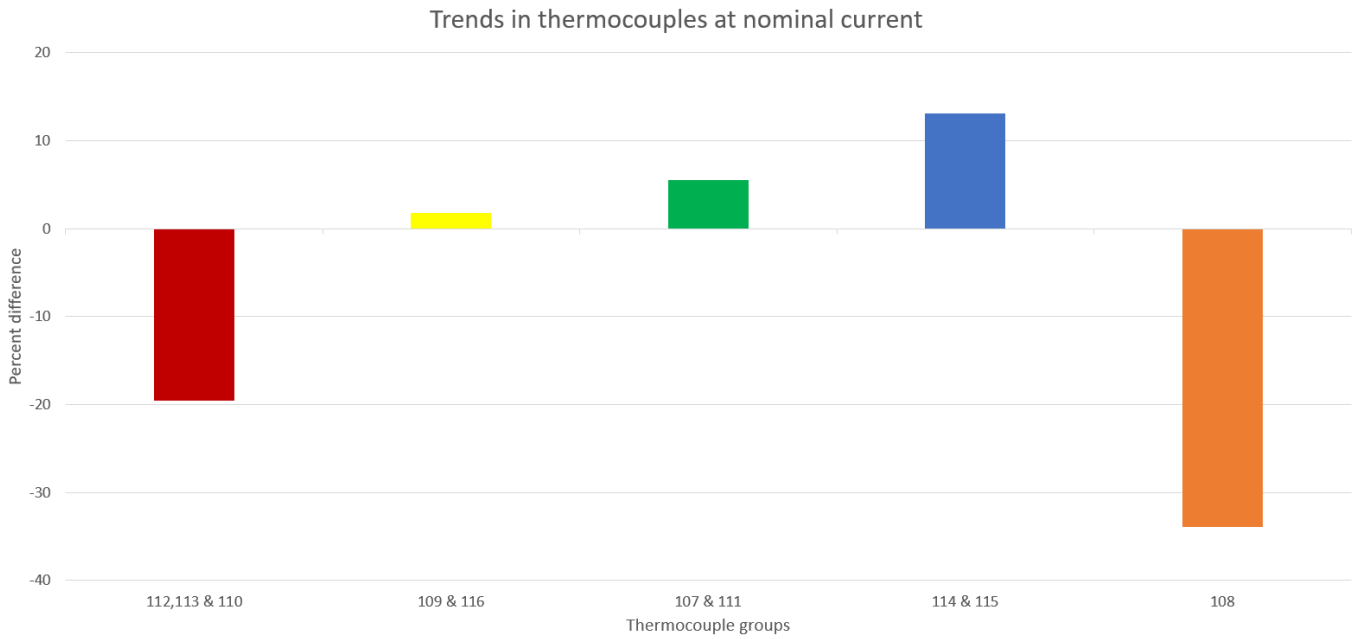


Figure 4.17: The major trend of the differences found in thermocouples, nominal current.

The gradients used to calculate these values are found in equations 4.5 and 4.6 Section C.2.2 in the appendix.

Twice nominal current

In Table 4.13, the measured and simulated losses for twice nominal current is presented together with the difference between these two. It is sorted after the thermocouples placed on the windings.

Table 4.13: The losses [W/m] calculated from the temperature measured using twice nominal current.

Thermocouple	107	108	109	110	111	112	113	114	115	116
From measurements [W/m]	5.52	4.70	5.58	5.61	5.51	5.71	5.75	5.90	5.89	5.61
From simulations [W/m]	5.15	7.14	5.62	7.14	5.15	7.14	7.14	5.12	5.12	5.62
Difference in %	7.19	-34.2	-0.772	-21.5	7.04	-20.1	-19.5	15.1	15.0	-0.271

As was the case for Tables 4.10, 4.11 and 4.12, there is a certain pattern to the difference between the losses measured and the losses simulated. This pattern is fairly similar to the patterns explained above for the cases for half and nominal current applied. There are some variations between all the loss differences at the various currents, but in general the differences are the very similar.

These trends are summed up in Figure 4.18.

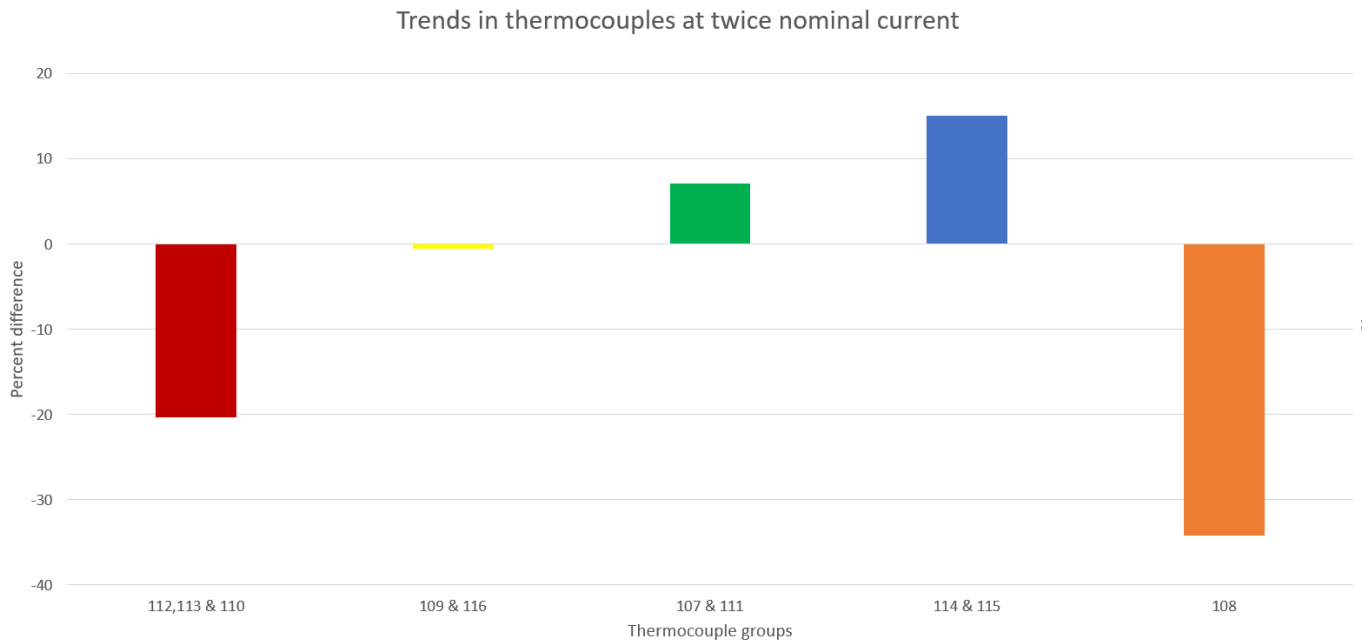


Figure 4.18: The major trend of the differences found in thermocouples, twice nominal current.

It should be noted from Figures 4.16, 4.17 and 4.18 that the major trends at different currents are quite similar.

The gradient used to performed the calculations for the measured power is found in Equation 4.8 and Section C.2.3 in the appendix.

4.5 Comparisons for different simulation methods

In Section D of the appendix, the Tables D.1, D.2 and D.3 are presented. These tables are found using the method presented in Section 3.6.

From Table D.1, the difference in % between the losses in each turn found using the magnetodynamic and semi-analytical loss calculation method can be observed. From this, it can be found that the difference in general is rather small. They are larger closer to the leakage field, but they are still minute in this area. For the secondary winding, the difference, though small, is largest in the uppermost turn, with the exception of the innermost parallel. This holds true also for the primary winding.

In Tables D.2 and D.3, the difference in % between applying and not applying circulating current in the semi-analytical loss calculation method is presented. As one can observe, the differences vary with the parallels of the winding. For the secondary winding, the differences is smallest in parallel 1 and increases with each parallel as they get closer to the leakage channel. In parallel 2 in the secondary winding, the losses without considering circulating currents are the largest. For the other parallels closer to the leakage channel, the opposite is true. For the two closest to the leakage channel, the differences are the largest. From Tables D.2 and D.3, it is clear that the parallel closest to the leakage channel has the largest losses when considering circulating currents compared with the case without circulating currents. The difference is nearly 38 %.

For the differences in the primary winding seen in Tables D.2 and D.3, variations between the parallels can be seen. In the parallel furthest from the leakage channel the losses without the circulating currents is almost 10 % larger. The difference is rather small for the middle parallel in the primary winding, with it being the smallest in the upper most turn. The difference in losses in the parallel closest to the leakage channel is as with the secondary winding the largest. In this parallel, the losses with circulating currents is almost 20 % larger.

5 | Discussion

5.1 Short circuit measurement

When comparing the largest delivered active effect seen in Figure 4.1 with the copper losses presented in Table 3.1, one can see that these two values are very close. The copper losses from Table 3.1 are at 1329.37 W while the delivered active power to the test transformer was at 1320 W. This gives a difference of 0.7 %. This difference is negligible and could be due to inaccuracy in measurement. This shows that the copper losses given in the rated data is measured at normal operation after the transformer has reached the operating temperature.

From Figure 4.1, one can notice that the active power delivered to the test transformer increases with time. From Figure 4.2 one can also notice an increase in temperature in the turns at different points. It should be noted that thermocouple 114 fell off during measurement and this is why it does not have a similar shape as the others, as seen in Figure A.0.1. From Equation 2.11, it's clear that the resistivity of a material increases with the temperature. As the temperature rises in the winding, the resistance is increased and the current applied decreases, as the voltage is constant from the energy source transformer. As one can see from Figure 4.1, the increases in delivered active power is not a smooth function. This is due to the current staying equal while the resistance of the windings increases with the temperature. Voltage is increased manually to maintain the desired current. This is why the delivered active power increases until it stabilizes at -1.32 kW.

When observing Figure 4.2, one can notice different behaviours of the temperature at different times. When discussing short circuit measuring, the temperature between 120 minutes and 300 minutes is of the biggest interest, as this is the region where the temperature is stabilizing and the increase in temperature is small. However, even after 5 hours, the temperature is still increasing. A possible explanation for this has to do with the iron core. This can be observed from the plot labeled 111 in Figure A.0.1, representing the measurement done at the iron core. The iron core has no current within it and does not have an increase in temperature caused by active power. It is on the other hand surrounded by windings that are getting warmer as current is running through them. Therefore the iron core gets warmer steady but slowly, as can be observed in Figure A.0.1. As the winding reaches operating temperature, the iron core is still getting warmer as this is a slower process. The increasing heat from the iron core affect the windings and causes small increases of temperature to continue. This is a possible reason for the small, but present temperature increase from 120 minutes to 300 minutes.

5.2 Circulating currents

The losses presented in Section 4.2.3 gave a total loss of 931.7 W. The losses calculated in the specialization project when not taking into account the circulating currents was 841.3 W after correction for the geometry. This gives an increase in losses of 10.7 %.

This increase in loss when taking into account circulating currents occurs because of the increased uneven currents in certain parallels. As explained in Section 2.5, circulating currents occur because of the leakage field and the geometry of the winding. As each parallel experience different induced voltages due to the leakage field, currents start to circulate to compensate this difference. This cause higher current in parallels closest to the leakage channel and smaller currents further from the leakage channel due to the distribution of the leakage field. Adding to this is the geometry of the parallels, as some parallels are shorter with smaller resistances, and others are longer with larger resistances. This difference in resistance affects the flow of the current. Since losses are calculated using the square of the current, as explained in Section 2.4, the increase in loss can be understood to happen because of the increased current density and the circulating currents taking place in the parallels.

When comparing the calculated total losses with the measured losses, one sees that the losses are not quite equal. The measured loss was 1.11 kW, as seen in Figure 4.1, while the calculated loss was at 931.7 W at the room temperature. This is a difference of 16 % between the calculated and measured losses. There are several possible explanation for why this has happened. The first one is imprecise calculations. This could be due to assumptions made not being accurate enough, the tightness of the mesh, etc. In short, this could be because of human fault. The difference could also be because of the resistivity of the conductor. It is assumed that the copper is rather pure in the COMSOL calculations. This may not be the case, as seen from Table 4.7. The calculated resistance is smaller than the measured resistance, and from Equation 2.9 it can be understood that the actual resistivity of the conductor being larger than assumed could cause this difference. Further research into the exact resistivity of the conductor would be beneficial.

A source of fault could also be the area and length of the windings. The assumptions about these elements could not accurate enough and cause the difference, as these elements affect the resistance of the conductor. Another possible explanation are losses in joints and connections in the transformer. In the transformer, there are several several joints and connections that have not been modelled due to a lack of information about the geometry of these. Lastly, losses may occur in the structural parts of the transformer that also were not modelled in COMSOL for the same reasons.

5.2.1 The measurement of the circulating current

The measurement of the circulating current that can be observed in Table 4.4 when compared with the calculated average values, from Tables 4.3 and 4.2, are quite similar. The differences are presented in Table 5.1.

Table 5.1: The difference in % between the simulated and measured circulating current.

Difference between measured and simulated			
Parallels	1	2	3
Difference in %, absolute value current	1	2.76	-0.388
Difference in %, phase angle	1.68	-0.80	-4.92

As seen in Table 5.1, the difference between the simulated currents and the measured currents are minute. The same is the case when looking into the phase angle, with the biggest difference occurring in parallel 3. This might be due to faults in measurements, considering it is still quite small. In general, one could consider the simulated circulating currents to match the measured circulating currents fairly well and understand the simulation to match the physical transformer well in this aspect.

5.3 Resistance measurement

In this section, the result from the resistance measurements are discussed and commented.

5.3.1 Before the heat run test

Before the heat run test, all the phases have more or less equal resistance in their respective winding, as can be seen from Table 4.6. The variation between the different phases could be caused by slightly different lengths of copper wire in the windings. These differences are generally so small that they are negligible.

In Table 4.7, the temperature and the resistivity is equal for the two windings. This occur due to the measurement being performed at room temperature and the transformer being subjected to room temperature for a long time. This causes all of the parts of the transformer to have equal temperature. From Equation 2.11, one can see that equal temperature would cause equal resistivity, as it is independent from the length of the conductor and only depends on the temperature.

The difference between the calculated and measured value is at 7.65 % for the secondary winding and 8.22 % for the primary winding. This difference may occur because of several factors. One is geometry. To calculate the length of the windings, only the part of the winding surrounding the core leg was used. The possible additional length in the connections leading to the terminals are not added, which would increase the calculated resistance. Another possibility related to the geometry is inaccuracy in the modelled windings. As seen from Equations 3.3 and 3.2, the calculation

of the resistance is dependent on the length of the parallels and the area of the conductor. If these values are not sufficiently accurate, the calculated resistance could end up not matching the measured resistance. This could be a possible explanation for the difference observed.

Another source, as mentioned when discussing the difference in simulated and measured loss, could be the resistivity of the conductor. The reason given in Section 5.2 about the resistivity could be a cause for the difference in the resistances.

5.3.2 After the heat run test

By observing the Tables 4.6 and 4.8, one can see that the resistance in both windings has increased after the heat run test. This is as expected, as the temperature after an heat run test is higher, as seen in Figure B.0.1. From Table 4.9, one can observe that the resistivity has increased with the temperature. This makes sense when taking into consideration Equation 2.11, which states that the increased temperature leads to increased resistivity. This again causes a higher resistance, as understood from Equation 2.9. As was the case with the measurement before the heat run test, the average resistance is larger in the primary winding than in the secondary winding.

One should notice that the resistivity is slightly larger in the secondary winding. This might be due to the placement of the secondary winding compared to the primary winding. As the secondary winding is placed closer to the core leg and with the primary winding surrounding it, less cooling takes place. This might cause the secondary winding to be warmer and for it to have a higher average temperature. Unfortunately, placing a thermocouple in the leakage channel in the middle of the secondary winding was not possible during the measurement, therefore there is not measurements to compare the temperature in the middle of the secondary winding.

The calculated temperature in the primary winding was found to be 76.94 °C, while the measured temperature after 4 minutes in thermocouple 115 was 78.48 °C. These two values are very close and only have a difference of 2%. It is assumed that the average temperature of the winding can be compared with the measurement from thermocouple 115 since it is placed in the middle of the leg. This is because of an assumption of a linear temperature profile throughout the winding.

All the resistances in the different phases are quite similar. It should be noted that the later resistance measurements are smaller than the earlier one. This is due to the temperature decreasing, as understood from Figure B.0.1. A notable exception is phase v. It has the largest resistance, for both primary and secondary winding, regardless of the time of measurement. This might be caused by the placement of the phase. Phase v is the phase that is situated around the middle leg of the transformer. As it is surrounded by the other phases, it receives heat from both of these windings. This causes the phase v to cool more slowly compared to the two other phases. And as explained earlier, as phase v is warmer, the resistance is higher, as can be observed for both windings.

5.4 Temperature measurement

Even though the method for measuring the losses on the secondary winding was presented in Section 3.3, there were unfortunately no measurements performed. This is due to the limited time for experiments, since restrictions were imposed by NTNU due to COVID-19.

5.4.1 Linear regression analysis

In the analyses presented in Section 4.4.1, thermocouple 110 is used. The measurement for this thermocouple is chosen arbitrarily as an example and is used to show the trends that can be observed by all the thermocouples in Section C.2 in the appendix.

When observing Figure 4.8, one can conclude that the temperature rise the first 10 minutes is fairly linear. Since the temperature and the suggested plot match to such a degree, one can conclude that the first 10 minutes are fairly close to having adiabatic heating as assumed.

Even with this, the gradient from the linear regression analysis performed using the data from 1 to 2 minutes is the gradient used to calculate the active power losses presented in Section 4.4.3. This decision can be argued for taking

into account Figures 4.7, 4.9, 4.10 and 4.13. Even though the plot suggested from 0 to 10 minutes is rather close to the entire temperature plot, the plot suggested from 1 to 2 minutes follows the temperature in this time interval much closer. As time passes, the assumption of adiabatic heating becomes invalid as cooling increases. This can be observed from Figure A.0.1. The increase in temperature declines until temperature equilibrium is achieved. Because of this, the data from the 1 to 2 minutes is used for all the measurements, as the cooling effects are closer to being negligible in this time frame compared to from 0 to 10 minutes.

For half the nominal current, the increase in temperature is rather small. As seen in Figure 4.6, the temperature increases from about 19.5 °C to 22.8 °C over 10 minutes. This is due to the relationship between current and power explained in Section 2.4, as the current is reduced by half, the power in the transformer turns becomes a fourth of the power compared to nominal current.

When looking at Figure 4.7, one can observe that the temperature has more noise in its measurement, compared to the measurements done at nominal and twice nominal current, seen in Figures 4.9 4.10 and 4.13. This might be happening since less power is delivered to the windings, making the increase in temperature less pronounced. Therefore the natural variations are made clearer than for the cases with twice nominal and nominal current, as a smaller scale for the y-axis is necessary. As seen from Figure 4.7, the temperature increase is small, going from 19.87 °C to 20.25 °C. This is a much smaller increase compared with the other measurements. As a result, the suggested gradient from Equation 4.2 for half the nominal current is a lot smaller than for the measurements at other currents.

For the temperature increase for nominal current, shown in Figure 4.8, it goes from approximately 20 °C to approximately 32 °C. This is larger than what was observed with half the nominal current. This is reflected in the gradients suggested in Equations 4.5 and 4.6. These gradients are nearly 4 times larger than the gradient for half the nominal current shown in Equation 4.2. This can be explained with the assumption of adiabatic heating and the difference in current. As explained above, in the time interval from 1 to 2 minutes that there approximately adiabatic heating, causing the temperature increase to be linear with the power. Since the current is twice as large between the two measurements, the power delivered becomes 4 times as large, causing the temperature increase to be 4 times as large as well. When investigating the relationship between temperature gradients for twice and half the nominal current, one can observe that the gradient for twice the nominal current, from Equation 4.8, is almost 16 times larger than the gradient for half the nominal current, which matches with what is explained above considering the difference in temperature increase.

For the measurement done with twice the nominal current, the temperature increase is a lot larger than all of the other measurements, best presented in Figure 4.14. Due to the great increase in temperature at twice the nominal current, the measurements at half and nominal current almost look like they are parallel. This happens because of the increase from 20 °C to 68 °C for the measurement with twice the nominal current, causing the scaling of the y-axis to be so large that details about the measurements at half the nominal and nominal current to be less pronounced. Since the temperature increase is so large at twice nominal current, the current changing throughout the measurement must be considered. For all the other measurement, the current was more or less constant throughout measurement as can be observed in Section C.1 of the appendix. This is not the case for the measurement done at twice nominal current. The increase in temperature causes an increase in resistivity, as explained in Equation 2.11, causing an increased resistance. The voltage from the energy source transformers is constant, causing the current to drop as the increase in temperature continues. This can be observed in Figure 4.12. To put it into perspective, the decrease in current from 1 to 2 minutes at twice nominal current of 1 A is equal to the current drop for the other measurements from 0 to 10 minutes. For comparisons between simulated losses and measured losses, the twice nominal current was set at 231.5 A, which is the average current in the time interval of 1 to 2 minutes.

5.4.2 Comparisons between measured and calculated power loss

From the tables in Section 4.4.3, one can see a clear correlation with the difference in losses and with the parallel where the thermocouple is placed. From Table 4.4, one can see when applying nominal current, different currents are in the three parallels in the primary winding. This causes three different losses to occur in each of the parallel since, as explained in Section 2.4, loss is in correlation with the square of the current. This could be why there's such an apparent pattern in the differences, regardless of the amount of current applied. This is made clear from Figure 4.16, 4.17 and 4.18, showing the major trends in the differences measured. This apparent pattern could mean that there is not a large fault in the measurements.

The difference between the losses, excluding thermocouple 108, is greatest for the parallel closest to the leakage channel. This is true regardless of the current being applied. From Table 4.4, it's clear that this parallel in the primary winding is the one with the largest current, and therefore the largest losses. The difference for this parallel is between 17.5 %

and 22.5 % larger in the simulations compared with all the measurements performed. A possible explanation could be that there is some heat being conducted into the connections and joints of the transformer, even though it is assumed that the heating is very close to being adiabatic. Another could be because of heat being conducted down into the turns situated further down. To truly uncover why this happens, further measurements would have to take place. Unfortunately, this was not possible for this master thesis due to restrictions imposed because of COVID-19.

For the difference in losses in parallel 2, it can be observed that it is rather small, especially compared with the difference in losses for the other parallels. It could be noted that the current in this parallel is the closest to being equal to the current when not taking into account circulating currents, as seen in Tables D.2 and D.3. For the difference in loss in parallel 3, it varies between 5.37 % and 7.91 %. In this case the measured loss is smaller than the simulated loss. One can also observe from Table 4.4 that this parallel has the smallest current. As with the case for the parallel closest to the leakage channel, further research and measurements are needed to understand how these differences occur.

For the difference in thermocouple 114 and 115, which are placed around turn 30 from the top, there is also a significant difference between what was measured and simulated. From Tables 4.10, 4.11 and 4.13, one can observe that the largest losses are measured with these thermocouples. For Table 4.12 the losses measured with thermocouples 114 and 115 are some of the highest for the beta measurement. By observing Figure 2.6, the uppermost turns in parallel 3 should have higher losses due to higher current density, as explained in Section 2.2.2. This is reflected in the simulated losses, with the losses simulated where thermocouples 107 and 111 are placed being larger than the simulated losses where thermocouples 114 and 115 are placed. This is not the case with the measured losses. This could be since so much area is surrounding thermocouples 114 and 115. Some of the power in the other turns could be measured by the thermocouple 114 and 115, causing this large difference between simulated and measured loss. Further measurements, as mentioned above, and alternative placement of the thermocouples would be beneficial to gather more information about this.

From theory, the losses should be increasing the closer to the leakage channel the turn is, as observed from Figure 2.6. This is the case for the losses measured and simulated, regardless of the current applied. This shows that even though some results do not match the theory explained earlier, other results do. From Table 4.4, one sees that the currents in the parallel measured, matches the losses found using the thermocouple when considering how the losses and currents are distributed in the parallels in the primary winding.

Lastly for this section, the result measured by thermocouple 108 should be discussed. From Figure 3.12b, it becomes clear that this thermocouple is different in placement, as it is the only thermocouple placed on the bottom of the winding. It also stands out in regards to result, as it can be seen from the figures in Section 4.4.3, as it is the only one with a difference at the various currents at around 30-34 %. This might be because of the construction of the transformer. At the bottom of the winding, as can be seen in Figure 3.1, there is a thick layer of tape. In addition, there is a thick layer of lacquer that the entire winding is dipped in. Due to gravity, the lacquer has trickled down and set itself in a thicker layer at the bottom of the winding. This thick layer of tape and lacquer might be the cause of this large difference, as they might function as a form of insulation for the winding and reduce the power losses registered from the temperature increase. Therefore, the measurement from thermocouple 108 stands out and could be considered not valid for comparisons.

5.5 Comparisons for different methods

From Table D.1, it is clear that the difference in using the semi-analytical loss calculation method and the magnetodynamic loss calculation method is so small that both methods can be used freely for 2D simulations at 50 Hz. The largest difference is from the parallels closest to the leakage field, which could be because of the difference in leakage field between the two methods, since the semi-analytical method calculates a magnetostatic field and adds the eddy current losses analytically using Equation 2.10. Therefore where the leakage field is greatest, which can be observed to be in the leakage channel from Figure 2.6a, the biggest difference will occur as the losses calculated magnetodynamically will take more into consideration the field, as can be seen from Section 2.2.2. At such low frequencies however, this has little effect, as can be seen from the very small differences in Table D.1. When compared with the conclusion about the two loss calculation methods from the specialization project[10], it is clear that that conclusion that at low frequencies, the methods could be used interchangeably is also valid when taking into consideration circulating currents.

When it comes to the comparison presented in Tables D.2 and D.3 between losses simulated with and without circulating current, the story is something else. The differences vary with the parallels. This occurs because different

voltages get induced in the different parallels for the case with the circulating current, as explained in Section 2.5, causing different currents to flow. Since a larger voltage gets induced due to leakage field in the parallels closest to the leakage channel, a larger current circulates in these parallels. This can be observed from Tables D.2 and D.3, where the losses with circulating losses compared with no circulating currents are around 38 % larger in the secondary winding's parallel and around 20 % larger in the primary winding's parallel closest to the leakage channel. The further from the leakage channel the parallels are, the larger the losses without circulating currents compared to the case with circulating currents are, especially for the primary winding. Another part for this case, as mentioned in Section 2.5, is the geometry of the primary winding. As parallel 3 in the primary winding is the parallel furthest from the iron core, it is the longest parallel and therefore has the largest resistance, considering Equation 2.9. Therefore less current will flow in this winding. When considering this being the parallel with the weakest leakage field for the primary winding, it becomes clear why this is the parallel in the primary winding to have the smallest amplitude compared with the loss calculation where circulating currents is taken into consideration.

For the secondary winding presented in Tables D.2 and D.3, the pattern that was clear the primary winding is not as clear for this case. When looking for the parallel with the largest losses for the case without circulating currents compared to the case with, it becomes apparent that this occurs in parallel 2, and not parallel 1. A possible explanation for this is the geometry of these two parallels. Parallel 1 is the parallel in the secondary winding closest to the iron core and is therefore the shortest. As explained for the primary winding, for Equation 2.9 this causes the resistance to be the smallest in this parallel of the two. Adding to this, from Figure 2.6a, the leakage field these two parallels are subjected to is quite similar, so this could be why it is parallel 2 and not parallel 1 who has the largest difference between the losses calculated where the case without circulating currents is the largest. For the two innermost parallels in the secondary winding, the same pattern discussed for the primary winding is apparent, as the difference becomes larger the closer to the leakage channel the parallels are with the losses being largest for the case with circulating currents.

6 | Conclusion

The short circuit heat run test showed that the copper losses given in the rated data from the producer of the test transformer was performed at operating temperature. There was only a small difference between the measured copper loss and the copper loss from the rated data.

When taking into consideration circulating currents in the model, the measured copper losses of 1.11 kW was still larger than the simulated losses at 931.7 W. This simulated losses increased from the losses found in the specialization project[10]. The circulating currents were measured and were quite close to the currents found using a 3D model in COMSOL multiphysics, both in regard to the amplitude and the phase angle of the current in the different parallels of the primary winding. As expected from the theory, the current in the parallel closest to the leakage channel was the largest and the parallel furthest from the leakage channel had the smallest current amplitude.

From the resistance measurements, it became clear that the primary winding had the largest resistance in the winding. There were some differences between the measured resistance and the calculated resistance from the temperature measured at room temperature. This could be due to faults in measuring, faults in calculating the geometry of the transformer or faults in the assumptions of the resistivity of the conductor. After the heat run test, the average temperature of the windings was calculated to be a little higher in the secondary winding than in the primary winding, assumed due to the placement and limited cooling in the secondary winding compared with the primary winding. The measured average temperature of the primary winding was close to the calculated average value.

The linear regression analyses performed on the measurements of the temperature increase show that in the first 10 minutes of applying current, the assumption of approximated adiabatic heating is valid. The temperature increased at the same rate as the power as the current applied increased. The temperature increase was largest for the case with twice the nominal current and smallest for the case with half the nominal current. Variations in ventilation affected the room temperatures and the likeness at the two measurements at nominal current, but the gradient for both were fairly similar.

When comparing the measured and simulated power loss in the primary winding, a clear pattern emerged between the difference between the losses and where the thermocouple was placed. It is unclear why this happened, and further measurements is necessary. Some of the measurements followed the theory quite nicely, for example that the largest losses on top of the winding was measured closest to the leakage channel while the smallest loss was furthest away. Other parts on the other hand, as with the losses registered in thermocouples 107 and 111, and thermocouples 114 and 115, did not follow the theory. A possible explanation could be the thermocouples 114 and 115 had large areas around them and registered more heat than just from 1 turn, but this claim need more research before it can be said to be true. Due to the construction of the transformer where thermocouple 108 was placed, this result is assumed to be invalid.

A comparison between the magnetodynamic and semi-analytical loss calculation method was performed, taking into consideration circulating currents. As was concluded in the specialization project, the difference between these two methods at 50 Hz was so small, that these methods could be used interchangeably. This makes it clear that for the frequencies tested in the master thesis, the accuracy of the semi-analytical loss calculation method is precise enough to do simulations of transformer windings, including the losses generated from eddy currents in 2D models. This holds true when taking into consideration circulating currents. The differences between losses with and without circulating currents was also presented and showed how circulating currents generate larger losses in the parallels closest to the leakage channel. It also demonstrated the impact of geometry for circulating currents, as the secondary winding did not have the largest loss without circulating currents compared to with circulating currents in parallel 1, but in parallel 2, while this happened in the primary winding in parallel 3.

7 | Further works

For further work based on this master thesis, more measurements could be performed. Due to restrictions imposed by NTNU because of COVID-19, the amount of measurements done was severely limited. There were only measurements from the primary winding and only on one of the phases. In addition to this, there were only measurements done at 50 Hz. For future works, the thermal elements could be placed on other phases, below the yoke, and to other turns as a part of the measurements. There could also be measurements performed on the secondary windings. This would give an increase in the data point available and make it possible to get better comparisons with the losses simulated using COMSOL multiphysics.

By performing measurement with different frequencies, the semi-analytical loss calculation method could be further tested, due to its dependency of frequency as a constant, as seen in equation 2.10. This would be useful to be able to do comparisons with simulated losses at both higher and lower frequencies in COMSOL multiphysics. This would be helpful because it would further test the validity of the semi-analytical loss calculation method, especially as additional losses occur at higher frequencies.

Another aspect that need further work is the differences between the losses measured and the losses simulated using COMSOL multiphysics. The discrepancy between what was simulated and what was measured need to be further investigated to find out why it happened. To accurately measure the resistivity of the conductor would be beneficial in regards to further works.

There should also be measurements performed when the transformer enclosure is around the test transformer. When performing the measurements in this master thesis, all were done with the transformer enclosure taken off. For normal operation of the transformer, this would not be the case. The transformer enclosure is used to secure the transformer within it, and to protect people. There are loss effects associated with the transformer enclosure since it is made from a magnetic material. By doing the measurements with the transformer enclosure, it could give a better picture of the losses in the turns during normal operation.

Another part of this master thesis that could be expanded on, is to model the joints and connections that were not included in the model used. However, these elements could be modeled through thorough measurements of the test transformer and added in the model. This could lead to a greater accuracy in the losses simulated in COMSOL.

A possible direction the work based on this master thesis could take is to do the measurements and loss simulations on another air insulated transformer. This would make it possible to further verify whether the losses calculated match simulated losses and could eliminate the possibility of the test transformer being a form of exception.

Bibliography

- [1] Working group A2.38. “Transformer Thermal Modelling”. In: *CIGRE* 1.1 (2016).
- [2] D.A. Koppikar; S .V. Kulkarni; G. Ghosh; S.M. Ainapure; J.S. Bhavsar. “Circulating current loss in transformer windings”. In: *IEE Proceedings - Science, Measurement and Technology* 4 (1998).
- [3] I J Nagrath D P Kothari. *Electrical machines*. 4th ed. Mc Graw Hill Education, 2016.
- [4] hyperPhysics. *Resistivity and Temperature Coefficient at 20 C*. 2020. URL: <http://hyperphysics.phy-astr.gsu.edu/hbase/Tables/rstiv.html#c1> (visited on 03/26/2020).
- [5] COMSOL Multiphysics. *The COMSOL® Software Product Suite*. 2019. URL: <https://www.comsol.com/products> (visited on 12/09/2019).
- [6] Robert Nilssen. *Electromagnetics in Power Engineering*. University Compendium, TET 4140 and TET5100. 2017.
- [7] Arne Nysveen. *Power Transformers*. University Compendium, TET4195. 2015.
- [8] Morten Gleditsch; Camilla Aabakken; Astri Gillund; Synnøve Lill Paulen. *Det høyspente distribusjonsnett*. Tech. rep. 2014.
- [9] Johannes Skaar. *Elektromagnetisme*. University Compendium, TFE4120. 2013.
- [10] Marianne Waagan. *Eddy current losses in transformer windings*. Specialization project. 2019.
- [11] Wikipedia. *Electrical resistivity and conductivity*. 2020. URL: https://en.wikipedia.org/wiki/Electrical_resistivity_and_conductivity#Temperature_dependence (visited on 03/26/2020).
- [12] Wikipedia. *Finite element method*. 2019. URL: https://en.wikipedia.org/wiki/Finite_element_method (visited on 03/19/2020).

A | Short circuit test

In Figure A.0.1, the temperature measurement done during the short circuit test. Each plot represent the temperature measurement done using thermocouples.

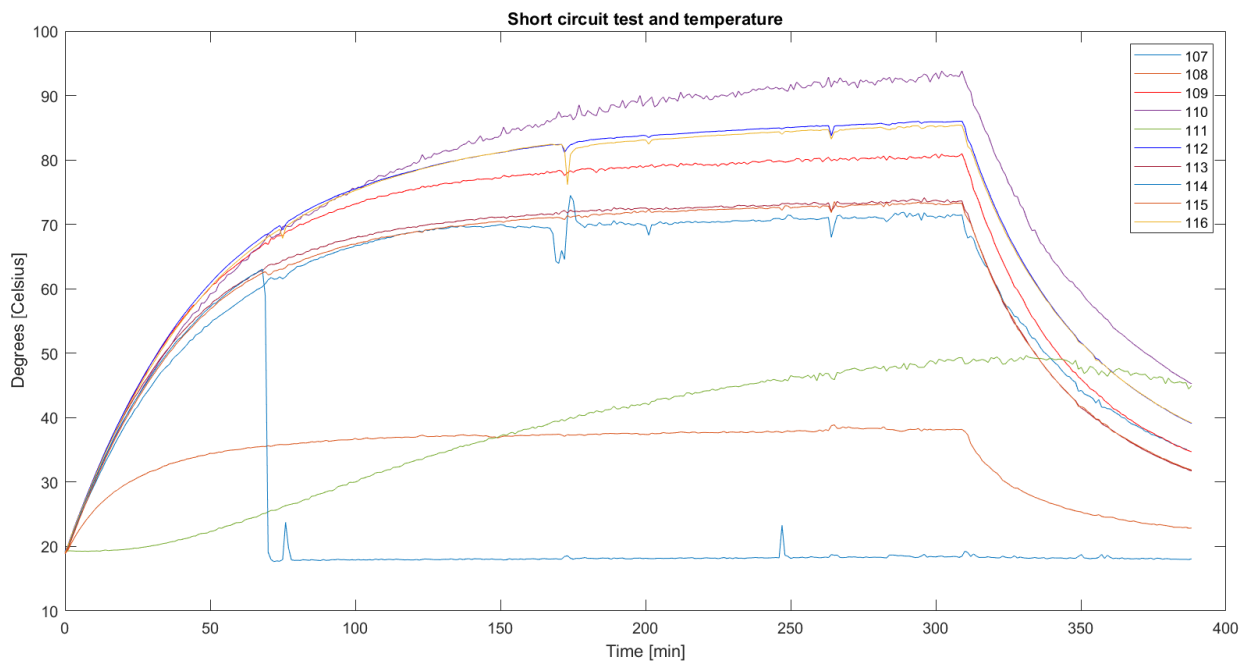


Figure A.0.1: All measurements of the short circuit test.

B | Resistance measurement

In Figure B.0.1, the temperatures during resistance measurements are presented. The x axis is the time in minutes, while the y axis is the temperature in °C.

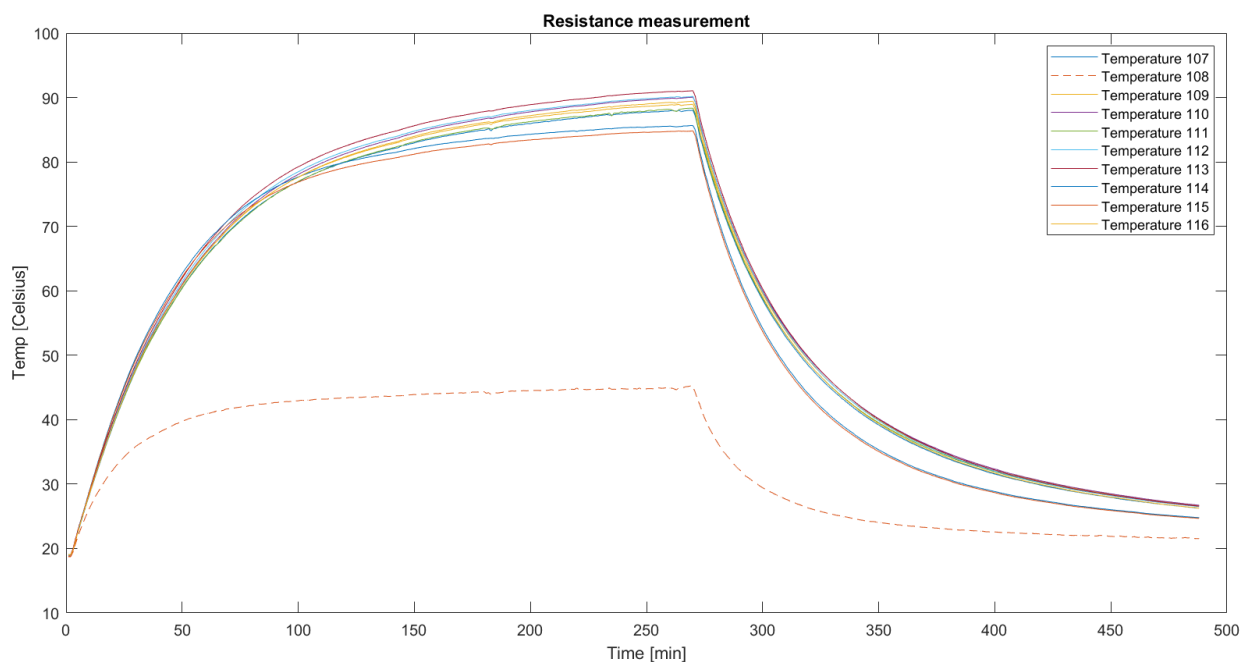


Figure B.0.1: Temperature [°C] over time for resistance measurement.

From the above figure, one can observe that the temperature increases quite rapidly for the first 100 minutes or so, then the temperature increase reduces in all the thermocouples until steady state is more or less reached around 270 minutes. After this, the power delivered is shut off, and the temperature gradually goes back to room temperature.

C | Temperature measurements

C.1 Current applied during temperature measurement

In this section, the currents applied during the temperature measurements are presented.

C.1.1 Half the nominal current

In Figure C.1.1, the current applied for the temperature test using half nominal current is presented. This figure shows the current from 0 to 10 minutes of measurement.

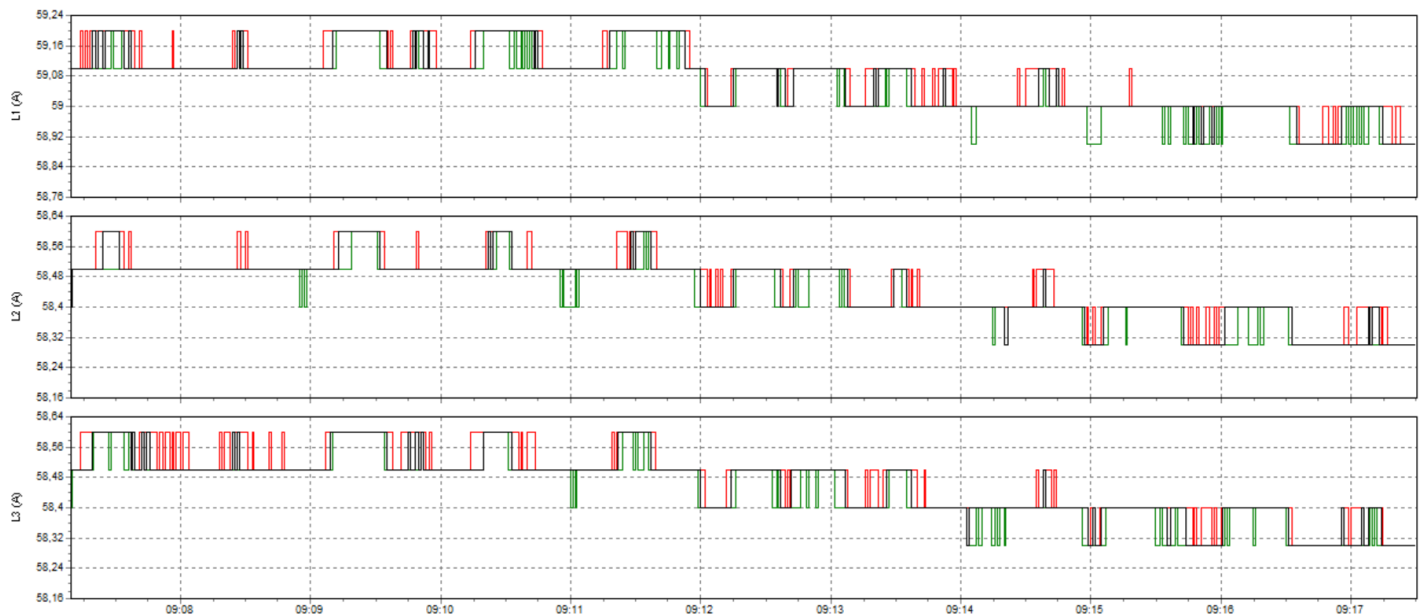


Figure C.1.1: The current [A] applied during temperature measurement for half nominal current.

The current decreases from 58.5 A to 58.4 A within 10 minutes of measurement.

C.1.2 Nominal current

Alpha measurement

In Figure C.1.2, the current applied for the temperature measurement using nominal current is presented.

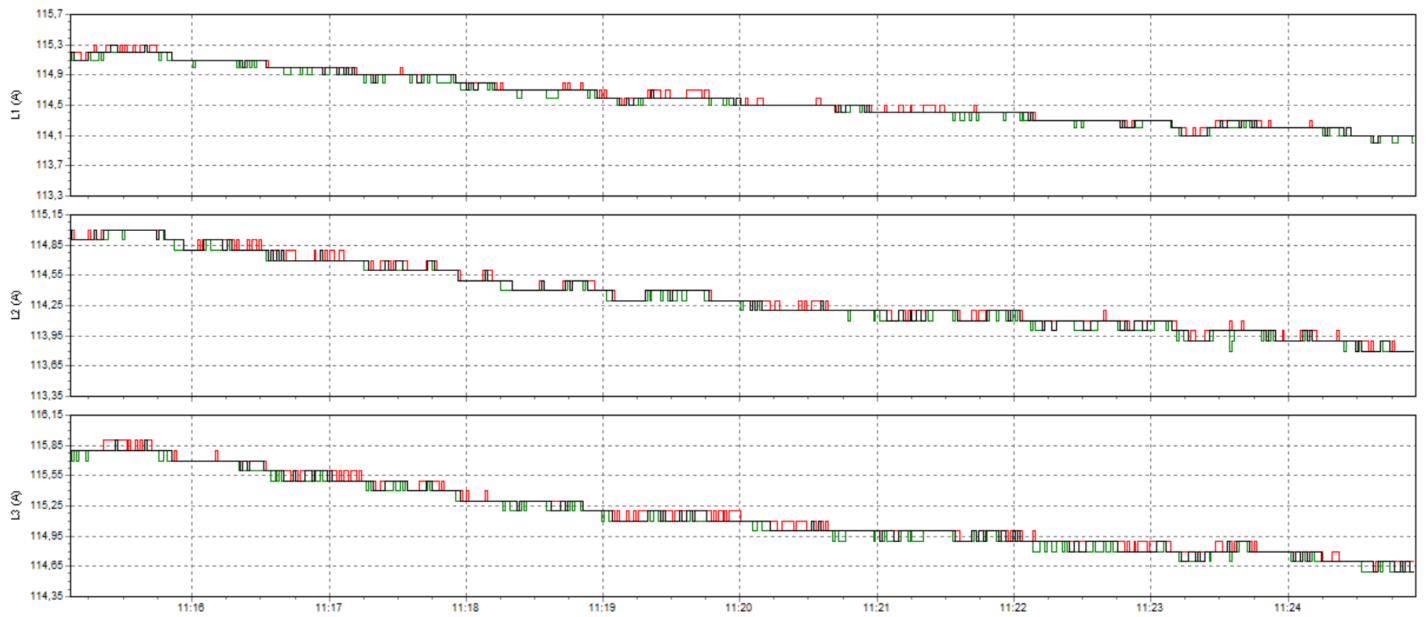


Figure C.1.2: The current [A] applied during the alpha temperature measurement for nominal current.

The current decreases from 115,4 A to 114 A over the 10 minutes.

Beta measurement

In Figure C.1.3, the current applied for the temperature measurement using nominal current is presented.



Figure C.1.3: The current [A] applied during the beta temperature measurement for nominal current.

The current decreases from 115 A to 113,7 A over 10 minutes.

C.2 linear regression analyses

C.2.1 Half the nominal current

Thermocouple 107

In Figure C.2.4, the temperature measurement done by thermocouple 107 and the linear regression analysis performed is shown. This measurement is done with twice the nominal current. This only is valid for 1 to 2 minutes of the measurement. The blue dotted plot represents the temperature measurement while the red plot represent plot found using the linear regression analysis.

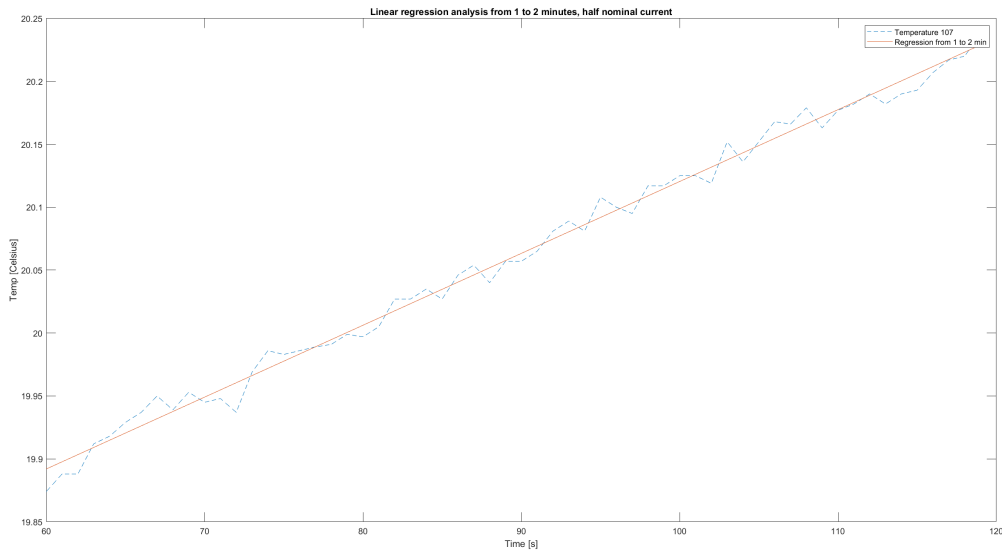


Figure C.2.4: The temperature [°C] and the linear regression analysis for thermocouple 107, from 1 to 2 minutes, at half the nominal current.

One can observe that the two plots follow one another fairly well. The red plot can be described using Equation C.1. Y represents temperature and x represent time in seconds.

$$y = 19.6 + 0.00571 \cdot x \quad (\text{C.1})$$

Thermocouple 108

In Figure C.2.5, the temperature measurement done by thermocouple 108 and the linear regression analysis performed is shown. This measurement is done with twice the nominal current. This only is valid for 1 to 2 minutes of the measurement. The blue dotted plot represents the temperature measurement while the red plot represent plot found using the linear regression analysis.

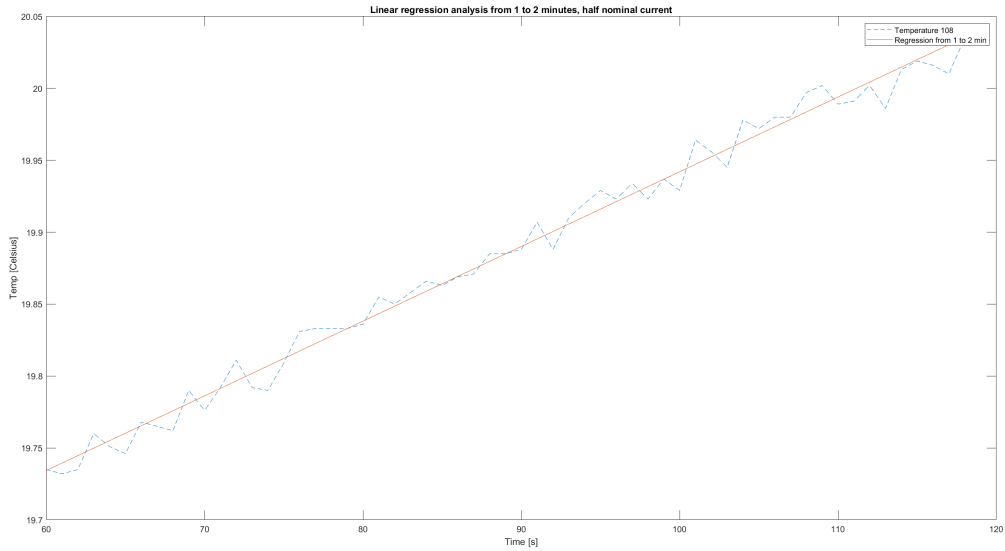


Figure C.2.5: The temperature [°C] and the linear regression analysis for thermocouple 108, from 1 to 2 minutes, at half the nominal current.

One can observe that the two plots follow one another fairly well. The red plot can be described using Equation C.2. Y represents temperature and x represent time in seconds.

$$y = 19.4 + 0.00519 \cdot x \tag{C.2}$$

Thermocouple 109

In Figure C.2.6, the temperature measurement done by thermocouple 109 and the linear regression analysis performed is shown. This measurement is done with twice the nominal current. This only is valid for 1 to 2 minutes of the measurement. The blue dotted plot represents the temperature measurement while the red plot represent plot found using the linear regression analysis.

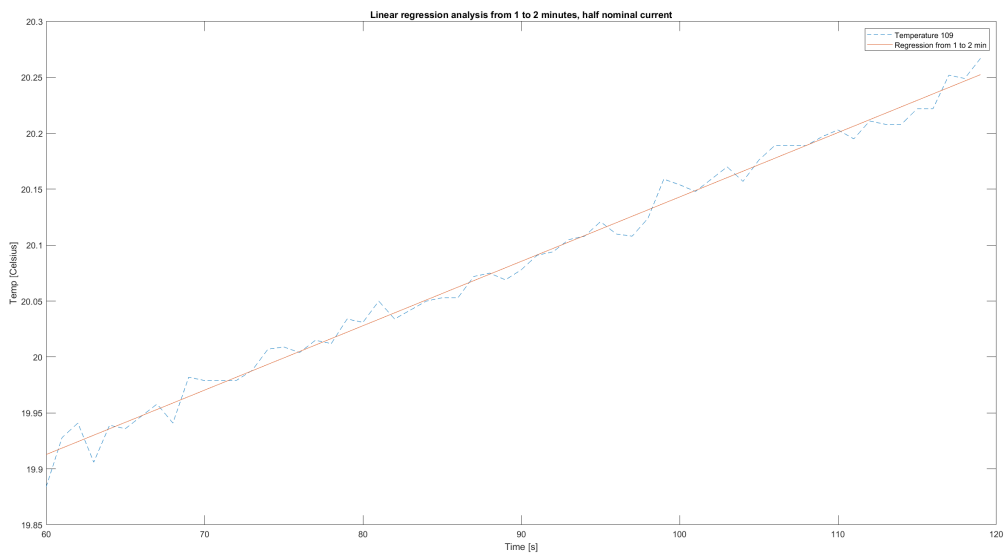


Figure C.2.6: The temperature [°C] and the linear regression analysis for thermocouple 109, from 1 to 2 minutes, at half the nominal current.

One can observe that the two plots follow one another fairly well. The red plot can be described using Equation C.3. Y represents temperature and x represent time in seconds.

$$y = 19.6 + 0.00576 \cdot x \tag{C.3}$$

Thermocouple 111

In Figure C.2.7, the temperature measurement done by thermocouple 111 and the linear regression analysis performed is shown. This measurement is done with twice the nominal current. This only is valid for 1 to 2 minutes of the measurement. The blue dotted plot represents the temperature measurement while the red plot represent plot found using the linear regression analysis.

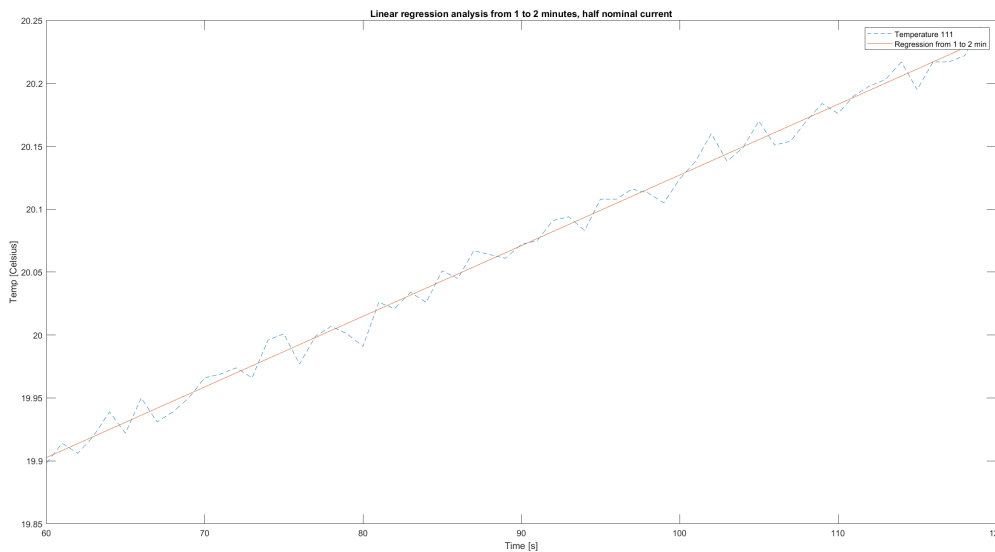


Figure C.2.7: The temperature [°C] and the linear regression analysis for thermocouple 111, from 1 to 2 minutes, at half the nominal current.

One can observe that the two plots follow one another fairly well. The red plot can be described using Equation C.4. Y represents temperature and x represent time in seconds.

$$y = 19.6 + 0.005615 \cdot x \tag{C.4}$$

Thermocouple 112

In Figure C.2.8, the temperature measurement done by thermocouple 112 and the linear regression analysis performed is shown. This measurement is done with twice the nominal current. This only is valid for 1 to 2 minutes of the measurement. The blue dotted plot represents the temperature measurement while the red plot represent plot found using the linear regression analysis.

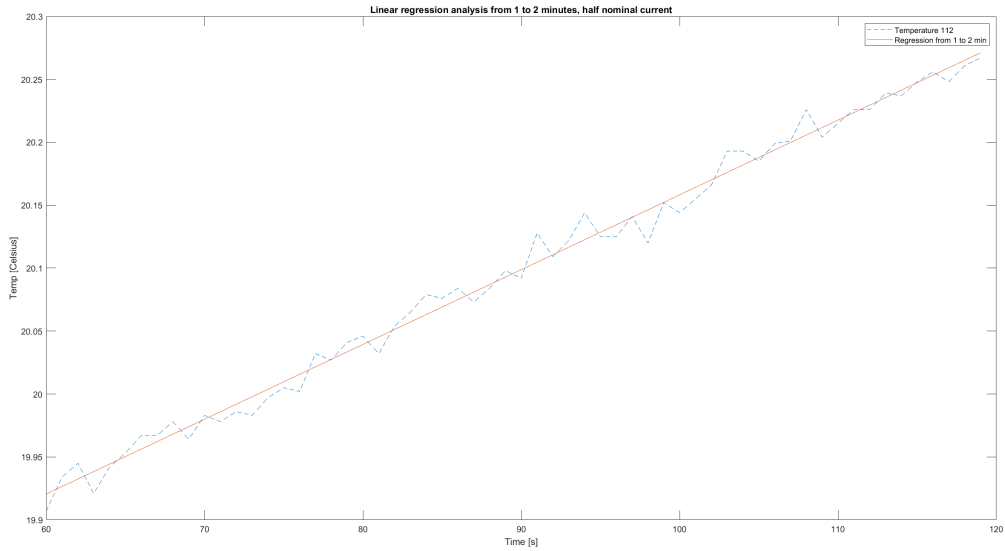


Figure C.2.8: The temperature [°C] and the linear regression analysis for thermocouple 112, from 1 to 2 minutes, at half the nominal current.

One can observe that the two plots follow one another fairly well. The red plot can be described using Equation C.5. Y represents temperature and x represent time in seconds.

$$y = 19.6 + 0.00594 \cdot x \tag{C.5}$$

Thermocouple 113

In Figure C.2.9, the temperature measurement done by thermocouple 113 and the linear regression analysis performed is shown. This measurement is done with twice the nominal current. This only is valid for 1 to 2 minutes of the measurement. The blue dotted plot represents the temperature measurement while the red plot represent plot found using the linear regression analysis.

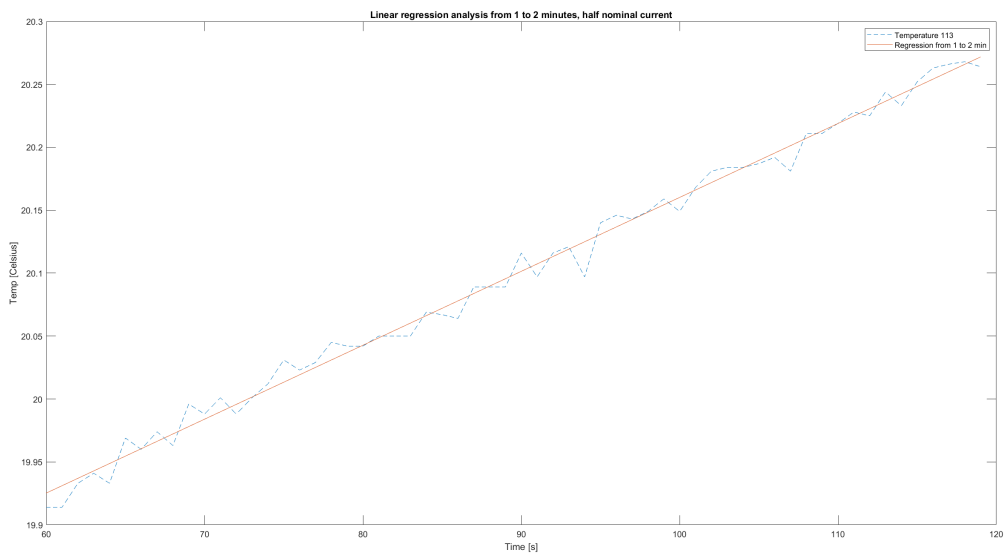


Figure C.2.9: The temperature [°C] and the linear regression analysis for thermocouple 113, from 1 to 2 minutes, at half the nominal current.

One can observe that the two plots follow one another fairly well. The red plot can be described using Equation C.6. Y represents temperature and x represent time in seconds.

$$y = 19.6 + 0.00587 \cdot x \tag{C.6}$$

Thermocouple 114

In Figure C.2.10, the temperature measurement done by thermocouple 114 and the linear regression analysis performed is shown. This measurement is done with twice the nominal current. This only is valid for 1 to 2 minutes of the measurement. The blue dotted plot represents the temperature measurement while the red plot represent plot found using the linear regression analysis.

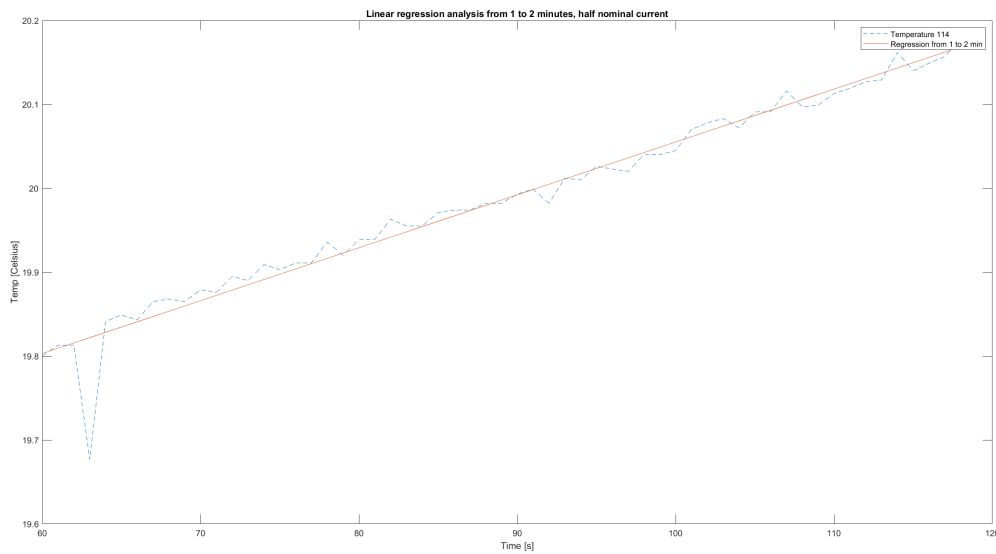


Figure C.2.10: . The temperature [°C] and the linear regression analysis for thermocouple 114, from 1 to 2 minutes, at half the nominal current.

One can observe that the two plots follow one another fairly well. The red plot can be described using Equation C.7. Y represents temperature and x represent time in seconds.

$$y = 19.5 + 0.00630 \cdot x \tag{C.7}$$

Thermocouple 115

In Figure C.2.11, the temperature measurement done by thermocouple 115 and the linear regression analysis performed is shown. This measurement is done with twice the nominal current. This only is valid for 1 to 2 minutes of the measurement. The blue dotted plot represents the temperature measurement while the red plot represent plot found using the linear regression analysis.

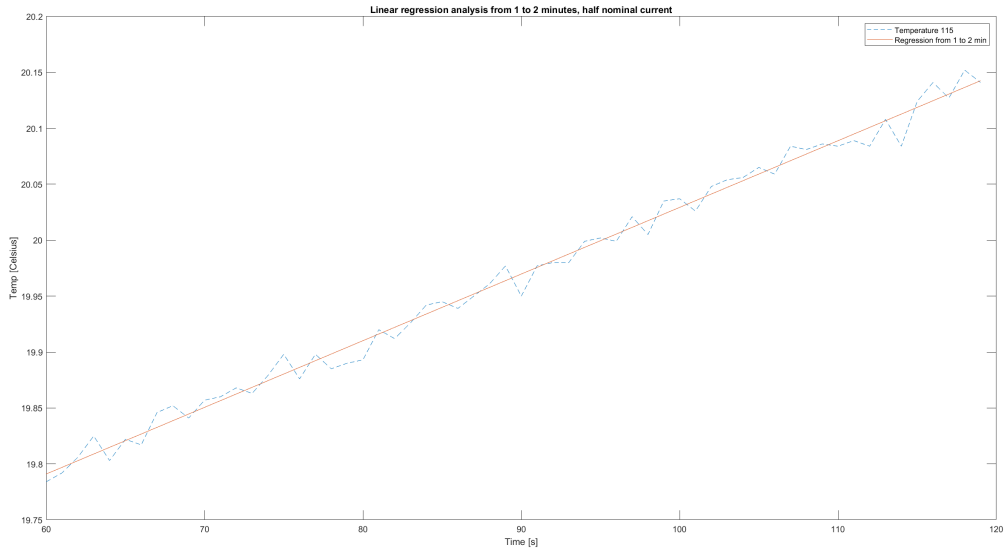


Figure C.2.11: . The temperature [°C] and the linear regression analysis for thermocouple 115, from 1 to 2 minutes, at half the nominal current.

One can observe that the two plots follow one another fairly well. The red plot can be described using Equation C.8. Y represents temperature and x represent time in seconds.

$$y = 19.4 + 0.00596 \cdot x \tag{C.8}$$

Thermocouple 116

In Figure C.2.12, the temperature measurement done by thermocouple 116 and the linear regression analysis performed is shown. This measurement is done with twice the nominal current. This only is valid for 1 to 2 minutes of the measurement. The blue dotted plot represents the temperature measurement while the red plot represent plot found using the linear regression analysis.

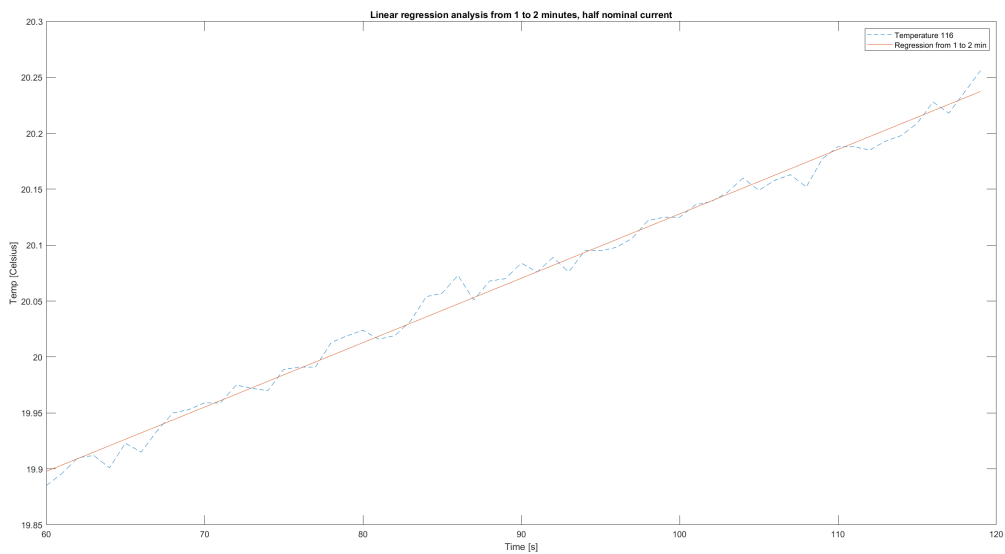


Figure C.2.12: . The temperature [°C] and the linear regression analysis for thermocouple 116, from 1 to 2 minutes, at half the nominal current.

One can observe that the two plots follow one another fairly well. The red plot can be described using Equation C.9. Y represents temperature and x represent time in seconds.

$$y = 19.6 + 0.00576 \cdot x \tag{C.9}$$

C.2.2 Nominal current

Thermocouple 107

In Figure C.2.13, the temperature measurement done by thermocouple 107 and the linear regression analysis performed is shown, for both alpha and beta measurement. This only is valid for 1 to 2 minutes of the measurement. The red and black plot represent the alpha and beta temperature measurement, respectively, while the blue and yellow dotted plot represent plots found using the linear regression analysis for alpha and beta measurement, respectively.

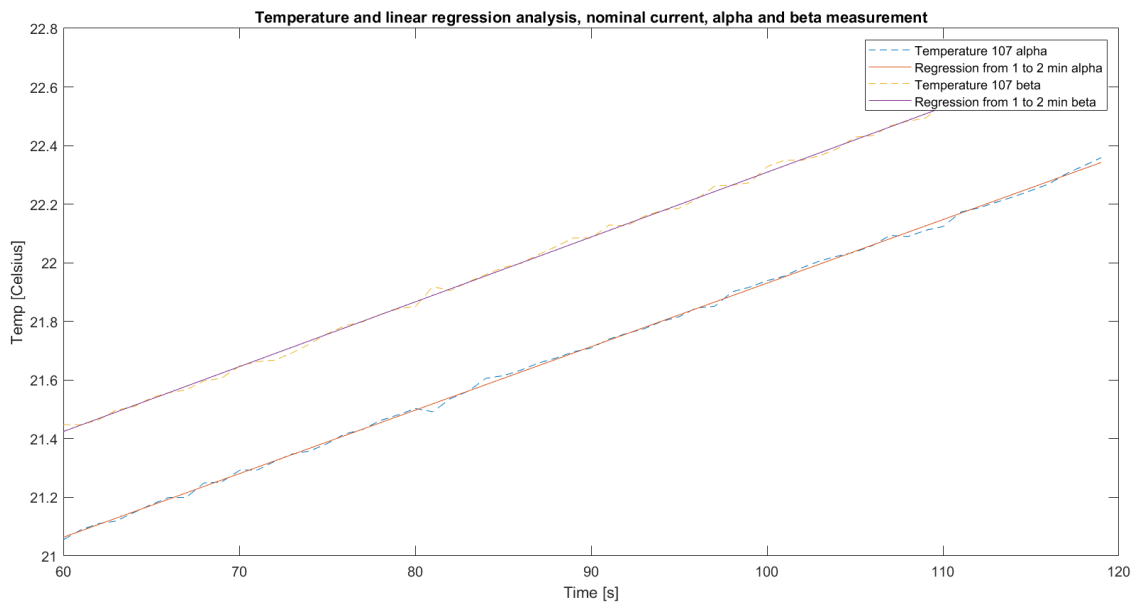


Figure C.2.13: . The temperature [°C] and the linear regression analysis for thermocouple 107, from 1 to 2 minutes, alpha and beta measurement.

One can observe that the linear regression plots follow the temperature plots another fairly well. The two different plots are nearly parallel with the beta plot being at a higher temperature. The linear regression analysis plots can be described using equations C.10 and C.11. Y represents temperature and x represent time in seconds.

$$y_{alpha} = 19.8 + 0.0217 \cdot x \tag{C.10}$$

$$y_{beta} = 20.1 + 0.0221 \cdot x \tag{C.11}$$

Thermocouple 108

In Figure C.2.14, the temperature measurement done by thermocouple 108 and the linear regression analysis performed is shown, for both alpha and beta measurement. This only is valid for 1 to 2 minutes of the measurement. The red and black plot represent the alpha and beta temperature measurement, respectively, while the blue and yellow dotted plot represent plots found using the linear regression analysis for alpha and beta measurement, respectively.

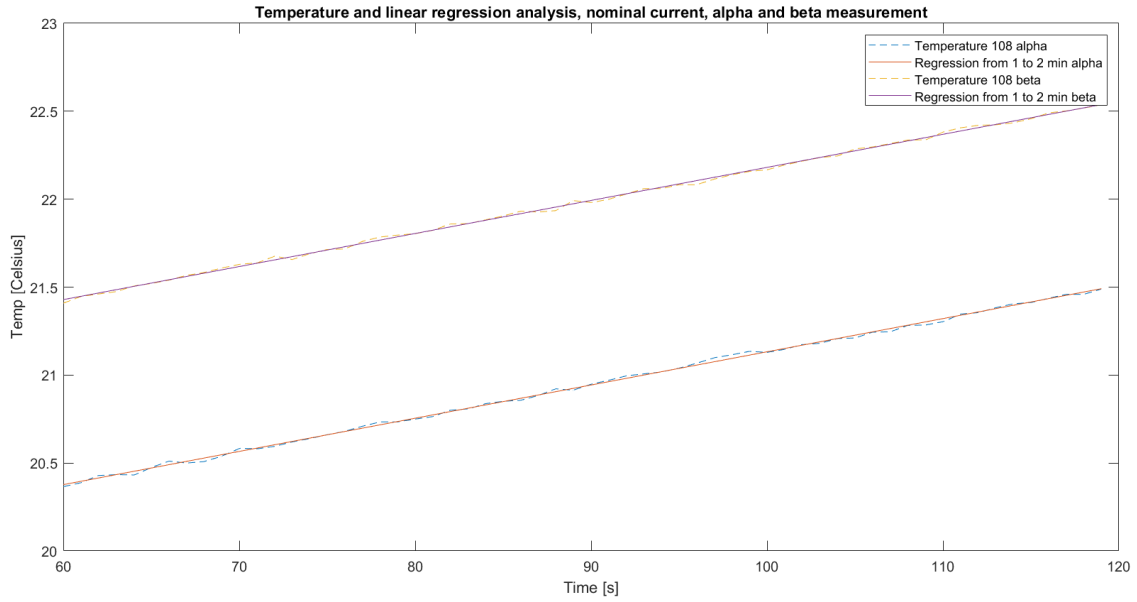


Figure C.2.14: . The temperature [°C] and the linear regression analysis for thermocouple 108, from 1 to 2 minutes, alpha and beta measurement.

One can observe that the linear regression plots follow the temperature plots another fairly well. The two different plots are nearly parallel with the beta plot being at a higher temperature. The linear regression analysis plots can be described using equations C.12 and C.13. Y represents temperature and x represent time in seconds.

$$y_{alpha} = 19.3 + 0.0189 \cdot x \quad (C.12)$$

$$y_{beta} = 20.3 + 0.0188 \cdot x \quad (C.13)$$

Thermocouple 109

In Figure C.2.15, the temperature measurement done by thermocouple 109 and the linear regression analysis performed is shown, for both alpha and beta measurement. This only is valid for 1 to 2 minutes of the measurement. The red and black plot represent the alpha and beta temperature measurement, respectively, while the blue and yellow dotted plot represent plots found using the linear regression analysis for alpha and beta measurement, respectively.

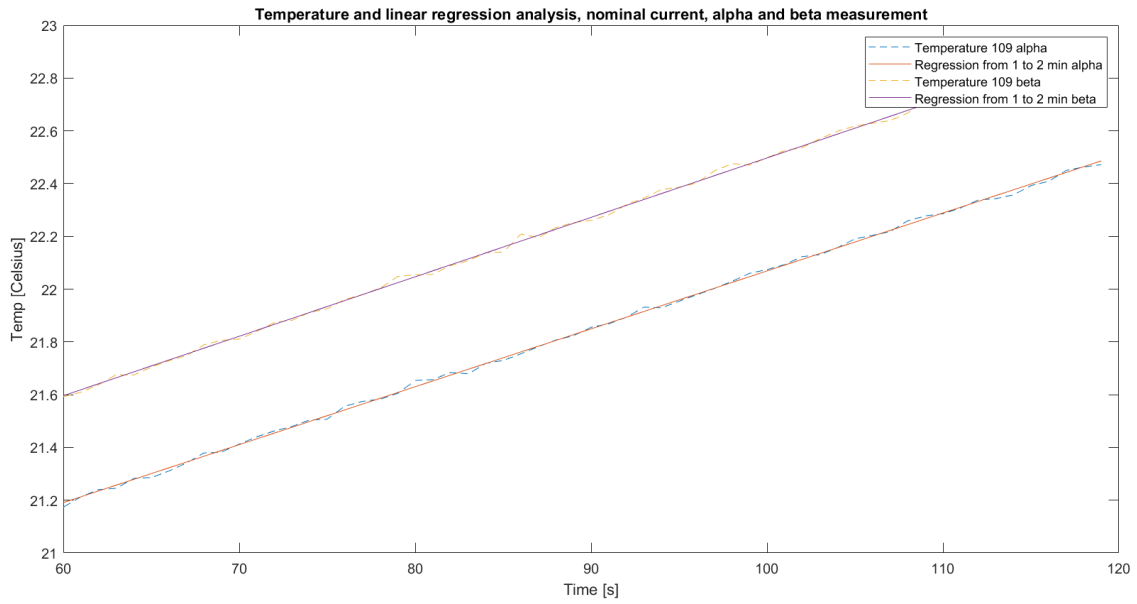


Figure C.2.15: . The temperature [°C] and the linear regression analysis for thermocouple 109, from 1 to 2 minutes, alpha and beta measurement.

One can observe that the linear regression plots follow the temperature plots another fairly well. The two different plots are nearly parallel with the beta plot being at a higher temperature. The linear regression analysis plots can be described using equations C.14 and C.15. Y represents temperature and x represent time in seconds.

$$y_{alpha} = 19.9 + 0.0220 \cdot x \quad (C.14)$$

$$y_{beta} = 20.3 + 0.0225 \cdot x \quad (C.15)$$

Thermocouple 111

In Figure C.2.16, the temperature measurement done by thermocouple 111 and the linear regression analysis performed is shown, for both alpha and beta measurement. This only is valid for 1 to 2 minutes of the measurement. The red and black plot represent the alpha and beta temperature measurement, respectively, while the blue and yellow dotted plot represent plots found using the linear regression analysis for alpha and beta measurement, respectively.

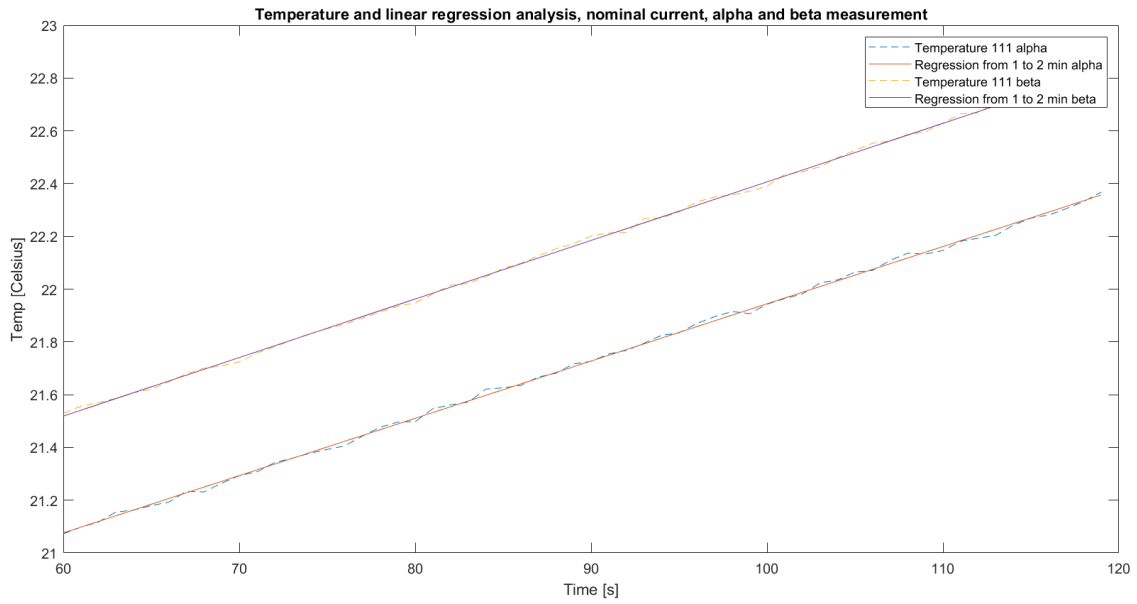


Figure C.2.16: . The temperature [°C] and the linear regression analysis for thermocouple 111, from 1 to 2 minutes, alpha and beta measurement.

One can observe that the linear regression plots follow the temperature plots another fairly well. The two different plots are nearly parallel with the beta plot being at a higher temperature. The linear regression analysis plots can be described using equations C.16 and C.17. Y represents temperature and x represent time in seconds.

$$y_{alpha} = 19.8 + 0.0217 \cdot x \tag{C.16}$$

$$y_{beta} = 20.2 + 0.0222 \cdot x \tag{C.17}$$

Thermocouple 112

In Figure C.2.17, the temperature measurement done by thermocouple 112 and the linear regression analysis performed is shown, for both alpha and beta measurement. This only is valid for 1 to 2 minutes of the measurement. The red and black plot represent the alpha and beta temperature measurement, respectively, while the blue and yellow dotted plot represent plots found using the linear regression analysis for alpha and beta measurement, respectively.

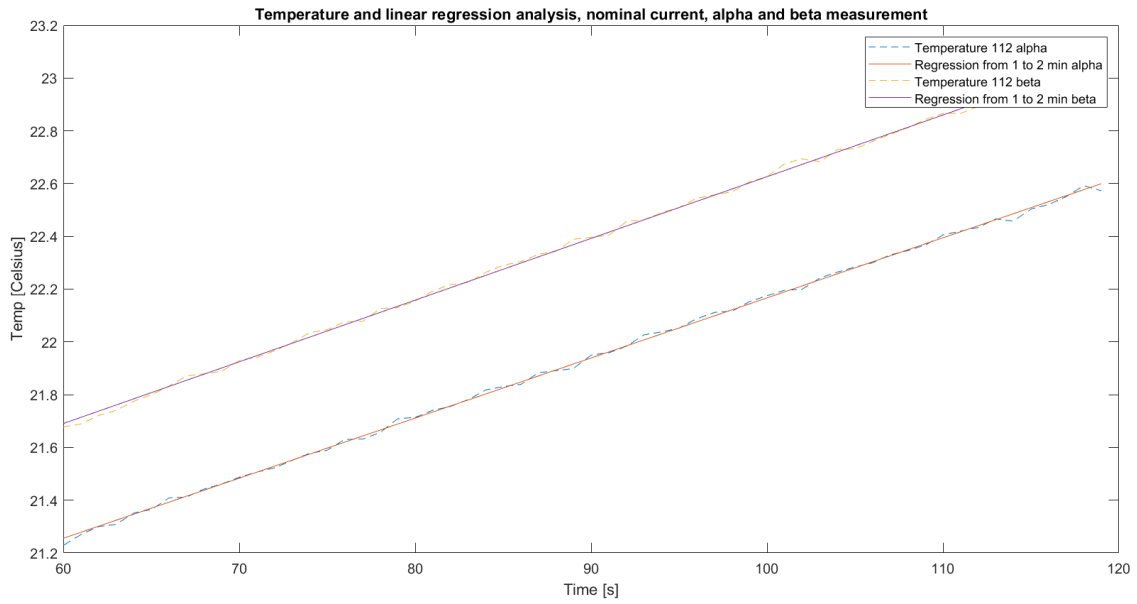


Figure C.2.17: . The temperature [°C] and the linear regression analysis for thermocouple 112, from 1 to 2 minutes, alpha and beta measurement.

One can observe that the linear regression plots follow the temperature plots another fairly well. The two different plots are nearly parallel with the beta plot being at a higher temperature. The linear regression analysis plots can be described using equations C.18 and C.19. Y represents temperature and x represent time in seconds.

$$y_{alpha} = 19.9 + 0.0228 \cdot x \quad (C.18)$$

$$y_{beta} = 20.3 + 0.0234 \cdot x \quad (C.19)$$

Thermocouple 113

In Figure C.2.18, the temperature measurement done by thermocouple 113 and the linear regression analysis performed is shown, for both alpha and beta measurement. This only is valid for 1 to 2 minutes of the measurement. The red and black plot represent the alpha and beta temperature measurement, respectively, while the blue and yellow dotted plot represent plots found using the linear regression analysis for alpha and beta measurement, respectively.

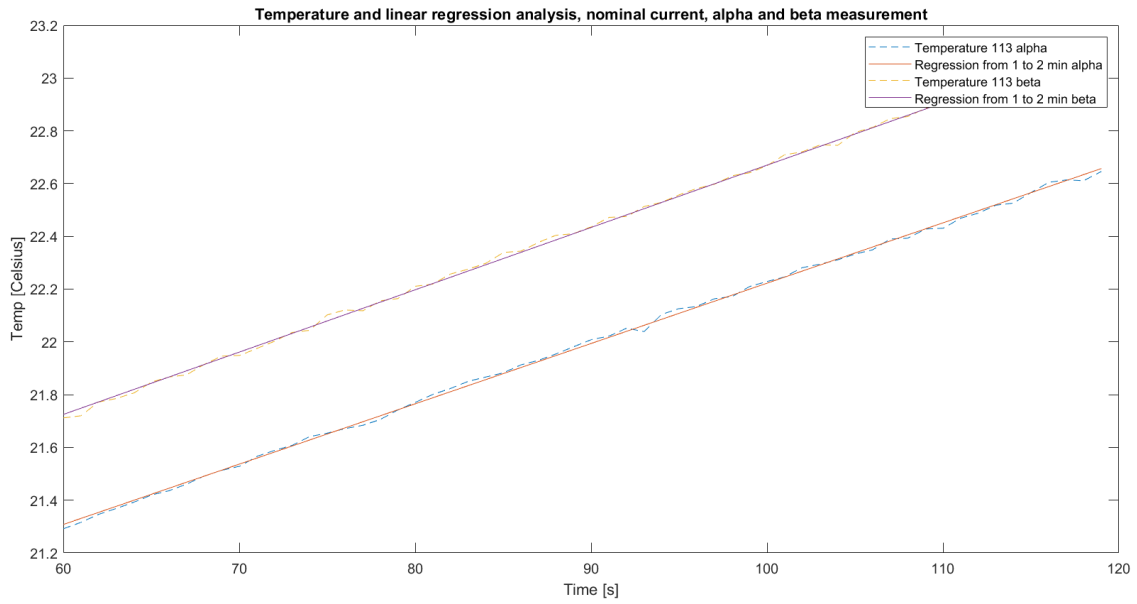


Figure C.2.18: . The temperature [°C] and the linear regression analysis for thermocouple 113, from 1 to 2 minutes, alpha and beta measurement.

One can observe that the linear regression plots follow the temperature plots another fairly well. The two different plots are nearly parallel with the beta plot being at a higher temperature. The linear regression analysis plots can be described using equations C.20 and C.21. Y represents temperature and x represent time in seconds.

$$y_{alpha} = 19.9 + 0.0229 \cdot x \quad (C.20)$$

$$y_{beta} = 20.3 + 0.0236 \cdot x \quad (C.21)$$

Thermocouple 114

In Figure C.2.19, the temperature measurement done by thermocouple 114 and the linear regression analysis performed is shown, for both alpha and beta measurement. This only is valid for 1 to 2 minutes of the measurement. The red and black plot represent the alpha and beta temperature measurement, respectively, while the blue and yellow dotted plot represent plots found using the linear regression analysis for alpha and beta measurement, respectively.

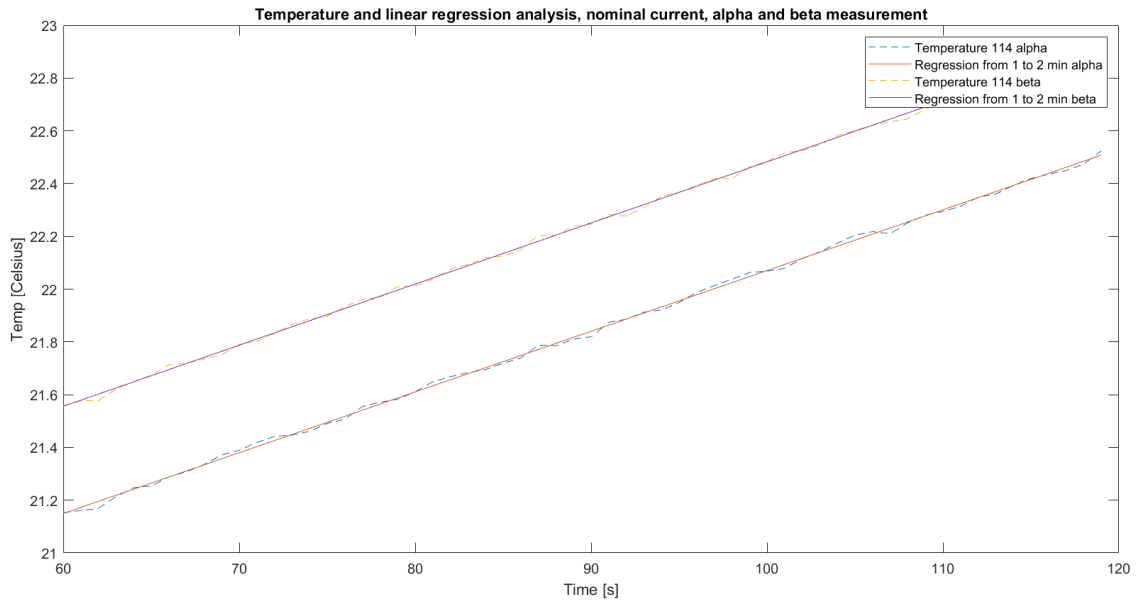


Figure C.2.19: . The temperature [°C] and the linear regression analysis for thermocouple 114, from 1 to 2 minutes, alpha and beta measurement.

One can observe that the linear regression plots follow the temperature plots another fairly well. The two different plots are nearly parallel with the beta plot being at a higher temperature. The linear regression analysis plots can be described using equations C.22 and C.23. Y represents temperature and x represent time in seconds.

$$y_{alpha} = 19.8 + 0.0230 \cdot x \quad (C.22)$$

$$y_{beta} = 20.2 + 0.0232 \cdot x \quad (C.23)$$

Thermocouple 115

In Figure C.2.20, the temperature measurement done by thermocouple 115 and the linear regression analysis performed is shown, for both alpha and beta measurement. This only is valid for 1 to 2 minutes of the measurement. The red and black plot represent the alpha and beta temperature measurement, respectively, while the blue and yellow dotted plot represent plots found using the linear regression analysis for alpha and beta measurement, respectively.

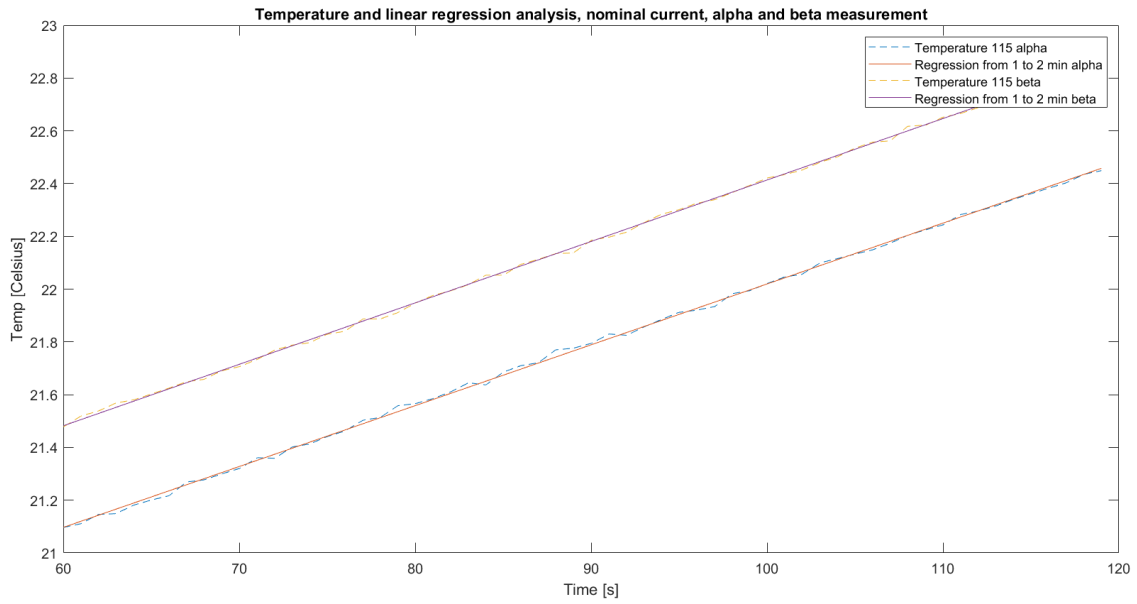


Figure C.2.20: . The temperature [°C] and the linear regression analysis for thermocouple 115, from 1 to 2 minutes, alpha and beta measurement.

One can observe that the linear regression plots follow the temperature plots another fairly well. The two different plots are nearly parallel with the beta plot being at a higher temperature. The linear regression analysis plots can be described using equations C.24 and C.25. Y represents temperature and x represent time in seconds.

$$y_{alpha} = 19.7 + 0.0231 \cdot x \quad (C.24)$$

$$y_{beta} = 20.1 + 0.0233 \cdot x \quad (C.25)$$

Thermocouple 116

In Figure C.2.21, the temperature measurement done by thermocouple 116 and the linear regression analysis performed is shown, for both alpha and beta measurement. This only is valid for 1 to 2 minutes of the measurement. The red and black plot represent the alpha and beta temperature measurement, respectively, while the blue and yellow dotted plot represent plots found using the linear regression analysis for alpha and beta measurement, respectively.

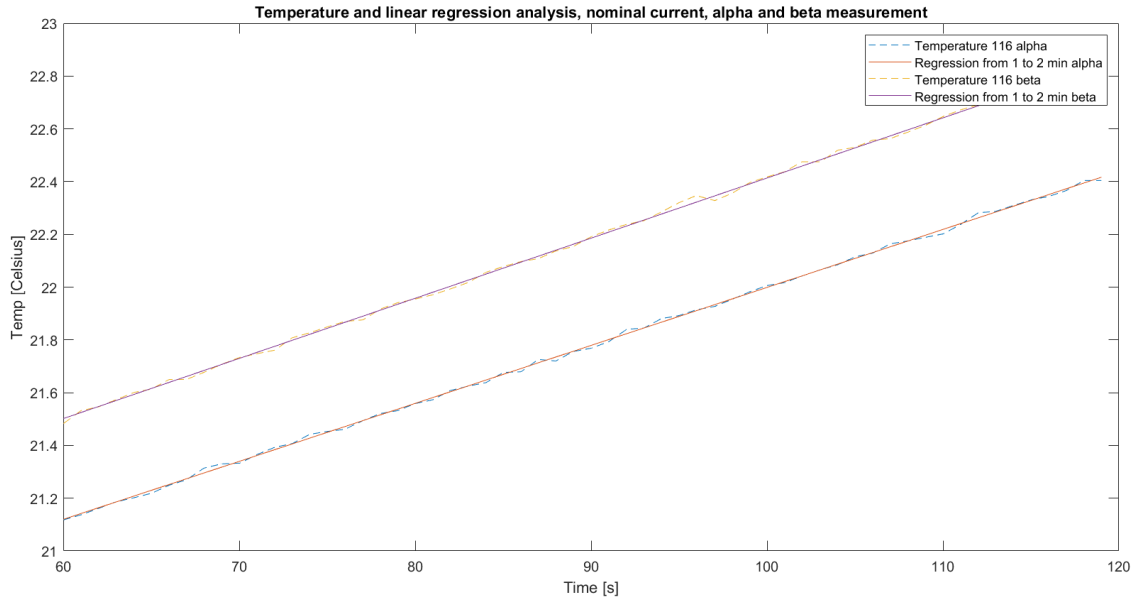


Figure C.2.21: . The temperature [°C] and the linear regression analysis for thermocouple 116, from 1 to 2 minutes, alpha and beta measurement.

One can observe that the linear regression plots follow the temperature plots another fairly well. The two different plots are nearly parallel with the beta plot being at a higher temperature. The linear regression analysis plots can be described using equations C.26 and C.27. Y represents temperature and x represent time in seconds.

$$y_{alpha} = 19.7 + 0.0231 \cdot x \quad (C.26)$$

$$y_{beta} = 20.1 + 0.0228 \cdot x \quad (C.27)$$

C.2.3 Twice the nominal current

Thermocouple 107

In Figure C.2.22, the temperature measurement done by thermocouple 107 and the linear regression analysis performed is shown. This measurement is done with twice the nominal current. This only is valid for 1 to 2 minutes of the measurement. The red plot represents the temperature measurement while the blue plot represent plot found using the linear regression analysis.

Linear regression analysis from 1 to 2 minutes for thermal couple 107, twice nominal

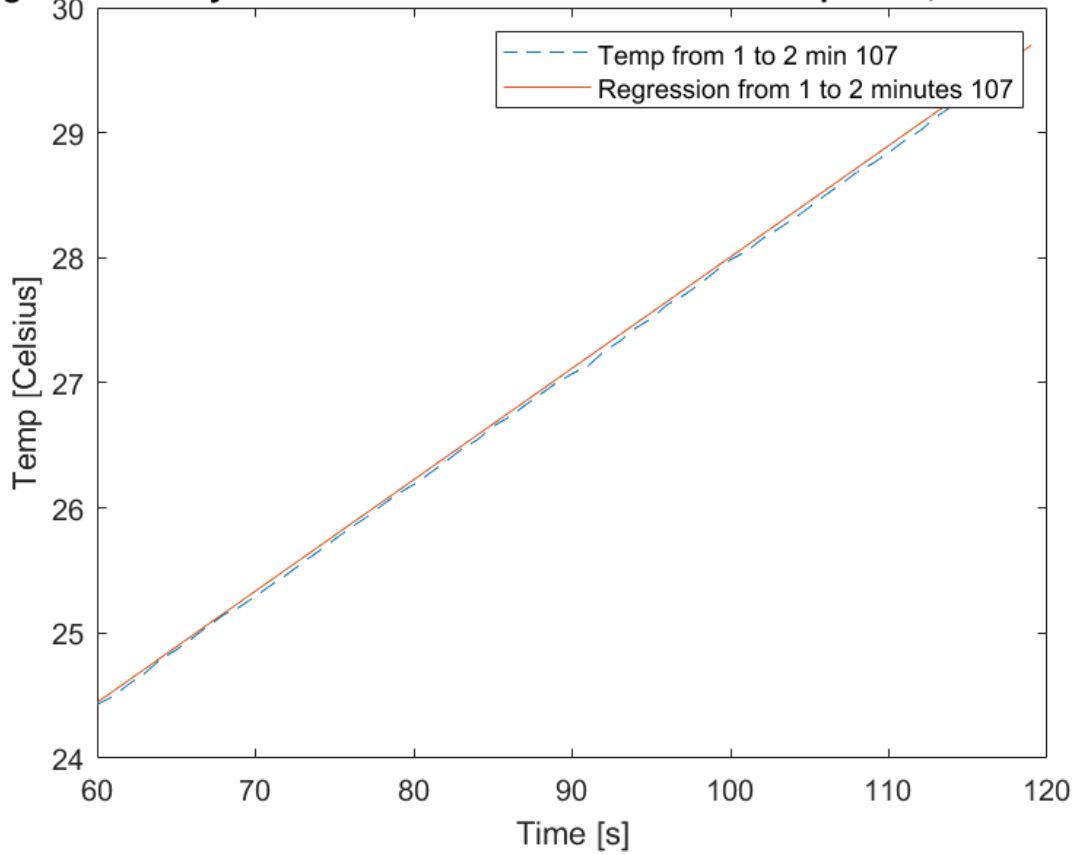


Figure C.2.22: . The temperature [°C] and the linear regression analysis for thermocouple 107, from 1 to 2 minutes, at twice nominal current.

The two plots follow one another fairly well. The blue plot can be described using Equation C.28. Y represents temperature and x represent time in seconds.

$$y = 19.1 + 0.0891 \cdot x \tag{C.28}$$

Thermocouple 108

In Figure C.2.23, the temperature measurement done by thermocouple 108 and the linear regression analysis performed is shown. This measurement is done with twice the nominal current. This only is valid for 1 to 2 minutes of the measurement. The red plot represents the temperature measurement while the blue plot represent plot found using the linear regression analysis.

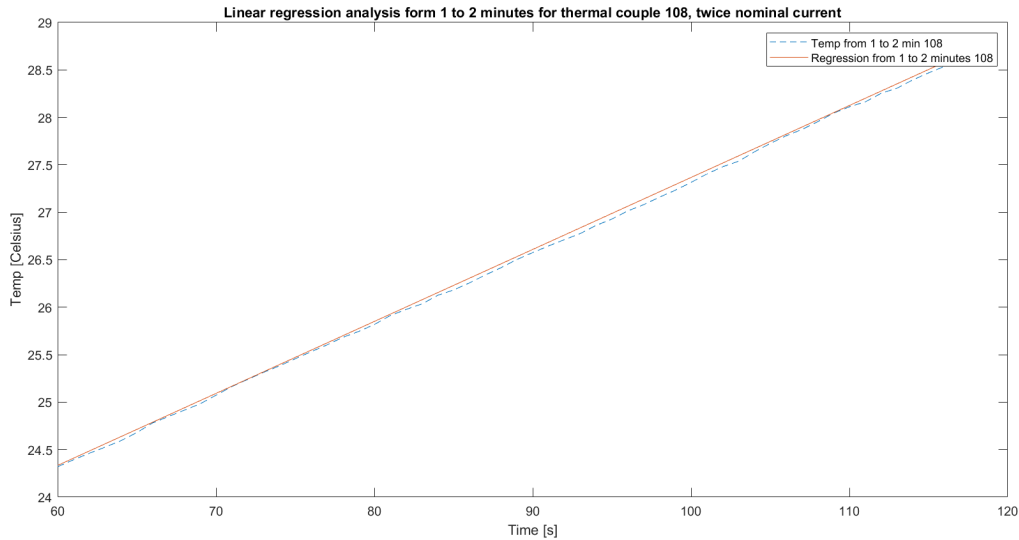


Figure C.2.23: . The temperature [°C] and the linear regression analysis for thermocouple 108, from 1 to 2 minutes, at twice nominal current.

The two plots follow one another fairly well. The blue plot can be described using Equation C.29. Y represents temperature and x represent time in seconds.

$$y = 19.8 + 0.0758 \cdot x \tag{C.29}$$

Thermocouple 109

In Figure C.2.24, the temperature measurement done by thermocouple 109 and the linear regression analysis performed is shown. This measurement is done with twice the nominal current. This only is valid for 1 to 2 minutes of the measurement. The red plot represents the temperature measurement while the blue plot represent plot found using the linear regression analysis.

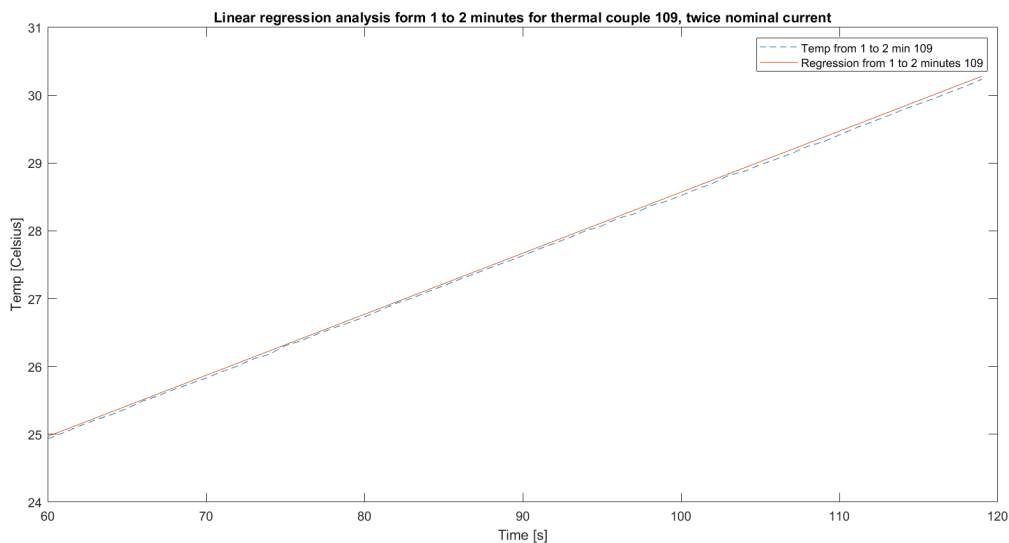


Figure C.2.24: . The temperature [°C] and the linear regression analysis for thermocouple 109, from 1 to 2 minutes, at twice nominal current.

The two plots follow one another fairly well. The blue plot can be described using Equation C.30. Y represents

temperature and x represent time in seconds.

$$y = 19.6 + 0.0901 \cdot x \tag{C.30}$$

Thermocouple 111

In Figure C.2.25, the temperature measurement done by thermocouple 111 and the linear regression analysis performed is shown. This measurement is done with twice the nominal current. This only is valid for 1 to 2 minutes of the measurement. The red plot represents the temperature measurement while the blue plot represent plot found using the linear regression analysis.

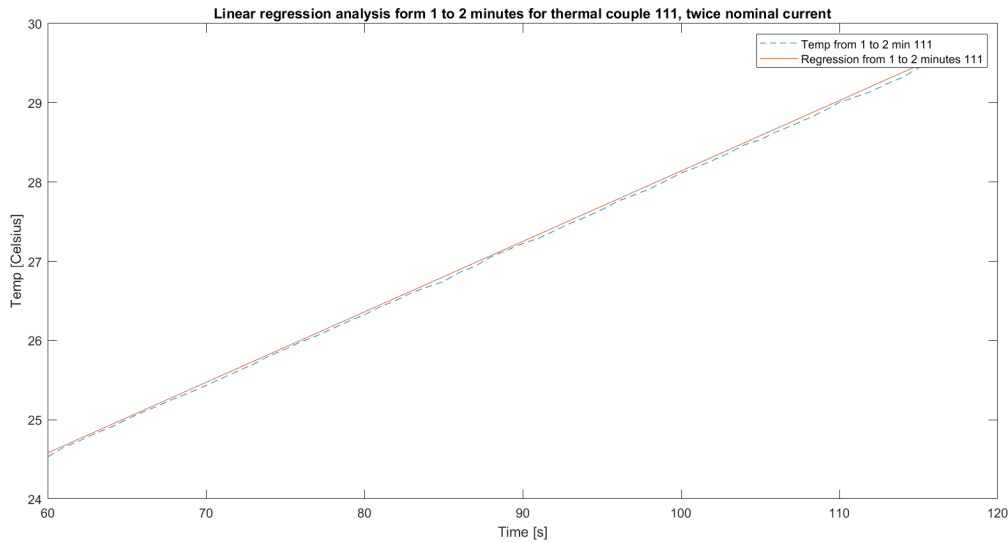


Figure C.2.25: . The temperature [°C] and the linear regression analysis for thermocouple 111, from 1 to 2 minutes, at twice nominal current.

The two plots follow one another fairly well. The blue plot can be described using Equation C.31. Y represents temperature and x represent time in seconds.

$$y = 19.2 + 0.0889 \cdot x \tag{C.31}$$

Thermocouple 112

In Figure C.2.26, the temperature measurement done by thermocouple 112 and the linear regression analysis performed is shown. This measurement is done with twice the nominal current. This only is valid for 1 to 2 minutes of the measurement. The red plot represents the temperature measurement while the blue plot represent plot found using the linear regression analysis.

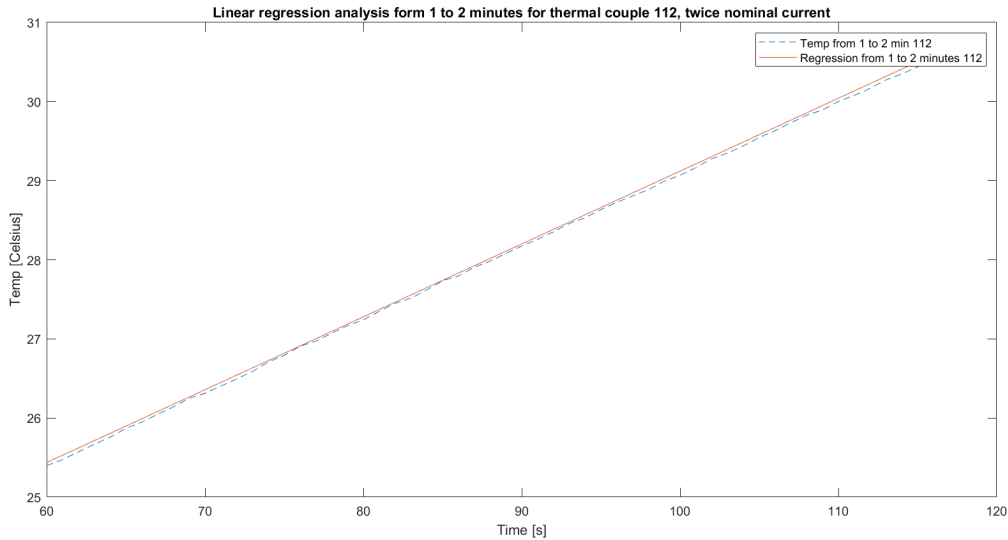


Figure C.2.26: . The temperature [°C] and the linear regression analysis for thermocouple 112, from 1 to 2 minutes, at twice nominal current.

The two plots follow one another fairly well. The blue plot can be described using Equation C.32. Y represents temperature and x represent time in seconds.

$$y = 19.9 + 0.0921 \cdot x \tag{C.32}$$

Thermocouple 113

In Figure C.2.27, the temperature measurement done by thermocouple 113 and the linear regression analysis performed is shown. This measurement is done with twice the nominal current. This only is valid for 1 to 2 minutes of the measurement. The red plot represents the temperature measurement while the blue plot represent plot found using the linear regression analysis.

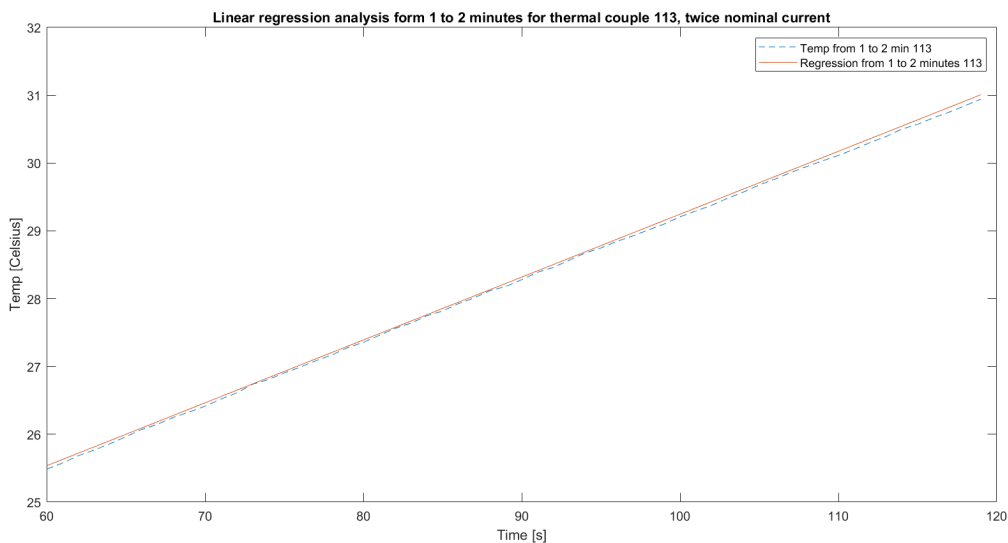


Figure C.2.27: . The temperature [°C] and the linear regression analysis for thermocouple 113, from 1 to 2 minutes, at twice nominal current.

The two plots follow one another fairly well. The blue plot can be described using Equation C.33. Y represents

temperature and x represent time in seconds.

$$y = 20.0 + 0.0928 \cdot x \tag{C.33}$$

Thermocouple 114

In Figure C.2.28, the temperature measurement done by thermocouple 114 and the linear regression analysis performed is shown. This measurement is done with twice the nominal current. This only is valid for 1 to 2 minutes of the measurement. The red plot represents the temperature measurement while the blue plot represent plot found using the linear regression analysis.

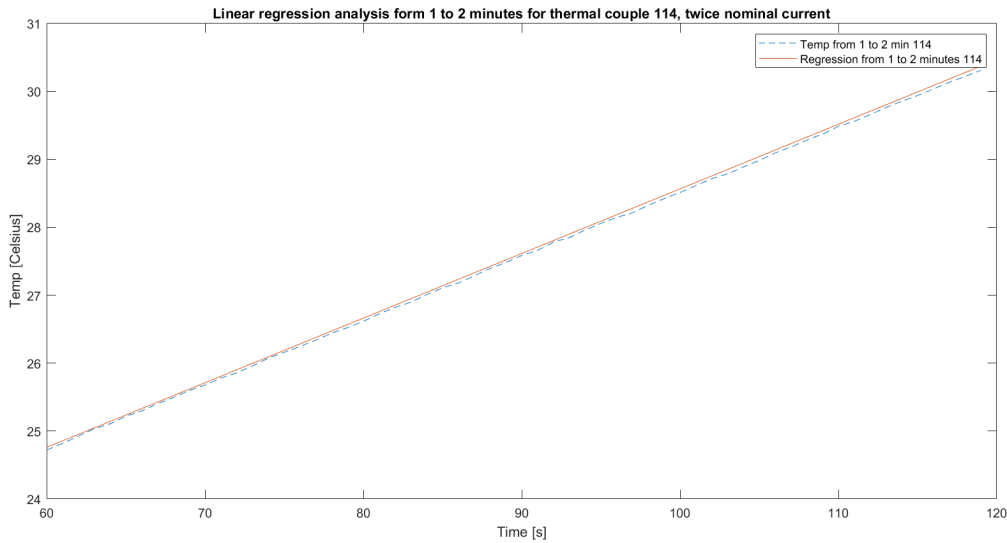


Figure C.2.28: . The temperature [°C] and the linear regression analysis for thermocouple 114, from 1 to 2 minutes, at twice nominal current.

The two plots follow one another fairly well. The blue plot can be described using Equation C.34. Y represents temperature and x represent time in seconds.

$$y = 19.1 + 0.0951 \cdot x \tag{C.34}$$

Thermocouple 115

In Figure C.2.29, the temperature measurement done by thermocouple 115 and the linear regression analysis performed is shown. This measurement is done with twice the nominal current. This only is valid for 1 to 2 minutes of the measurement. The red plot represents the temperature measurement while the blue plot represent plot found using the linear regression analysis.

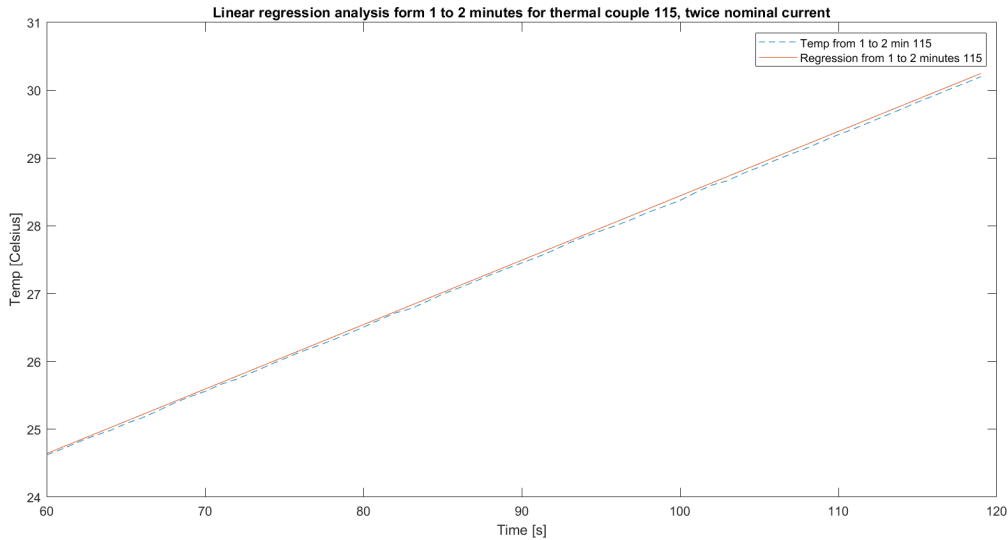


Figure C.2.29: . The temperature [°C] and the linear regression analysis for thermocouple 115, from 1 to 2 minutes, at twice nominal current.

The two plots follow one another fairly well. The blue plot can be described using Equation C.35. Y represents temperature and x represent time in seconds.

$$y = 18.9 + 0.0950 \cdot x \tag{C.35}$$

Thermocouple 116

In Figure C.2.30, the temperature measurement done by thermocouple 116 and the linear regression analysis performed is shown. This measurement is done with twice the nominal current. This only is valid for 1 to 2 minutes of the measurement. The red plot represents the temperature measurement while the blue plot represent plot found using the linear regression analysis.

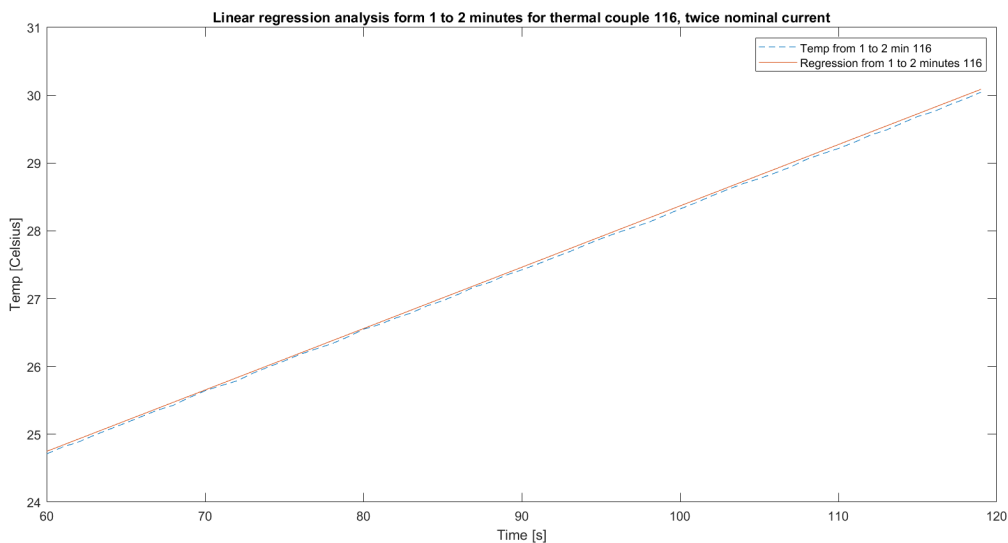


Figure C.2.30: . The temperature [°C] and the linear regression analysis for thermocouple 116, from 1 to 2 minutes, at twice nominal current.

The two plots follow one another fairly well. The blue plot can be described using Equation C.36. Y represents

temperature and x represent time in seconds.

$$y = 19.3 + 0.0905 \cdot x \tag{C.36}$$

D | Ratio between different methods

In Table D.1, the differences in percent between the magnetodynamic and semi-analytical loss calculation method are presented. Each of the cells in the table represents a turn from the top of the windings. This difference is for the case with circulating currents.

Table D.1: Difference in loss in % between the magnetodynamic and semi-analytical loss calculation method.

Difference in loss in %						
Secondary				Primary		
0.685537	0.813208	0.464774	-0.29794	-0.01807	0.454437	0.472507
0.260726	0.200059	-0.01681	-0.36001	-0.1359	0.057612	0.12815
0.128237	0.050912	-0.09736	-0.30185	-0.12461	-0.00074	0.052931
0.07764	0.009913	-0.09942	-0.24226	-0.10025	-0.00799	0.038141
0.056594	0.000525	-0.08633	-0.20025	-0.08314	-0.00396	0.033694
0.046833	8.02E-05	-0.07226	-0.1704	-0.06584	-0.00217	0.036183
0.042238	0.001947	-0.06159	-0.15081	-0.06012	0.003687	0.032051
0.038893	0.005007	-0.05494	-0.13727	-0.05489	0.00533	0.035748
0.03799	0.006301	-0.04842	-0.12828	-0.05199	0.002115	0.032784
0.037593	0.007913	-0.04516	-0.122	-0.04579	0.007758	0.037437
0.036734	0.009437	-0.04253	-0.11684	-0.04396	0.007543	0.035242
0.036875	0.009322	-0.04015	-0.114	-0.04015	0.008542	0.033343
0.036857	0.009893	-0.03864	-0.11227	-0.04176	0.010399	0.038881
0.036735	0.010984	-0.03827	-0.10957	-0.04204	0.012969	0.037442
0.036556	0.011238	-0.03701	-0.10895	-0.0412	0.009112	0.03619
0.036348	0.011834	-0.03614	-0.10698	-0.03943	0.012968	0.035103
0.03613	0.011441	-0.03588	-0.10649	-0.0369	0.010111	0.034168

In Tables D.2 and table D.3, the comparison between the losses when applying circulating currents and not applying circulating currents to the semi-analytical loss calculation method is presented. The difference in losses is presented as the percent difference between the them. Each cell in the table represent a turn, from the top of the winding.

Table D.2: Difference in loss in % between the semi-analytical loss calculation method applying and not applying circulating currents, from turn 0 to 30 from the top.

Difference in loss in %						
Secondary				Primary		
-0.25848	3.166711	-9.58637	-38.4335	-19.9985	0.497007	9.198471
0.132991	3.797429	-9.17508	-38.321	-19.8929	0.89032	9.595751
0.261154	3.956779	-9.09688	-38.2877	-19.8843	0.95469	9.685393
0.311802	4.001675	-9.08561	-38.2717	-19.8882	0.962692	9.707483
0.333954	4.013564	-9.08886	-38.2615	-19.8919	0.960042	9.712201
0.344399	4.015421	-9.09416	-38.2542	-19.8939	0.956268	9.71245
0.349646	4.014449	-9.09866	-38.2484	-19.8946	0.953117	9.711735
0.352449	4.012947	-9.1019	-38.2439	-19.8946	0.950847	9.710959
0.354042	4.0116	-9.10419	-38.2401	-19.8942	0.949183	9.710308
0.354986	4.010539	-9.1056	-38.237	-19.8936	0.947863	9.709787
0.355588	4.009748	-9.10654	-38.2343	-19.8931	0.946992	9.709363
0.355982	4.009158	-9.10704	-38.2321	-19.8925	0.946205	9.709003
0.356237	4.008707	-9.10737	-38.2302	-19.8919	0.945572	9.708697
0.35642	4.008374	-9.10761	-38.2286	-19.8914	0.945092	9.708423
0.356544	4.008101	-9.10771	-38.2272	-19.891	0.944619	9.708194
0.356631	4.007882	-9.10778	-38.2261	-19.8907	0.944224	9.707983
0.356689	4.007703	-9.1078	-38.2251	-19.8903	0.943905	9.707797
0.356728	4.007548	-9.10787	-38.2243	-19.89	0.943591	9.707641
0.356755	4.007401	-9.10798	-38.2235	-19.8898	0.943353	9.70749
0.356769	4.007289	-9.1079	-38.223	-19.8897	0.943191	9.707366
0.356778	4.007184	-9.10797	-38.2224	-19.8895	0.942886	9.707251
0.35678	4.007098	-9.10805	-38.222	-19.8894	0.942801	9.707162
0.356783	4.007004	-9.10805	-38.2217	-19.8893	0.942645	9.707073
0.356773	4.006914	-9.10807	-38.2214	-19.8893	0.942492	9.706989
0.356773	4.006841	-9.1081	-38.2212	-19.8892	0.94234	9.706929
0.356758	4.006773	-9.10815	-38.221	-19.8892	0.942262	9.706865
0.356755	4.006707	-9.10821	-38.2209	-19.8892	0.942112	9.706807
0.356737	4.006645	-9.10829	-38.2209	-19.8893	0.942037	9.706753
0.356728	4.006572	-9.10837	-38.2209	-19.8893	0.94189	9.706703
0.356719	4.006515	-9.10847	-38.2209	-19.8894	0.941817	9.706666

Table D.3: Difference in loss in % between the semi-analytical loss calculation method applying and not applying circulating currents, from turn 30 to 61 from the top.

Difference in loss in %						
Secondary				Primary		
0.356698	4.006435	-9.10858	-38.221	-19.8895	0.941672	9.706617
0.356678	4.00637	-9.1087	-38.2212	-19.8897	0.9416	9.70658
0.356661	4.006282	-9.10894	-38.2214	-19.89	0.941458	9.70653
0.356643	4.006209	-9.10908	-38.2217	-19.8901	0.941316	9.706485
0.356612	4.0061	-9.10924	-38.2221	-19.8904	0.941103	9.706444
0.356588	4.005994	-9.10952	-38.2225	-19.8907	0.941037	9.706392
0.356558	4.005878	-9.10981	-38.223	-19.8912	0.940827	9.706337
0.356525	4.005739	-9.11012	-38.2236	-19.8917	0.940546	9.706279
0.356491	4.005578	-9.11055	-38.2243	-19.8922	0.940267	9.706204
0.356456	4.005408	-9.111	-38.2252	-19.8928	0.940062	9.706136
0.35641	4.005204	-9.11149	-38.2263	-19.8936	0.939716	9.706044
0.356372	4.004953	-9.11211	-38.2275	-19.8945	0.939299	9.705953
0.356331	4.004669	-9.11287	-38.2289	-19.8955	0.938812	9.70584
0.356293	4.00434	-9.11367	-38.2306	-19.8968	0.938257	9.705724
0.356262	4.003954	-9.11474	-38.2327	-19.8982	0.937707	9.70558
0.356246	4.003486	-9.11608	-38.2351	-19.8999	0.937015	9.705418
0.35624	4.002899	-9.1176	-38.2381	-19.9018	0.936113	9.705243
0.356278	4.002182	-9.11955	-38.2418	-19.9042	0.935144	9.705038
0.356363	4.001261	-9.12204	-38.2463	-19.9071	0.934038	9.704799
0.356542	4.000061	-9.12524	-38.2522	-19.9106	0.932579	9.704513
0.356889	3.998484	-9.12963	-38.2598	-19.9148	0.930841	9.704171
0.357537	3.996397	-9.1354	-38.2699	-19.9202	0.928682	9.70375
0.358759	3.99368	-9.14344	-38.2838	-19.9272	0.925962	9.70322
0.361158	3.990337	-9.15447	-38.303	-19.9366	0.922359	9.702592
0.366024	3.986869	-9.16946	-38.3301	-19.9496	0.917556	9.702044
0.376327	3.985381	-9.18913	-38.3692	-19.968	0.911631	9.702413
0.399237	3.99286	-9.21111	-38.4252	-19.9943	0.906273	9.706886
0.453466	4.03242	-9.22229	-38.5033	-20.0294	0.910937	9.72712
0.594185	4.18734	-9.1628	-38.5987	-20.0601	0.971599	9.808663
1.035965	4.831336	-8.73208	-38.6384	-19.9866	1.362869	10.1773

